SUSTAINED LOAD BEHAVIOUR

OF REINFORCED CONCRETE FRAMES

BY

RONALD C. T. DANIELSEN, B. ENG.

A THESIS
SUBMITTED TO THE FACULTY OF GRADUATE STUDIES
IN PARTIAL FULFILLMENT OF THE REQUIREMENTS
FOR THE DEGREE
MASTER OF ENGINEERING

McMASTER UNIVERSITY
HAMILTON, ONTARIO

MARCH, 1970

MASTER OF ENGINEERING (1970)
(Civil Engineering)

McMASTER UNIVERSITY
Hamilton, Ontario

TITLE: Sustained Load Behaviour of Reinforced Concrete Frames

AUTHOR: Ronald C. T. Danielsen, B. Eng. (McMaster)

SUPERVISOR: Dr. R. G. Drysdale

NUMBER OF PAGES: ix, 195

SCOPE AND CONTENTS: Methods are presented for the prediction of the short-term and sustained load behaviour of reinforced concrete frames. These procedures are evaluated by an experimental program using a particular structure and loading configuration. The results of two short-term tests and one sustained load test are compared with the analytic predictions. The inadequacy of classical methods of structural analysis for sustained load problems is also discussed. It is concluded that the methods using small elements, numerical integration and successive iterations can provide accurate predictions of short-term and sustained load behaviour of reinforced concrete frames.

ACKNOWLEDGEMENTS

The author would like to express his appreciation to Dr. R. G. Drysdale for his guidance and advice during the course of this investigation. The assistance provided by Mr. Jan Svihra and Mr. Laird Smith is gratefully acknowledged.

The author also takes this opportunity to thank the following:

1) McMaster University for financial support during this research.
2) The staff of the Applied Dynamics Laboratory for their help in the experimental program.
3) The personnel of the McMaster University Computer Centre for helping to overcome programming difficulties.
4) The Steel Company of Canada for providing the reinforcing steel.

And finally, the author wishes to express his gratitude to his sister, Liz, for her assistance in preparing this thesis.

TABLE OF CONTENTS

		PAGE
Chapter 1	INTRODUCTION	
1.1.	Proposal	1
1.2.	Background	1
1.3.	Scope of Research	2
Chapter 2	LITERATURE REVIEW	
2.1.	Introduction	4
2.2.	The Nature of Creep	4
2.3.	Factors Affecting Creep	9
2.4.	Investigations of Creep in Structures	10
Chapter 3	FRAME SELECTION, FABRICATION & MATERIALS	
3.1.	The Concrete Frame	12
3.2.	Concrete	13
3.3.	Reinforcing Steel	15
3.4.	Forms	16
3.5.	Cage	16
3.6.	Fabrication	17
Chapter 4	TEST APPARATUS	
4.1.	Introduction	20
4.2.	Instrumentation	20
4.2.1.	Bases	20
4.2.2.	Dial Gauges	22

4.2.3. Demec Strain Measurement 22

4.2.4. Load Cells 23

4.3. Short-Term Test Apparatus 24

4.4. Long-Term Test Apparatus 24

4.4.1. Introduction 24

4.4.2. Controlled Atmosphere Tent 25

4.4.3. Sustained Load Systems 28

Chapter 5 TEST PROCEDURE AND GENERAL OBSERVATIONS

5.1. Introduction 32

5.2. Frame R1 32

5.2.1. Introduction 32

5.2.2. Test Procedure 32

5.2.3. Observations 32

5.2.4. Resulting Modifications 33

5.2.5. Conclusions 34

5.3. Frame L1 34

5.3.1. Introduction 34

5.3.2. Test Procedure 34

5.3.3. Observations 35

5.3.4. Resulting Modifications 36

5.3.5. Conclusions 36

5.4. Frame R2 36

5.4.1. Introduction 36

5.4.2. Procedure 37

5.4.3. Observations 37

5.4.4. Conclusions 38

5.5. Sources of Error in Testing 39

5.5.1. Introduction 39

5.5.2. Summary of Testing Errors 41

Chapter 6 METHODS OF COMPUTING CREEP

6.1. Introduction 43

6.2. Effective Modulus Method 45

6.3. Rate of Creep Method 45

6.4. Method of Superposition 46

6.5. Modified Method of Superposition 47

6.6. Evaluation of Methods of Computing Creep 50

Chapter 7 METHODS OF ANALYSIS

7.1. Introduction 52

7.2. Mechanism Method 53

7.2.1. Assumptions 53

7.2.2. Effective Member Lengths 55

7.2.3. Results 55

7.2.4. Discussion 56

7.2.5. Conclusion 58

7.3. Elastic Slope-Deflection Equations 59

7.3.1. Assumptions 59

7.3.2. Procedure 59

7.3.3. Use of Slope-Deflection Equations to Determine the Effects of Base Movements 60

7.3.4. Results 62

7.3.5. Discussion 62

7.3.6. Conclusions 64

7.4. Plastic Slope-Deflection Equations 65

7.4.1. Introduction 65

7.4.2. Procedure 65

7.4.3. Results 65

7.5. Numerical Procedure Using the Moment-Curvature Relationships for Short-term Loads 66

7.5.1. Introduction 66

7.5.2. Assumptions 66

7.5.3. The Frame Model 68

7.5.4. Moment-Curvature Computation 71

7.5.5. The Influence of Concrete Tensile Strength on Frame Behaviour 81

7.5.6. Comparison Between the Moment-Curvature Element Method and Slope-Deflection Equations 84

7.6. Numerical Integration Using Element Slices and Creep Data for Sustained Loads 86

7.6.1. Introduction 86

7.6.2. The Solution of Forces, Moments, Rotation and Displacement for Each Element 87

7.6.3. Concrete Strength 90

7.6.4. Shrinkage 90

7.6.5. Changes in Load 92

Chapter 8 COMPARISON AND EVALUATION OF RESULTS

8.1. Introduction 93

8.2. Moments Calculated from Demec Readings 93

8.3. Extreme Fibre Strains from Demec Readings 94

8.4. Frame R2 95

8.4.1. Introduction 95

8.4.2. Moments from Testing and Analysis 95

8.4.3. Deflections - Predicted and Experimental 97

8.5. Frame L1 104

8.5.1. Introduction 104

8.5.2. Short-Term Test 104

8.5.3. Sustained Load Test 107

8.6. Resume 117

Chapter 9 SOURCES OF ERROR

9.1. Introduction 127

9.2. Errors in Conventional Methods of Analysis 127

9.3. Errors Common to the Element Methods 128

9.3.1. Introduction 128

9.3.2. Concrete Stress-Strain Relationship 128

9.3.3. Reinforcing Steel 129

9.3.4. Shrinkage 129

9.4. Errors in Moment-Curvature Computation 130

9.4.1. Introduction 130

9.4.2. Tension in Concrete 131

9.4.3. Moment-Curvature Expressions 131

9.5. Moment Calculation from Demec Readings 132

9.5.1. Data from Demec Points 132

9.5.2. Calculations 132

9.6. Extreme Fibre Strains from Demec Readings 133

9.7. Frame Analysis Using the Moment-Curvature Element Method 134

9.7.1. Calculations for Each Element 134

9.7.2. Solution for the Frame 136

9.7.3. Bases 139

9.8. Frame Analysis Using Sustained Load Element Method 139

9.8.1. Introduction 139

9.8.2. Creep Expression 140

9.8.3. Shrinkage 140

9.8.4. Concrete Stress-Strain Relationship 141

9.8.5. Solution for Each Element 141

9.8.6. Total Precision for the Frame Solution 142

9.9. Summary of Errors in Analysis 142

Chapter 10 CONCLUSIONS AND RECOMMENDATIONS

10.1. Introduction 144

10.2. Methods of Analysis 144

10.2.1. Conventional Methods 144

10.2.2. The Element Methods 145

10.3. Test Apparatus and Procedures 150

10.3.1. Introduction 150

10.3.2. Loading Systems 150

10.3.3. Instrumentation 150

10.3.4. Recommended Changes in Testing 152

10.4. Additional Recommendations for Further Research 152

10.5. Resume 153

APPENDIX A	CONCRETE CYLINDER TESTS	154
APPENDIX B	COMPUTER PROGRAMS	156
B1	Moment-Curvature Relationships from Demec Readings	159
B2	Theoretical Moment-Curvature Relationships	163
B3	Strain Distribution from Demec Readings	168
B4	Short-Term Analysis	170
B5	Sustained Load Analysis	178
APPENDIX C	TENSILE TESTS ON REINFORCEMENT	191
BIBLIOGRAPHY		193

Chapter 1

INTRODUCTION

1.1. Proposal

This investigation formed part of an extensive program at McMaster University to study creep and shrinkage in concrete. Initiated in 1967 by R. G. Drysdale, [5] the series has included the testing and analysis of concrete prisms with the aim of obtaining an empirical method of predicting creep under varying stress. Gray [11] did the first work on this phase of the program.

The object of this investigation was to develop a method of analysis for simple framed structures subjected to sustained loading using the data from prism tests to predict the influence of creep and shrinkage. The procedure was to be sufficiently general that the behaviour of a large range of structures and loading conditions could be determined without the necessity of experimental comparison.

1.2. Background

During the twentieth century, a great number of papers have been written on creep in concrete with the result that an enormous amount of data has been accumulated, and numerous theories have been presented. Despite this substantial background of experience, two important limitations must be recognized. First, the exact nature of creep and how it affects reinforced concrete is not known, and, second, the influence of creep on all but a few specialized structures, such as pinned-ended columns, cannot be predicted accurately. The main reason for this uncertainty is the number of variables involved. Creep is dependent on atmospheric conditions, the type of cement, the magnitude and nature of loading, time, concrete strength, age at loading, aggregate, member cross-section, and numerous other factors not all of which are known.

Most work on creep has concentrated on one of two areas; the nature of the phenomenon, or its effects on structures. In the former case, all of the factors mentioned above have been studied by attempting to isolate their influence. This is a difficult task in itself and does not account for inter-relationships between the various factors. Based on this experimental evidence, models for creep have been devised.

Using prism tests to study the nature of creep, and tests on common structures such as columns and frameworks to determine its influence, an empirical appreciation of creep has been obtained. But, because of the complexity of this phenomenon, testing for each individual case has been the only sure way of obtaining an accurate solution.

1.3. Scope of Research

In order to achieve the objective, the method of analysis had to be sufficiently general that it could accomodate any functional relationship between creep and time, and a range of structures and load conditions. The analysis developed was applied to a specific structure for the purpose of experimental verification, but could be easily modified to satisfy the requirement of generality.

Test materials and conditions were limited by the desire to use creep data obtained previously by Drysdale.(5) Hence, the concrete mix, steel, section properties, temperature, humidity, and age at loading were fixed. For comparison between tests and the analysis, the frame geometry and loading configuration were not changed during the program.

The investigation was conducted in two phases. The first was a study of the short-term behaviour of the frame, and the second was a study of the sustained load response. Comparative analyses and experiments were provided for these conditions. Of specific interest was the increase in deformation and the redistribution of frame moments caused by creep.

Chapter 2

LITERATURE REVIEW

2.1. Introduction

This chapter includes a brief review of some of the creep research by previous investigators. Because it is essential to understand as clearly as possible how creep occurs in order to study its effects on frame behaviour, some recent theories on the nature of creep are presented. The only factors influencing creep which were allowed to vary in this investigation were time and stress. The reader is referred to Neville's work[19] for the effects of other variables. Previous sustained load studies on various structures are also outlined in this chapter.

2.2. The Nature of Creep

A number of authors have concentrated on trying to determine the nature of creep and shrinkage phenomena, their causes and their effects.

In 1958, Washa and Fluck[6] wrote a review of creep research up to that time with references to publications as far back as 1905. They attributed creep to closure of internal voids, viscous flow of aggregates, and the flow of water out of the gel due to load and drying.

Freudenthal and Roll[7] did extensive work on creep under high compressive stress. It had been recognized for many years that the relationship between creep and stress was non-linear above a certain stress level. Freudenthal and Roll developed a rheological model to explain this phenomenon, and in 1958 presented a theory of creep which included creep recovery and the effects of high stresses.

They attributed creep to four conditions:- viscous flow of the cement paste, seepage of adsorbed water from the gel under pressure, delayed elasticity due to the cement paste acting as a restraint on elastic deformation of the aggregate-cement crystal skeleton, and permanent deformation caused by local fracture. The decreasing rate of creep was considered to be caused by an increase in viscosity of the paste as it crystallized, by completion of the delayed elastic deformations, and by the termination of seepage. Creep recovery was explained by the reversal of seepage which could be recovered to various degrees. Other deformations were permanent.

Freudenthal and Roll presented generalized equations for creep as a result of their theory and tests. These equations were based on a rheological model which consisted of four units (each representing one of the creep conditions mentioned above) connected in series. Three were made up of a dashpot and spring in parallel and the fourth was a dashpot and spring in series. All of the units responded to increases in stress, while two of them allowed for irreversible creep by not reacting to decreases in stress. The spring constants and dashpot fluidities were determined experimentally.

The original expressions for creep strain were linear functions of stress and exponential functions of time.

In 1962, Glucklich and Ishai[10] ran a series of tests in an attempt to determine the true nature of creep. They investigated the viscous theory which considered the cement gel to act as a highly viscous fluid which flowed under external loading, and the seepage theory which considered the gel as a hygroscopic solid which creeps due to water migration in its channels. Using torsional loading and careful control of boundary conditions they showed that creep is almost non-existent in mortar deprived of almost all its water. Hence, creep was found to be conditional on the presence of evaporable water, and was not an inherent property of the gel, a solid unable to flow under load. This contradicted the viscous theory, but the seepage theory as previously presented was also inadequate since it considered only the movement of pore water and did not account for the complexity of creep particularly in almost dry concrete. Also, the original seepage theory was inaccurate under conditions of stress reversal with creep recovery, or after long periods of time.

The explanation of creep by Glucklich and Ishai, probably the most plausible to date, is presented as follows:

Hydration converts cement to a hygroscopic gel of enormous specific surface area (200 m^2/g) and a high percentage of voids (28%). The chemical reaction of cement and water forms an amorphous mass of colloidal size particles (the gel) which is porous with numerous very small voids corresponding to the thickness of four to five water molecules.* Besides this amorphous mass, coating the unhydrated cement particles and filling inter-granular gaps, rod, ribbon and crumpled foils, shaped crystals are formed with a length about one thousand times their width and an average spacing of fifteen angstroms. Also in the paste are larger voids called capillary pores which may be interconnected to form capillary channels.

---

* Glucklich and Ishai sized the gel pores and forty to fifty angstroms, but, since a water molecule is about 2.63 A, this would seem to be in error. A void size of ten to fifteen angstroms is probably more reasonable.

Because of its strong absorption capacity, the gel is saturated with water immediately on forming. If any evaporable water is present, it will first fill the gel voids and, in the absence of sufficient reserve, hydration will terminate even though the gel remains saturated. For hydration, 0.26 g of water are required per gram of cement. But, since the gel (with 28% voids) must be saturated for hydration to continue, the actual water/cement ratio for continued hydration through setting is 0.44 to 0.50 assuming no water can be added from outside sources. A water/cement ratio over 0.70 leads to too many capillary pores and channels and hence to a weak concrete. Hydration ceases when the vapour pressure in the paste drops below 80% of the saturated vapour pressure.

The water in the cement mass is classified as follows:-

1. capillary water (in channels)
2. voids gel water (in the voids of the amorphous mass)
3. intracrystalline water (zeolitic water)

Zeolitic water is very strongly bound to the solid and has almost infinite viscosity - it acts almost like a solid.

Gel water is also strongly bound since it is in small voids where friction forces are significant. Only very large forces will induce it to flow, and it is fairly insensitive to the humidity gradient between the concrete and the outside environment.

Because it is loosely bound, capillary water flows readily in and out through the channels in response to humidity gradients. However, since the channel diameters are large, the attractive forces between channel walls are small compared with the attractive van der Waal's forces between gel sheets and hence volume change on moisture movement is also small.

Shrinkage is greater when zeolitic or gel pore water is removed because of the close proximity of gel particles. Pressure produced in the pore water acts against the van der Waal's forces between particles. When this water is removed the attractive forces pull the gel particles closer together thus producing shrinkage.

The effect of evaporable water content on creep is explained as follows:

When a porous, fluid-containing body is loaded, pressure differences are set up which induce flow of liquid within the body at a rate depending on the diameter of voids and friction between liquid and solid. If the voids are empty, the body tends to deform elastically. The presence of fluid introduces a non-linearity of displacement rate, but the final displacement is the same as without fluid. In a saturated body, initial loading causes the voids to act as rigid spheres. Stress gradients cause the water to flow and stress is gradually transferred from liquid to solid. Flow stops when all stress is carried by the solid. This is the asymptotic limit to which creep tends. A rheological model for this process is illustrated in figure 2.1.

At a near saturated condition as exists during curing or shortly thereafter, rate of creep is high and is not proportional to water content, since all types of evaporable water are present, particularly low viscosity capillary water. As water is removed, creep rate diminishes rapidly since most water removed at this stage is capillary water. Once all capillary water is removed, gel water will leave. This water is more viscous and hence creep rate is further reduced and is more linear.

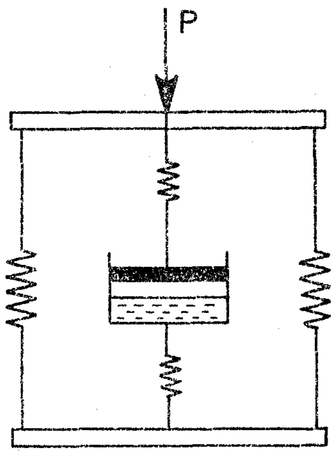

FIGURE 2·1 Rheological model for creep.

2.3 Factors Affecting Creep

Neville(19) has written an extensive summary of the affects of constituents, proportions, curing, storage, section dimensions, loading, temperature, humidity, and stress level on creep and shrinkage. His work indicates the enormous complexity involved in creep problems and the necessity of isolating specific variables in order to find useable solutions.

Lyse(15) also investigated the effects of stress level on creep and presented an empirical method for relating sustained load and cement content of the mix with creep and shrinkage.

Ross(20) studied creep under a stress gradient and presented an evaluation of methods for computing creep strains for increasing and decreasing stresses. The work of Ross is mentioned in more detail in Chapter 7.

2.4. Investigations of Creep in Structures

Considerable work has been done on the affects of creep on concrete components and structures.

A number of investigators have studied the effects of sustained load on slender reinforced concrete columns. In 1958, Gaede(9) tested pin-ended columns under sustained eccentric load and compared experimental results with a theoretical prediction based on the work of Krieg(13). Gaede noted a definite decrease in the buckling strength of columns as a result of creep.

In 1964, Breen and Ferguson(2) investigated the effects of sustained load on columns in a closed rectangular frame and found that, for the case studied, the increase in concrete strength during the time under test more than balanced the detrimental effects of the increased column deflection due to creep. A similar test by Furlong and Ferguson(8) indicated an overall decrease in strength due to creep.

In 1966, Manuel and MacGregor(17) investigated creep of restrained long columns analytically and compared their predicted results with the experimental findings of Green(12). Manuel and MacGregor presented a method of analysis for columns in frameworks which applied discreteness to cross-sections, member lengths and duration of sustained load. They also utilized numerical integration and iterative techniques to obtain framework equilibrium configurations. Good correlation was obtained between their analysis and the experimental findings of Green.

Drysdale(5) performed tests on slender pinned-end columns under sustained eccentric loading for uniaxial and biaxial bending.

He developed an analytic procedure using numerical integration, sectioning and iterative methods. The present study utilizes the work of Drysdale on concrete stress-strain formulation, shrinkage and creep under varying stress.

In 1968, Lehman[14] presented test results on the short-term behaviour of long columns in frames subjected to sidesway, and showed that elastic distribution of moments gave poor correlation with experimental data beyond working loads. A series of tests on model frames both single and two-bay provided considerable data on concrete frame action. The single bay frames tested by Lehman were approximately two feet square with column section $2\frac{1}{2}'' \times 2\frac{1}{2}''$ and beam section $2\frac{1}{2}'' \times 3\frac{1}{2}''$. Longitudinal reinforcement consisted of four number 2 bars. The large variety of data included load-moment interaction curves, frame deflections, variation in reactions with loading and crack propagation. Ball joints were used to provide a pinned-end support for the columns.

Chapter 3

FRAME SELECTION, FABRICATION AND MATERIALS

3.1. The Concrete Frame

In selecting a test frame a number of factors were considered. These included the size, the end conditions, the loading, the cross section, and the material properties.

The size of the frame was limited by the dimensions of the lateral loading bay used for sustained load tests. The largest frame which could be accomodated easily, with allowance for loading systems and instrumentation, was about ten feet wide. Since the anchor bolt holes in the test floor were spaced on three foot centres, it was decided to locate the columns nine feet apart. The final outside dimensions of the frame were 9' - 0 in height by 9' - 8 in width. By using a large scale model it was hoped that errors due to dimensional tolerances could be minimized and that the frame behaviour would be indicative of that encountered in engineering practice.

It was decided to use fixed column bases. Since one phase of the objective of the investigation was to study moment redistribution under sustained load, fixing the bases provided the maximum number of high moment regions at which changes could occur. Also, with rigid bases, two more plastic hinges were required for collapse in sidesway, and hence the amount of information on plastic deformation in concrete gained from each frame was increased.

The loading arrangement was designed to simulate both lateral and gravity loads on the frame. In order to simplify the loading systems required, point loads were used. One point load was applied horizontally at the top of the left column. A vertical point load of twice this magnitude was applied at midspan of the beam.

The member cross-sections were selected on the basis of providing realistic loads for the frame size. The same section was used for the beam and columns in order to simplify construction of the reinforcing cage and to provide approximately the same moment capacity at each hinge location. The section dimensions were 8 inches by 8 inches. Longitudinal reinforcement was provided by four number six bars, spaced on a square pattern with one inch cover from each face. This provided an under-reinforced section with the percentage of tension steel 1.66%. The cover was considered sufficient to provide bond between the concrete and steel. Use of an under-reinforced section was consistent with normal design procedure.

For the purpose of analysis, the properties of the concrete and reinforcing steel had to be known. Steel with a stress-strain relationship as close as possible to the ideal elastic-plastic case was required.

3.2. Concrete

The concrete mix used, as shown in Table 3.1., was identical to that used in the University of Toronto column test series,(5) and in other concrete work at McMaster. Cylinder test results were included in Appendix A.

Twelve cylinders and either two or three shrinkage prisms were cast with each frame. One of the prisms contained reinforcing identical to that of the frame, while the other was not reinforced.

Concrete components were prepared by weight and mixed in a horizontal drum mixer in batches of about six cubic feet. A slump of $2\frac{1}{2}$ to $3\frac{1}{2}$ inches was sought. Three lifts were required to cast the frame, prisms and cylinders; and these were placed in such a manner as to provide uniform layers of concrete throughout all the specimen.

The forms were overfilled to allow the layer with excess moisture to be trowelled off. The concrete was allowed to set for one hour before surface finishing. Demec gauge points as described in Section 4.2.3. for shrinkage measurement were cast in the concrete of the prisms.

The sides of the forms were removed eighteen to twenty-four hours after pouring. Then the specimen were moist cured on the casting bed using damp burlap for seven days before being moved to the test areas. The frame for sustained load testing was placed in a controlled atmosphere tent and was maintained at $75^{o}F$ and 50% relative humidity for the balance of the test period. The short-term frames were moist cured in their test position for an additional seven days. All frames were loaded twenty-eight days after casting. Cylinder tests were performed at seven, fourteen and twenty-eight days; and at the conclusion of testing for the sustained load frame.

TABLE 3.1.

CONCRETE MIX DATA

COMPONENT	PERCENT BY WEIGHT	WEIGHT PER BATCH
Portland Cement Type I	14.0	127.4
Water	9.1	82.6
Fine Aggregate (washed pit run sand, fineness modulus = 2.51)	46.6	424.0
Coarse Aggregate (3/8" maximum size crushed limestone)	30.3	275.5
	100.0	909.5

Slump for standard 12 inch high slump cone = $2\frac{1}{2}$"
Volume per batch = 6.0 cubic feet (approx.)

3.3. Reinforcing Steel

The stress - strain relationship for representative samples of the reinforcing steel was included in Appendix C. The behaviour was ideally elastic-plastic up to a strain of 0.005. Then strain hardening caused stress to increase with strain.

Local heating with an acetylene torch was used in bending the longitudinal steel for the first cage. Bending of the bars was accomplished by gripping a section with two pipe wrenches and then turning one wrench to produce a 90^{o} corner. A very small radius of curvature resulted. Because of brittle failure of the reinforcement during the first frame test, a number of tensile tests on reinforcement subjected to various degrees of heat treatment were performed. The results of these tests were presented in Appendix C. It was concluded that although the heat treatment used in bending the bars for the cage did not likely affect the strength of the steel or its behaviour, the deformation caused by bending around a small radius could have produced micro-cracks on the tension side of the corner. This condition was probably the cause of the premature failure.

From the heat treated tensile specimen, the yield strength of the reinforcing steel was found to be 59,800 ± 500 psi, and the ultimate tensile strength was 109,500 ± 700 psi. These strengths applied to steel bars heat treated in a manner similar to the conditions imposed during bending of the reinforcing for the frame corners. A series of bars were bent 45^{o} and then straightened. Tensile tests on some of these produced strengths close to those above, while others fractured at considerably lower stress levels. It was concluded that the micro-cracking caused by bending around a small radius rather than the heat treatment was responsible for premature steel failure in the frame.

Further tensile tests were performed in order to determine the yield strength, ultimate strength, and modulus of elasticity of non heat treated number six bars. The results of these tests were: yield strength 59,000 ± 500 psi, ultimate strength 108,500 ± 1700 psi, and modulus of elasticity $(29.6 \pm 0.6) \times 10^6$ psi. The stress-strain curve presented in Appendix C was based on this series of tests.

3.4. Forms

The forms for casting frames are shown in Figure 3.1. They were constructed of nine inch angle sections bolted to a plate back which was drilled to accomodate a number of specific section depths. In order to provide a section width of eight inches, a one inch thick plywood bottom was placed in the forms.

The forms were designed to accomodate a single bay or two bay frame. By using vertical plywood inserts, they could be used to cast columns, beams or prisms.

The steel forms provided durability, strength, and accuracy. The allowable dimensional tolerance was ± 1/8 inch. They could be easily cleaned and produced a smooth surface finish on the concrete. Each section of the forms was light enough that it could be handled by two men.

3.5. Cage

With the exception of the bars for the first cage, mentioned in Section 3.3., the number six bars which made up the longitudinal reinforcing were bent cold around a five inch diameter pipe. Continuous bars were provided from the base of one column around the frame to the base of the other column. Plywood templates were used to hold the bars on $5\frac{1}{4}$ inch centres until the stirrups were installed.

Stirrups were fabricated from plain $\frac{1}{4}$ inch diameter bars using the bar bending device shown in Figure 3.2. to a tolerance of ± 1/16 inch. Spacing of the stirrups was 6 inches in the columns and 3 inches in the beam. Wire ties were used to fasten the stirrups to the longitudinal reinforcing. In this manner the steel was located accurately and the cage was strong enough to be handled as a unit. The corners were made extremely stiff by the inclusion of additional reinforcing as shown in Figure 3.3.

3.6. Fabrication

Prior to installation of the cage, the forms were lubricated with mineral oil. The cage was held in position in the forms by small spacers fabricated from $\frac{1}{4}$ inch diameter bars.

For attaching the frames to the test floor, steel bases were fabricated from 8 inch wideflange sections. These were 8 inches long with four holes drilled through the webs to accomodate the longitudinal reinforcing.

The bases were placed in the forms at the correct locations so that the flanges would be in line with the inside and outside surfaces of the columns. Then the reinforcing bars were cut off so that they protruded about $\frac{1}{2}$ inch through the web. The reinforcing was welded to the wideflange on both sides of the web. The column bases were stiffened up to the edge of the wideflange flanges by welding hooks made from number three bars to the web and by welding cross-ties between the flanges.

FIGURE 3.1. FORMS

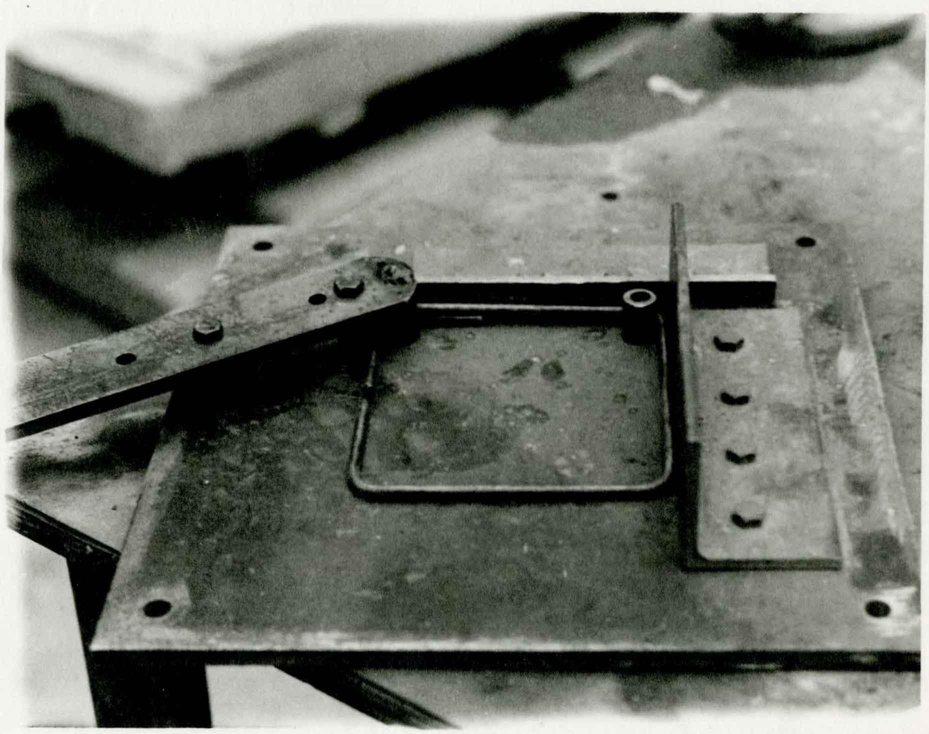

FIGURE 3.2. BAR BENDER

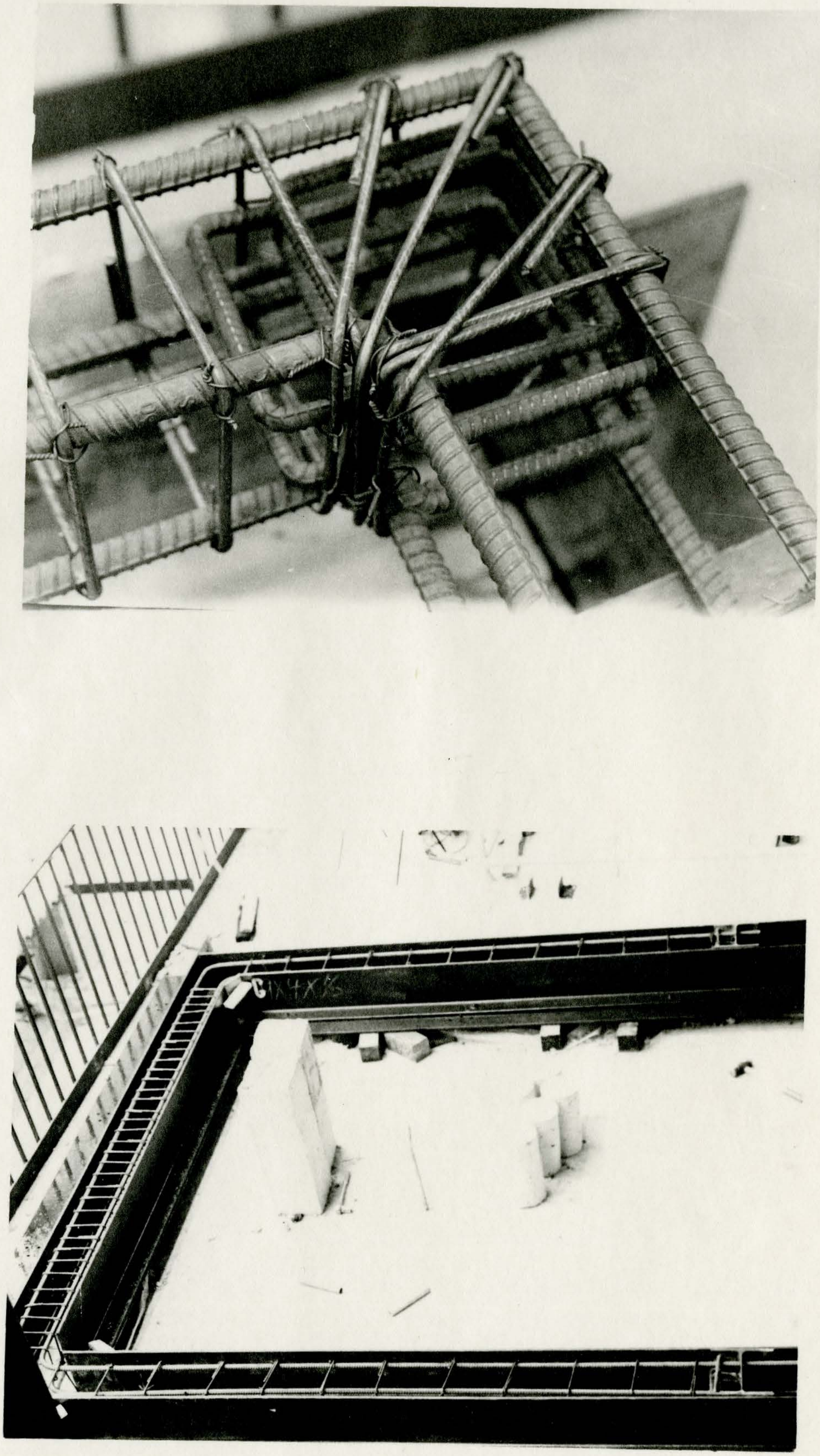

FIGURE 3.3. REINFORCING CAGE

Chapter 4

TEST APPARATUS

4.1. Introduction

Two separate sets of apparatus were used. The first was designed for short-term loading. The second was designed to provide a means of maintaining a sustained load on the frame over a long period of time. Several components of the test equipment were similar for both tests.

4.2. Instrumentation

4.2.1. Bases

Rigid bases were constructed as shown in Figure 4.1. Originally, the bases were designed so that the reactions could be measured using electric resistance strain gauges. These bases were to be stiff enough to resist significant motion of the concrete column bases while undergoing sufficient strains so that the reactions could be determined to a reasonable degree of accuracy.

Horizontal strain was registered by a cantilevered section held rigidly at one end and supported on rollers along its length. Several designs were attempted, the final choice being a solid steel block three inches high, eight inches wide and sixteen inches long. Between the rigid support and the concrete column base, a section of this block was machined out leaving an upper and lower flange each one quarter inch thick. On these flanges, electric resistance strain gauges were mounted to monitor horizontal strain of the base. By considering equilibrium of forces through this section, the moment and horizontal reaction could be determined. The large mass of this section was to absorb heat from welding the vertical portion of the base in place so that warping could be avoided. The rigid end connection was provided by two rows of ½" diameter bolts which connected the horizontal block to the one inch thick lower base plate.

Vertical strain was registered by electric resistance gauges mounted on the wideflange column bases described in Section 3.6. The gauges were mounted at half the distance from the web to the outside of the lower flanges. From them, the vertical reaction and moment at this section could be determined.

Base rotation was considered acceptable if it did not cause a reduction in base moment greater than 15% of the fixed end moment. Despite considerable refinement, rotation of the bases described above could not be restricted to tolerable levels. Since most rotation occurred in the cantilever block, the means of correction used was to fasten it rigidly to the lower base plate. This was accomplished by welding stiffening plates between the cantilever block and the base plate. Although this alteration greatly restricted rotation, it made it impossible to use the strain gauge readings from the horizontal block to determine the horizontal reactions.

The lower base plate was stiffened with eight inch channel sections as indicated in Figure 4.1. The entire assembly was bolted to the test floor using two 2 5/8 inch diameter anchor bolts which were prestressed to sixty kips.

For the short-term tests, the arrangement of anchor bolt holes in the test floor and the location of other testing apparatus made it necessary to mount the bases with their stiffer axes at right angles to the plane of loading of the frame. This configuration also placed the anchor bolts very near the axis of rotation for each column. For the sustained load tests, the bases could be positioned with their stiff axes parallel to the plane of the frame. Hence, greater support rigidity was obtained in the sustained load tests.

4.2.2. Dial Gauges

Frame deflections were recorded by dial gauges mounted on a framework as shown in Figure 4.3. This system was fastened directly to the test floor and was independent from the load system or frame supports. Dial gauges were also used to record movement and rotation of the column bases.

4.2.3. Demec Strain Measurement

Concrete strains were measured using a Demec gauge, a mechanical device with an eight inch gauge length.

The gauge points used to indicate strains consisted of ¼" diameter brass discs drilled with a number 60 centre hole. These were attached to the frame with sealing wax or epoxy cement. Demec points were placed for two gauge lengths at the base and top of each column, at each end of the beam, and to either side of the centre of the beam. At each location, they were installed 3/8" from the compression face, 2" from the compression face, and at the level of the tension steel.

From the Demec readings in the compression zone, the strain distribution at a section was determined as an average over the gauge length.

Using the Demec gauge, it was possible to repeat readings to ± 5 microstrain. The precision of strain determination was limited by the accuracy in location of the gauge points, by creep in the wax or cement, and by cracking of the concrete. These errors are discussed in more detail in Chapter 9.

4.2.4. Load Cells

Loads were measured using a variety of load cells. Although they varied in size and physical appearance, these were all similar in principle and function.

The load cell usually was a spool-shaped steel cylinder with four electric resistance strain gauges, two vertical and two horizontal, mounted on its outside surface midway between the ends. These gauges were wired as a full Wheatstone bridge and therefore were temperature compensating. Strains were registered by a switch and balance unit and a Budd Model P-350 strain indicator. The strain gauges on the load cell were protected by a wax coating.

Most of the load cells were prepared by lathe turning and centre boring round steel stock. They were sized so as to provide the full loads required for strains in the elastic range (usually between 300 and 700 microstrain). In one case, the piston of a hydraulic jack was used as a load cell by mounting strain gauges on it.

Prior to each test, the load cells were calibrated in a Tinius-Olsen universal testing machine. Loads and strains were recorded in increments up to the maxima required. Readings were made for several cycles of increasing and decreasing loads. Any load cell for which readings could not be repeated was discarded. Graphs relating applied loads to measured strains were prepared for use during frame tests.

After each test, the load cells were immediately re-calibrated.

4.3. Short-Term Test Apparatus

The concrete frame was transported from the casting area by overhead crane, and was positioned on the bases. Then the eight inch wideflange column ends were welded to the lower base assembleges.

Two fourteen inch wideflange columns were mounted on the test floor, one on each side of the frame at the centre of the beam as indicated in Figure 4.2. The anchor bolts for these columns were prestressed to 60 kips. The vertical load mechanism was placed between the columns using channel cross-members. This load system consisted of a 50 ton hydraulic jack mounted on a mechanical slide which allowed 8 inches travel from the centre of the beam in the direction of sidesway. The jack for the vertical load system had a six inch stroke, but because the piston was used as a load cell, only three inches of this could be utilized in loading. This jack was of the push to load, spring return type. Load was transferred to the frame through a ball joint and a set of three 3/4" diameter roller bearings placed on the beam.

A fourteen inch wideflange column was placed at one end of the frame to accomodate the horizontal load system. The jack for this system was of the push-pull type and had a nine inch stroke. It was mounted on a mechanical slide which allowed vertical travel up to 8 inches. Load was transferred to the frame through a load cell and ball joint.

4.4. Long Term Test Apparatus

4.4.1. Introduction

For the long term test it was necessary to maintain a constant load on the frame for a long period of time. Springs were used to store the energy required to accomplish this. The other primary requirement for the sustained load study was the preservation of constant temperature and humidity.

4.4.2. Controlled Atmosphere Tent

The long-term test was performed inside a polyethylene controlled atmosphere enclosure located in a lateral loading bay of the Applied Dynamics Laboratory. This "tent" had a floor area approximately eighteen feet square and a height of fifteen feet. On three sides there were walls fitted with vertical wideflange sections which could be used to apply horizontal loads.

It was desired to maintain a constant temperature of 75°F and a humidity of 50% during testing. To accomplish these requirements, the tent contained a humidifier, a dehumidifier, two electric heaters, and four fans. The atmospheric conditions were controlled by two thermostats mounted on opposite walls, and by a humidistat. These instruments were electronically coupled to the appropriate equipment.

Because there was no cooling system in the tent, it was impossible to control temperatures over 75°F as encountered during the summer months, but sustained periods of high temperatures were not encountered during the long-term test which commenced on September 13th. Relative humidity was adequately controlled except for occasional periods, particularly during the transition from hot, humid summer weather to cooler dryer winter conditions. During the sustained load test, the average daily humidity maximum was 50.44% with a standard deviation of 0.66%. The average daily minimum humidity was 48.22% with a standard deviation of 1.38%. The average daily temperature was 75.0°F with a standard deviation of 1.5°F.

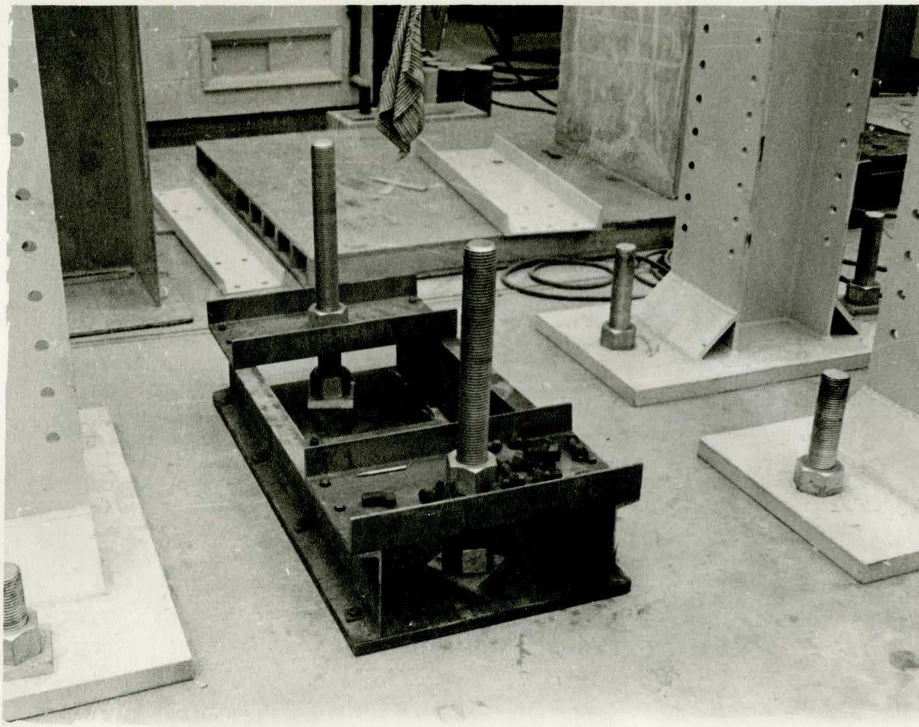

FIGURE 4.1. COLUMN BASES

FIGURE 4.2. SHORT-TERM TEST APPARATUS

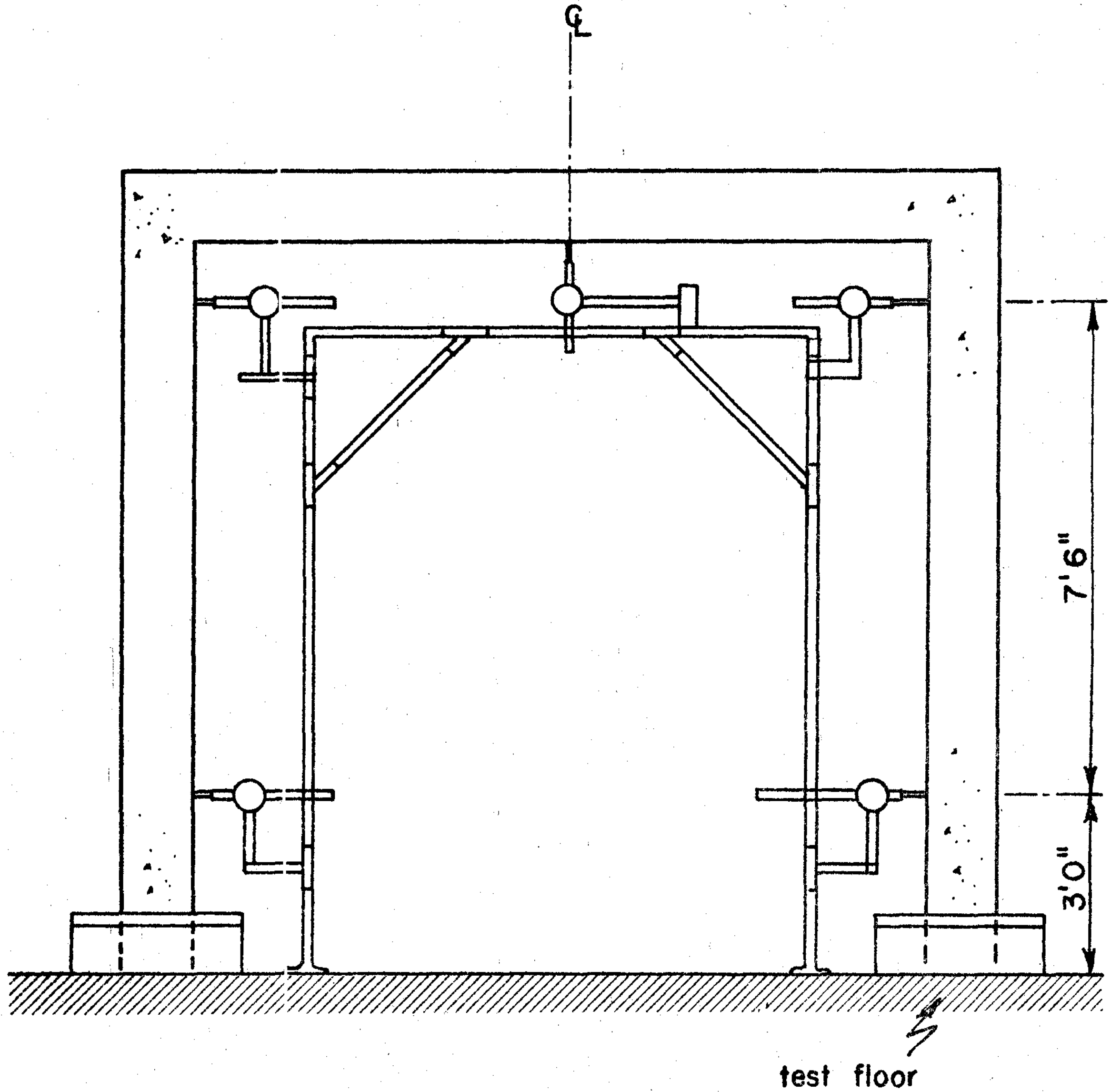

FIGURE 4·3 Dial gauge framework.

4.4.3. Sustained Load Systems

The sustained load mechanisms were as shown in Figure 4.4. Both the systems utilized coil springs to maintain loads on the frame.

4.4.3.1. Springs

The spring specifications called for a low spring constant so that frequent adjustment of the loads would not be required. As supplied, the vertical load springs were each guaranteed to deliver 4,900 pounds of force at a three inch deformation. This provided a spring constant of 1633 pounds per inch at the given load. The horizontal load springs were each guaranteed to deliver 1600 pounds at a deformation of three inches.

4.4.3.2. Vertical Load System

The four vertical load springs were stressed by pulling downward on four tension rods which extended from a plate on top of the springs to a base bolted to the test floor.

The base consisted of a rigid box with a slide plate located under the top. The tension rods passed through the top of this box and the slide plate. Both ends of the tension rods were threaded to accomodate adjusting nuts. The slide plate was held against the underside of the top of the box by nuts on the tension rods.

A one inch thick plate was supported by the tension rods about 1' - 2" below the top of the box. On this plate, a 50 ton hydraulic jack was placed to load the springs. Load was applied by jacking against the top of the box, thereby pulling downward on the tension rods and compressing the springs. With jacking pressure applied, the nuts holding the tension rods against the slide plate were tightened

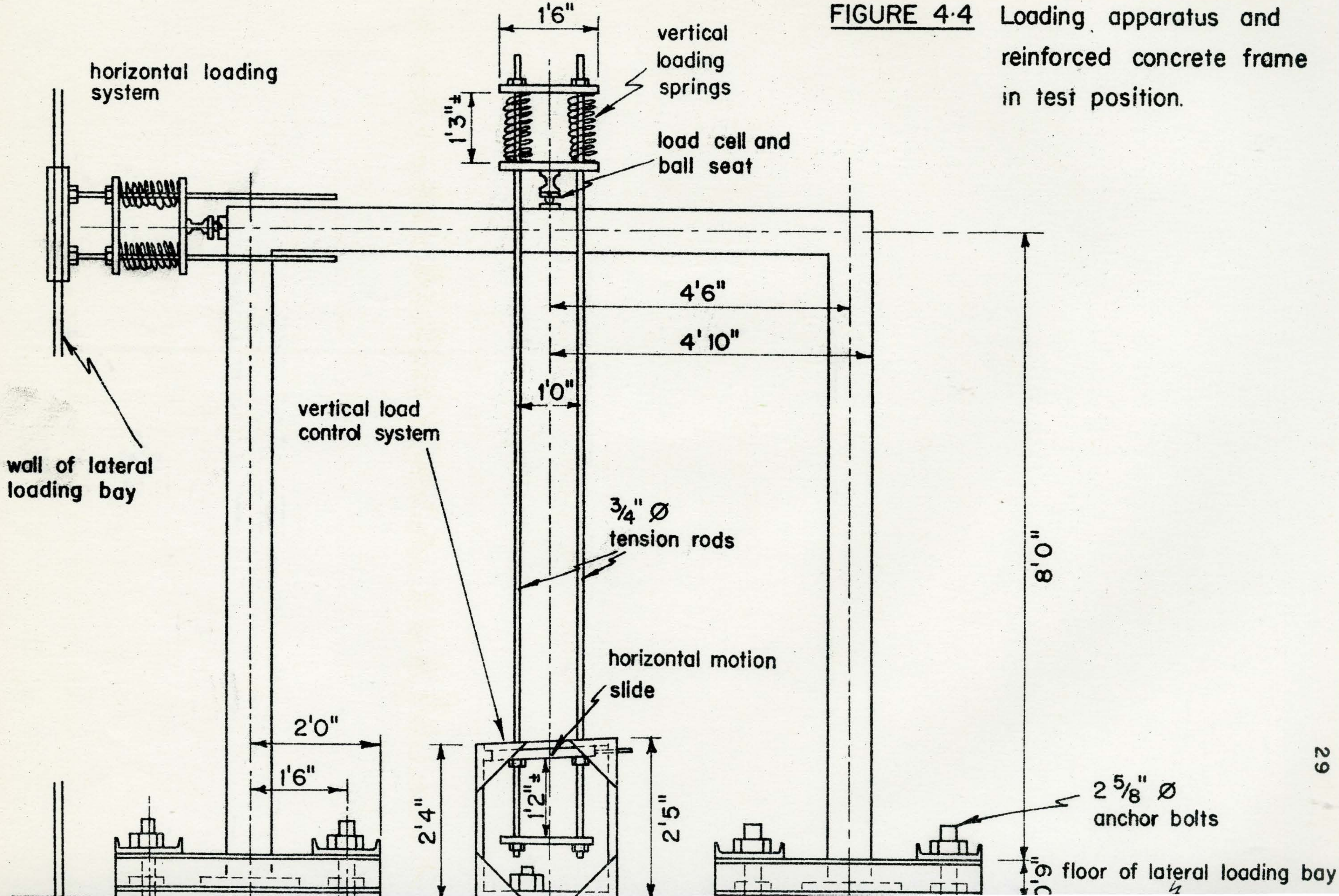

FIGURE 4·4 Loading apparatus and reinforced concrete frame in test position.

thus maintaining the displacement of the springs. Then the jack was removed. The decrease in load caused by deflection of the concrete beam with time was corrected by adjusting these nuts. Loads were not allowed to decrease by more than 2% without adjustment. Making this correction once daily was usually sufficient.

The underside of the top of the box and the upper surface of the slide plate were machined to a smooth finish and were lubricated with graphite. The load was kept vertical by moving the slide plate. This was accomplished by turning a nut which rested against the side of the box on a threaded shaft that passed through the side of the box and into the slide plate. Horizontal movement of the slide plate was assisted by an upward inclination of the top of the box of two degrees in the direction of motion. The coefficient of friction of the machined and lubricated surfaces was about 0.16. The slide plate allowed horizontal motion up to eight inches.

The working capacity of the vertical load system was thirty kips.

4.4.3.3. Horizontal Load System

The horizontal load system was mounted on one of the wideflange columns of the lateral loading bay. Four 3/4" diameter rods were threaded into a one inch thick plate which was clamped onto the flanges of the column at the required elevation. The rods were threaded throughout most of their length. They passed through a one inch plate about fourteen inches from the wall. This plate rested against nuts turned onto the wall side of the rods. The horizontal load springs were placed between this plate and another which bore on the frame through a load cell and ball joint. Load was applied to the springs by turning the adjusting nuts. Although it was not required, a hydraulic jack could have been accomodated between the wall and the spring retainer plate.

The working capacity of the horizontal load system was fifteen kips.

Chapter 5

TEST PROCEDURES AND GENERAL OBSERVATIONS

5.1. Introduction

In this chapter, the test procedure is described for each of the frame tests performed. Some observations of the general behaviour are included.

5.2. Frame R1

5.2.1. Introduction

The first frame was used in a preliminary test to evaluate the apparatus, instrumentation and procedure.

5.2.2. Test Procedure

The test procedure consisted of incrementing the horizontal and vertical loads proportionately to predetermined levels up to collapse. At each load stage, readings were made on the base electric resistance guages, the Demec points, and the dial gauges. Crack formation in the frame was also noted. Collapse was defined by the inability of the frame to sustain a further increase in load. This was indicated by the formation of a sufficient number of plastic hinges to form a mechanism. A hinge was said to have formed when the strain at the level of the tension steel exceeded yielding. Crushing of the concrete at the compression face denoted the limit of the constant moment relationship for the section. The order of formation of hinges was recorded as well as their location.

5.2.3. Observations

It was observed that the base rotation encountered was considerably greater than tolerable. Also the electric resistance strain gauges on the bases yielded conflicting readings which could not be used. A third problem concerned the lack of stiffness in the corners and the method of bending of the reinforcing. The longitudinal bars of this frame had been hot deformed and hence were subject to tensile cracking as mentioned in Chapter 3. Also there was no additional reinforcing included to stiffen the corners. Because of these conditions, the first hinge occurred in the corner between the beam and unloaded column.* Cracks proceeded diagonally across the corner from the outside and at a horizontal load of 8200 pounds and a vertical load of 16,400 pounds, the tension steel in the corner fractured. Final collapse occurred without appreciable increase in load by the failure of one of the welds holding the frame to the horizontal cantilever section of the base.

5.2.4. Resulting Modifications

As a result of this test, the following changes were made in subsequent frames:

(1) Electric resistance gauges were attached to the bases using heat cured epoxy rather than contact cement in an attempt to improve strain measurements.

(2) Longitudinal reinforcing was bent cold around a five inch diameter pipe rather than hot bending as performed previously. This was done to avoid cracking and brittle fracture of the steel at corners.

(3) The corners of the frame were stiffened by the addition of extra reinforcing to improve frame behaviour and simplify analysis.

---

* The column at which the horizontal load is applied is referred to as the loaded column or the left hand column. The right hand column is also referred to as the unloaded column.

(4) The horizontal cantilever part of the steel bases was redesigned to provide greater resistance to rotation.

5.2.5. Conclusions

As well as indicating problem areas in the model, this test provided an opportunity to develop procedures for loading and retrieving data from the frames. The jacking method which required constant monitoring of independent hydraulic systems during loading, worked well as did the load cells and ball joints. It was found that the screw mechanism of the slide on the vertical load system could be operated rapidly enough to keep the load over the beam centre during sway; however, the threaded block on the slide was not strong enough near ultimate load. This problem was later corrected by manufacturing a stronger slide. The demec points and the epoxy used to mount them performed well throughout the test as did the dial gauges.

5.3. Frame L1

5.3.1. Introduction

The sustained load test incorporated the modifications recommended as a result of the first short term test. These changes included corners stiffened with additional reinforcement, electric resistance gauges mounted using heat cured epoxy, improved bases which utilized a cantilever section of solid three inch thick steel, and cold deformed reinforcement.

5.3.2. Test Procedure

The first phase of the test consisted of short-term loading to a horizontal load (H) of 6.0 kips, and a vertical load (V) of 12.0 kips. From an approximate solution using the mechanism method of plastic analysis, the ultimate loads were predicted to be H = 11.0 kips and V = 22.0 kips. Analysis using slope-deflection equations indicated that the first hinge would occur at a horizontal load of 9.5 kips. Hence the applied loads (H = 6.0 kips, V = 12.0 kips) represented about 55% of ultimate load or 63% of the load required to form the first hinge; therefore, this could be considered a working load level.

The above load level was maintained until creep deformations became nearly static. After 53 days, the loads were increased to H = 7.5 kips and V = 15.0 kips (68% of predicted ultimate or 79% of the load required to form the first hinge). This new level was held for an additional 28 days, then the frame was quick loaded by increments to failure.

5.3.3. Observations

The first hinge formed at the upper right hand corner (the top of the unloaded column) at loads of H = 11.0 kips and V = 22.0 kips. This was followed almost immediately by a second hinge at the centre of the beam. As the loads were increased further, severe deformation occurred. At loads H = 12.6 kips and V = 25.2 kips, a third hinge formed at the right base (the lower end of the unloaded column). With further jacking, the loads dropped back gradually to H = 12.0 kips and V = 24.0 kips. The last hinge formed at the left base. Subsequent jacking caused the loads to decrease continuously.

Based on the test results, the first sustained load level represented 47.5% of final ultimate load or 54.5% of the load required to form the first hinge. The second sustained load level represented 59.5% of ultimate load or 68.2% of the load required to form the first hinge.

During the initial short-term loading phase, the column bases underwent severe rotations due to distortion of the thin part of the cantilever. The loads were removed and plates were welded between the sides of the cantilever and the bottom base plate. This restricted the rotations to an acceptable level (a maximum of 0.005 radians at ultimate load and 0.001 radians at the second sustained load level). However, welding the cantilever block down prevented use of the electric resistance gauges mounted on it. But, despite the use of heat-cured epoxy, the other electric resistance gauges still yielded conflicting results, so that the loss of the horizontal cantilever instrumentation was not a severe loss in itself.

5.3.4. Resulting Modifications

As a result of frame test L1, the following changes were made in the system:

(1) Electric resistance strain gauges were omitted from the basis since they did not previously produce useable readings.

(2) The steel column bases were welded directly to the lower base plate since use of the cantilever block had allowed too much rotation.

5.3.5. Conclusions

Despite the above mentioned difficulties, other facets of the system such as the load cells, springs, Demec points, and dial gauges performed well.

The detailed results of frame test L1 are presented in Chapter 8.

5.4. Frame R2

5.4.1. Introduction

The second short-term test was performed without the horizontal cantilever blocks on the bases. The wideflange column bases were welded directly to the lower baseplates. Also, the electric resistance strain gauges were omitted.

Frame R2 also incorporated the improvements made in frame L1, such as stiffened corners and cold-bent longitudinal bars.

5.4.2. Procedure

The procedure for this test was the same as that used for frame R1. Loads were applied proportionately to collapse, with strain and deflection readings taken at various levels.

5.4.3. Observations

According to Demec readings, the first hinge formed in the upper right hand corner (the top of the unloaded column) at H = 9.0 kips and V = 18.0 kips. Spalling occurred at the inside corner and severe cracking extended to both the top of the beam and the outside of the column, with the result that, although the actual corner block remained rigid, it was impossible to determine whether the actual hinge occurred primarily in the beam or in the column. After additional deformation due to jacking, but with no measurable increase in load, the second hinge formed at the centre of the beam. Formation of this hinge resulted in crushing of the concrete adjacent to the metal loading plate. At H = 11.0 kips and V = 22.0 kips, the third hinge formed at the right base.

Finally, at H = 11.5 and V = 23.0, the ultimate capacity of the frame was reached. Completion of the collapse mechanism by formation of the final hinge at the right base occurred following continued deformation, during which the applied loads decreased slightly.

After the development of the mechanism, the load carrying capacity of the frame decreased continuously with increasing deformation.

As a result of this test, and the others in the series, further modifications were proposed for future frames. These are discussed in Section 10.2.

5.4.4. Conclusions

As in the case of frame R1, the column bases were mounted with their stiff axes at right angles to the load plane, and the anchor bolts almost on the axes of rotation. Thus, although rotation was greatly improved as compared to that encountered during test R1, it was much more severe than that which occurred during test L1 which was performed in the tent with bases aligned in the direction of loading. Rotation of the right base reached 0.01 radians at H = 11.0 kips and V = 22.0 kips, while the left base had turned through 0.0047 radians at the same load level. From an elastic analysis a rotation of 0.001 radians was found to cause a reduction in moment at the right base of about 3%. Hence, prior to formation of the hinge at the right base, the moment was expected to be up to 30% lower than that which would have occurred if the base had been completely rigid. For a rigid base, elastic solution predicted the third hinge to form at 92.5% of ultimate load, indicating the effect of rotation. It was felt that the elastic reduction factor overestimated moment decrease substantially at these high load levels. This was confirmed by the result that formation of the expected mechanism occurred in a predictable manner despite fairly severe base rotations.

5.5. Sources of Error in Testing

5.5.1. Introduction

This section discusses a number of factors which affected the experimental results. These included the material properties, geometry and section variations, the behaviour of the bases, cracking of the concrete, and the loading systems.

(i) Concrete

The precision in knowing the actual concrete strength affected the analysis rather than the experimental results. However, the test data was influenced by variations in concrete properties at different locations, particularly since three batches were required to cast each frame. This error was minimized by pouring the frames in three lifts each of which provided a uniform layer of concrete throughout the entire frame, prisms and cylinders.

(ii) Steel

Since all of the steel was from the same heat, the strength of the bars was considered uniform. The behaviour caused by heat treating and severe bending encountered during frame test R1 was a major problem. However, the cold bending around a 5 inch diameter pipe used in subsequent tests eliminated brittle fracture. Stiffening of the corners also helped alleviate error caused by bending the reinforcement. It was felt that negligible error in testing was caused by the steel.

(iii) Geometry and Section Variations

Dimensional variations in the concrete section, frame positioning and location of the cage were sources of experimental errors. As mentioned previously in Chapter 3, the steel forms provided a tolerance in section dimensions of ± 1/8 inch. This allowed an error in concrete area of 3%, and a possible error in moment capacity of about 0.6%.

Using the bar bending device to fabricate the stirrups and by careful checking of dimensions, it was possible to keep the cage within a tolerance of ± 1/16 inch. This allowed a possible error in moment capacity of 1%.

(iv) Bases

Rotation and displacement of the steel bases were computed from dial gauge readings. The dial gauges recorded vertical and horizontal movement of the column bases relative to the test floor. The accuracy of most of the dial gauges was ± 0.0005 inches, but some had a precision of ± 0.0001 inches. Because the displacements were very small (usually 0.001 to 0.01 inches), the relative error was quite large. However, the effect on frame behaviour of these errors was not severe. The resulting error in base moments was about 2% at a load level of H = 6.0 K and V = 12.0 K.

(v) Cracking

Cracking of the concrete caused variations in stress distribution at various sections, particularly at high loads. Demec readings were severely affected by cracking in two ways. First, cracks in some regions loosened the concrete at the location of gauge points. Second, the variations in stress at different sections caused by cracking led to Demec readings which were not indicative of the strain which related to the average moment over the gauge length. However, since the strain computations were based on readings from the compression zone where cracking did not occur, only this second condition had any significant effect because of the influence of bond between the steel and concrete.

For analysis, the corners were considered rigid. Cracking in the corners affected the validity of this assumption. The extra reinforcing provided to solve this problem appeared adequate although cracking in the corners was not completely eliminated once hinges had formed.

(vi) Loading Systems

A possible critical source of error in testing involved use of the load cells. A faulty load cell would have meant that the load on the frame was not known correctly, and this could have led to a complete misinterpretation of results from the other instrumentation. Therefore, premature loading to failure or loading in the wrong proportions could have resulted. Although there was no way of directly checking the function of a load cell, the gauge pressure of each hydraulic jack was noted during short-term testing as a precaution. Immediately following a test, the load cells were removed and recalibrated without altering the balance setting of their strain gauges.

For the sustained load test, spring deflections of the loading systems were recorded to be used in the event of a load cell failure.

During this test series there was only one load cell failure. This occurred during initial loading of frame R1, and was revealed when the gauge pressure of the horizontal jack indicated disagreement with the load cell. The load cell was removed, recalibrated and found to be faulty. All other load cells performed well with strain differences always less than 1% for the full load range before and after each test.

5.5.2. Summary of Testing Errors

In summary, despite a large number of systematic errors, these were independent of each other, and hence were not cumulative in effect.

Every effort was made to control errors in the materials, dimensions, and systems for loading and instrumentation. Because the experimental errors were not large, most of the inaccuracy encountered would be due to the inability of the analysis to properly simulate the actual frame and/or materials. Discussion of these errors as applied to analysis is contained in Chapter 9.

Chapter 6

METHODS OF COMPUTING CREEP

6.1. Introduction

There are basically three methods for computing creep under varying stress. These are:

(1) the effective modulus method.

(2) the rate of creep method.

(3) the method of superposition.

All these procedures express creep as a function of time and stress only; therefore, all other influential factors have to be taken into account separately.

Expressions have been developed by L'Hermite[15] relating creep, shrinkage and humidity, and by Lyse[16] relating creep, shrinkage, stress and cement content of the concrete. Thus, it is possible to analyze situations involving a number of variables, but this develops into a very complex process. Attempts to inter-relate several creep influencing factors leads to confusing results which are difficult to separate as to cause and effect. Hence, it is advisable to question results obtained from investigations which did not control the variation of all boundary conditions. This is not because the data is invalid, but because it cannot be separated into relationships between creep and its parameters. The effects of most of these factors are sufficiently large that they cannot be ignored.

It is concluded that the most useful expressions relating creep, stress and time can be obtained by testing prisms of the same section properties as the structure in question. Sustained load should be applied to the prisms under conditions of constant temperature and humidity. From these tests, creep can be expressed as a function of time for a number of stress levels, using least-squares or other curve fitting techniques. A similar procedure may be used to correlate these curves to obtain creep as a function of time and stress.

This procedure was used by Drysdale[5] to develop expressions for creep as a function of time and stress level. Since a similar concrete mix and the same conditions of temperature and humidity were maintained it was assumed that these relationships could be used in the present investigation on frame behaviour. However, the section used in this investigation was eight inches square compared with a five inch square section used by Drysdale. For this reason, the creep expressions would tend to slightly overestimate the creep which occurred in the test frames.

The percentage of reinforcement used by Drysdale was greater than that used in the frame tests. For a given shrinkage strain, the stress in the concrete would be greater with more reinforcing. However, because of the greater restraint, it would be expected that less shrinkage would occur over a given time interval for the more heavily reinforced section. Upon loading, the specimen would be free to shrink, and shrinkage would be less for the larger section. Because of the interrelationship between creep and shrinkage, these factors would have some influence on the validity of the creep expressions, but this was not considered severe.

The creep-time expression used was linear with respect to the logarithm of time. It had the form:

$$C = -A + B \log_{10} t$$

where C was the creep strain, t was the time after loading, and A and

B were functions of stress determined by a least-squares fit of experimental data. This was similar to the expression $C = Bt^{1/A}$ presented by Shank[22].

6.2. Effective Modulus Method

This method requires calculation of the "specific creep" or the creep strain per unit stress. Since creep and stress relate linearly only up to 40 to 50% of ultimate strength, according to Ross[20], the specific creep is limited to working load studies.

The effective modulus method uses normal structural mechanics techniques, but replaces the elastic modulus Ec by a "reduced" modulus Ec^1 defined as follows:

$$Ec^1 = \frac{Ec}{1 + C_1 Ec}$$

In this expression, C_1 is the specific creep under one psi, at the appropriate time. Hence, both elastic and creep strains are included.

Although the reduced modulus method is easy to use, it is theoretically incorrect since it disregards stress history. Also it erroneously predicts a complete recovery of creep upon removal of stress.

6.3. Rate of Creep Method

The slope of the specific creep-time curve at any time t gives the rate of creep dc_1/dt. For a stress f, the increment of creep over interval dt is fdc_1. Hence, creep under variable stress after time t is:

$$c = \int_0^t f \frac{dc_1}{dt} dt$$

To some degree, this method includes stress history because it integrates incremental creep elements over the time of loading.

However, since fdc_1/dt is zero for zero stress, this method predicts no creep recovery upon unloading. Also stress history is not correctly included since this method does not consider previous stress levels, but merely assumes that the concrete will creep at the rate $f\ dc_1/dt$ regardless of how it was stressed at an earlier time.

Gray[11] used a similar procedure to predict creep under varying stresses, but instead of considering a constant rate of creep over a time interval, he developed an expression for creep as a function of time and elastic strain. Gray included previous stress history by the use of superposition of the effects of creep over discrete time intervals. This procedure became increasingly complex with the number of time intervals considered. The major limitation of this method was that it was developed only for the case where the entire section acted in compression.

6.4. Method of Superposition

This procedure involves superposing the creep strains for different stress levels at different times assuming stress remains constant over each time interval.

With reference to figure 6.1., consider a specimen loaded to stress σ_1, from time t_0 to t_1, and then loaded to stress t_2 from time t_1 to t_2. One part of the creep is taken as that which occurs from t_0 to t_2 under stress σ_1 when loaded at t_0. The other part is the creep due to σ_2 minus that due to σ_1 for the time interval $t_2 - t_1$ using creep curves for specimen loaded at time t_1. Total creep is the sum of the two components.

Although the method of superposition does not provide a general algebraic solution as do the other methods, it can be readily used in a numerical procedure, and it does take account of stress history. As presented above, this method predicts almost complete creep recovery on unloading. Also it overestimates creep for increasing stresses, and underestimates creep for decreasing stresses.

6.5. Modified Method of Superposition

Drysdale[5] presented a revised procedure which more accurately compensated for previous stress history.

This method assumed negligible error occurred through the use of constant stress creep curves to predict creep with a stress gradient. It was realized that this procedure would overestimate creep recovery upon removal of stress, but it was felt that since the stress change was gradual there would not be significant error.

In the present study, creep recovery could be important because of moment redistribution in the frame. Hence, despite the lack of experimental data, it was decided that some account should be taken for the amount of creep recovery. Based on test results presented by Ross [20], it was assumed that creep recovery would be two-thirds of the creep which would occur for a corresponding increase in stress. Although it is undoubtedly an oversimplified assumption, it was felt that it would yield a much more accurate result than provided by straight superposition, and hence would reduce the error in analysis considerably. Further study of the creep recovery phenomenon would be essential before attempting a more comprehensive solution.

The superposition method presented by Drysdale, utilized creep versus time curves for various values of "elastic" strain (the "elastic" strain being the equivalent short term cylinder strain). Creep equation parameters were strain functions obtained by a least-squares fit of experimental data. Because of lack of further results for the frame sections, and because of similarities between this test series and the University of Toronto column tests [5], the same expressions were considered adequate for use without serious error. The reason for using strain rather than stress in the creep expressions was that the increase in concrete strength and modulus of elasticity with time could be taken into account.

Figure 6.1. illustrates the method. Consider a specimen stressed to "elastic" strain Σ_1 from time t_0 to t_1 and Σ_2 from t_1 to t_2. The first part of the creep was that which would have occurred for an "elastic" strain Σ_1, for time interval t_0 to t_1. The second part, CREEP 2, was that which would have occurred for an "elastic" strain Σ_2 over time t_1 to t_2 with first loading at t_0.

The third part, CREEP 3, was that which would have occurred for elastic strain $\Sigma_2-\Sigma_1$, over time t_2-t_1, for a specimen loaded to that strain at t_1. Total creep over the interval was the sum of the three components.

Using this method, creep was computed as the sum of the strains which occurred over successive time intervals up to the time in question. Creep recovery was computed in the same manner but was reduced by one-third and was subtracted from the previous strains for increments in which "elastic" strains were reduced.

This method slightly underestimated creep for increasing stress. Its accuracy in following stress decreases was not known because of the constant factor used for creep recovery, but the error was not considered significant.

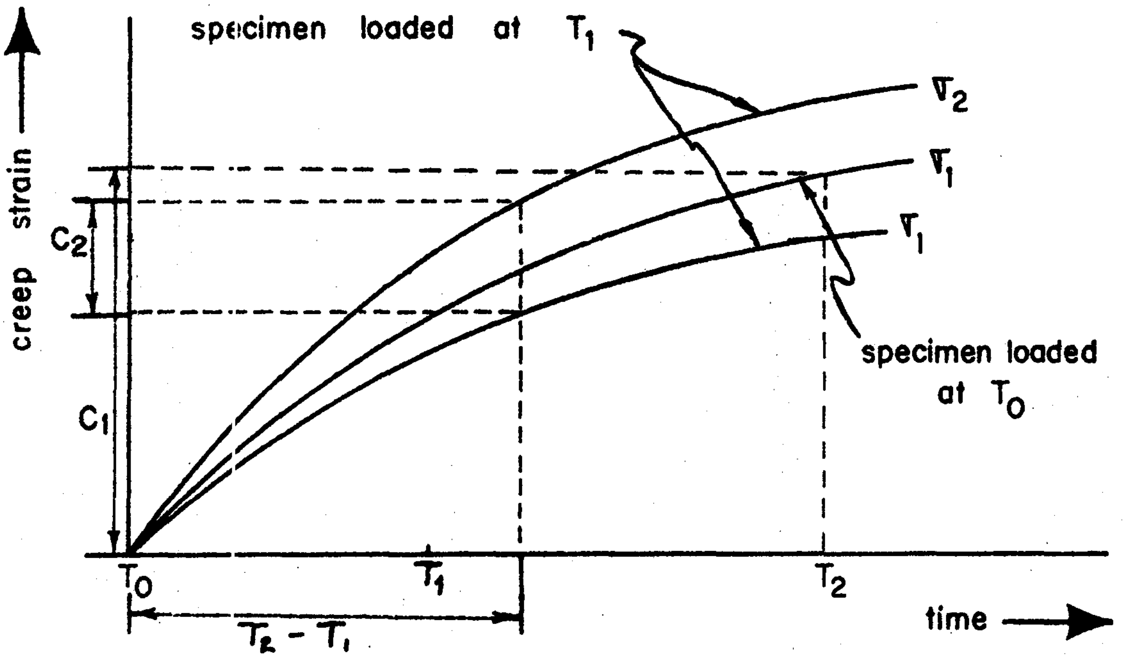

Specimen loaded to σ_1 from T_0 to T_1 and to σ_2 from T_1 to T_2

Total creep = $C_1 + C_2$ after time T_2.

Standard method.

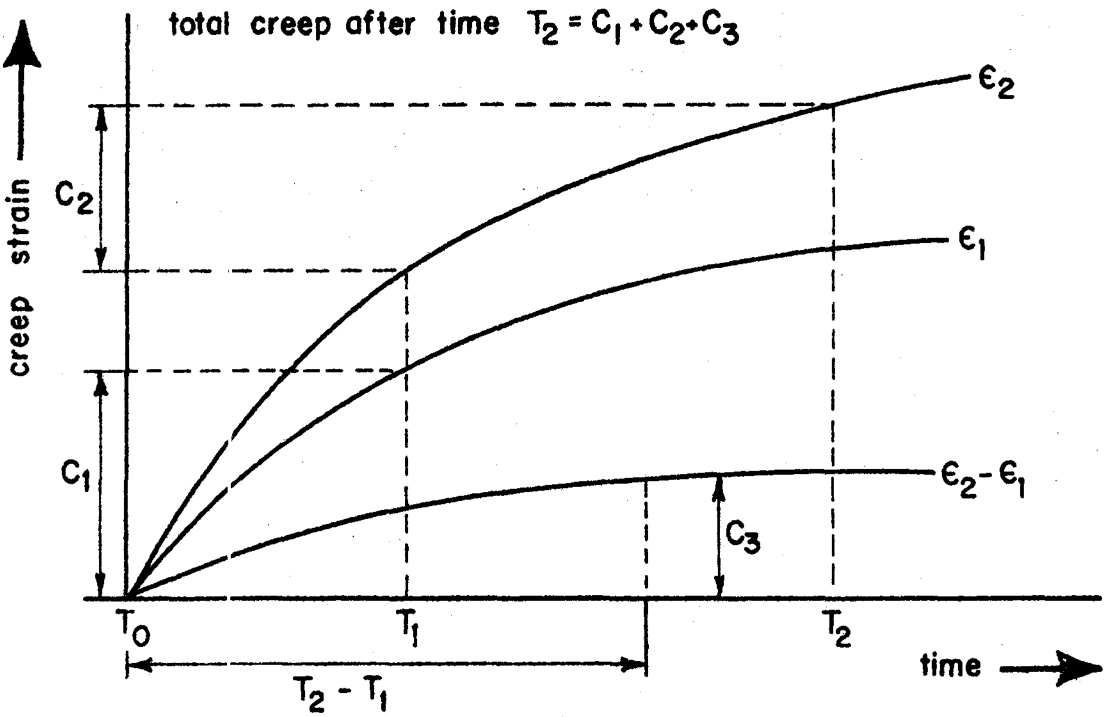

creep curves for constant 'elastic' strain.

Modified superposition method.

FIGURE 6·1 Methods of superposition.

6.6. Evaluation of Methods of Computing Creep

Ross [20] performed a number of tests to determine creep under conditions of severe variations in stress. He found that the effective modulus method gave very poor results for large stress fluctuations, underestimating the strain for decreasing stress and overestimating the strain for increasing stress. The effective modulus method predicted total creep recovery on unloading.

For increasing stresses, the rate of creep method gave surprisingly good results considering its theoretical inadequacy. It underestimated creep for increasing stresses to a degree that became worse with time and higher stress levels. Upon complete removal of load, this method yielded a horizontal straight line asymptotic to observed recovery. Under decreasing stresses, the rate of creep method overestimated strain.

Using the conventional superposition method, Ross found that the correct shape of the curves was obtained, but the magnitude of strain was no more accurately determined than by the rate of creep method. The superposition method overestimated strain for both increasing and decreasing stresses, but gave a much closer approximation than the effective modulus.

Ross concluded that, for general design use, the effective modulus method was preferable for conditions of relatively constant stress because of its simplicity and because, for these conditions, it yielded results comparable to the other methods. For use in practice, under severe stress gradients, he recommended the rate of creep method because of its simplicity and because it yielded reasonably accurate results without the necessity of experimental data.

The modified superposition method reduced the error by taking into account the length of time that the preceeding stress had been imposed on the element. The previous method incremented creep by taking the difference in the amount of creep which would occur for the two stresses considering them to have been applied at the beginning of the time interval under consideration. The modified method used the same time interval but considered it to commence at the beginning of loading and used a time dependent concrete stress-strain relationship in calculating the "elastic" portion of the strain to account for the increased age of the concrete. Drysdale[5] found that the modified superposition method underestimated creep for increasing stresses and overestimated creep for decreasing stresses, but with less error than in previous methods.

Hence, it is concluded that the modified superposition method yields the most accurate results for creep under stress gradients where creep can be determined as a function of time and "elastic" strain.

Chapter 7

METHODS OF ANALYSIS

7.1. Introduction

The following five types of analysis were performed on the rectangular portal frames:

(1) plastic analysis by the mechanism method

(2) elastic slope-deflection equations

(3) plastic slope-deflection equations

(4) numerical integration using the moment-curvature relationships for short-term loads

(5) numerical integration using cross-section elements to include creep effects for sustained loading.

The first three procedures were termed "linear" since they did not consider secondary moments produced by deflections. These were the methods commonly used in structural analysis. They included a number of simplifying assumptions particularly as applied to problems in reinforced concrete which exhibits significant "nonideal" behaviour. Also these methods could not take into account accurately the influence of a number of factors such as abrupt section changes, unusual characteristics of the structure (such as the bases), or secondary effects such as creep.

The last two procedures were developed to study accurately the behaviour of reinforced concrete frames and particularly those used in the tests. The aim was to predict the real behaviour by a mathematical model which would include secondary moments, the influence of particular characteristics such as the steel bases, nonlinear aspects of the concrete and, in the last method, the effects of creep under sustained load.

No attempt was made to formulate these techniques as general design procedures, although the theories involved could be applied to a large number of general problems.

Since the method of superposition, which provided the most accurate means of analyzing the effects of creep, required a numerical procedure and elemental approach, these techniques appeared to be the most suitable means of studying creep under conditions of variations in stress.

7.2. Mechanism Method

7.2.1. Assumptions

A number of assumptions had to be made in adopting this procedure.

Since no provision was made for the inclusion of the effects of base movement, it was assumed that both bases were fixed.

The section was considered to act in an idealized elastic-plastic manner. This implied a moment-curvature relationship similar to figure 7.1. When ultimate moment (equated to the plastic moment capacity M_p) was reached, further attempts to increase the load resulted in rotation without an increase in moment.

Failure by buckling prior to collapse was ignored. Since the axial forces caused by the particular loading configuration used were small, this was not considered a problem.

Deformation and loading were confined to the plane of the structure. Also, deflections were considered sufficiently small that secondary moments could be neglected. The effect of axial force on moment capacity was likewise disregarded.

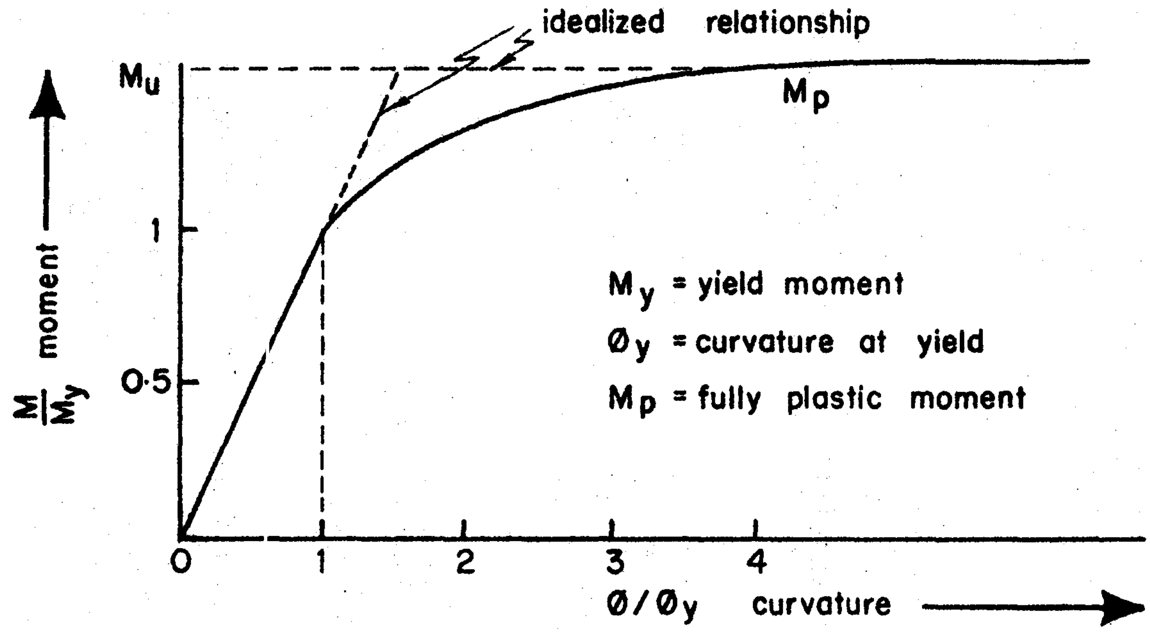

FIGURE 7·1 Ideal elastic-plastic moment curvature.

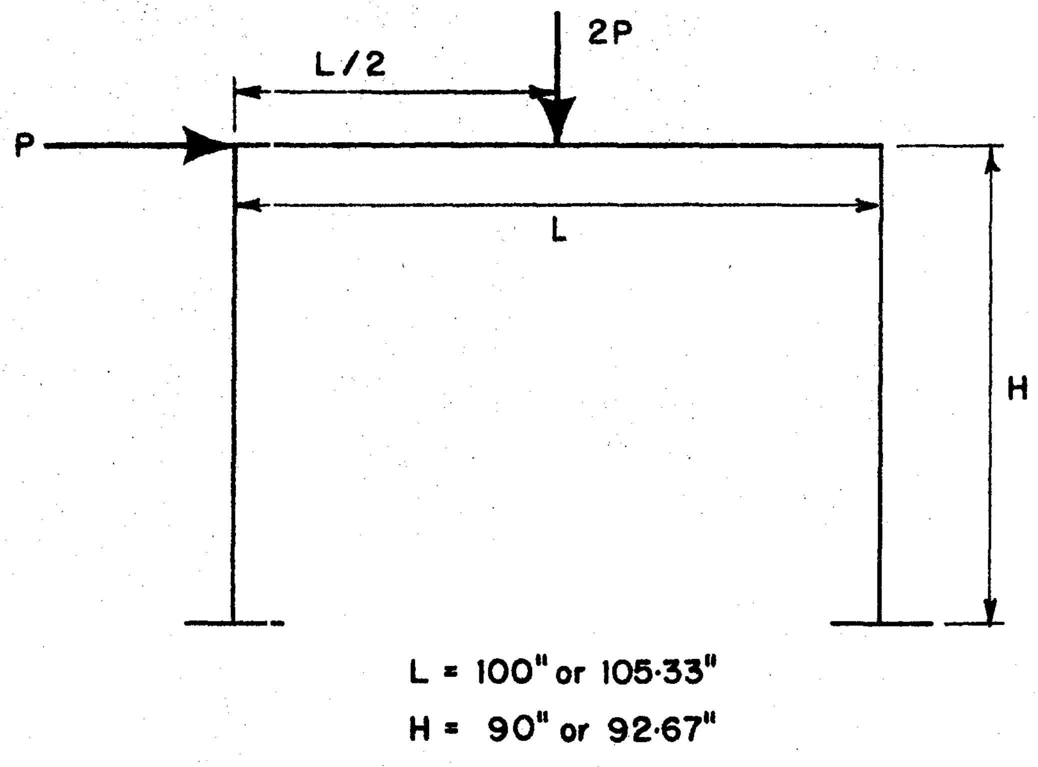

FIGURE 7·2 Frame model for classical analysis.

7.2.2. Effective Member Lengths

Figure 7.2. shows the frame model used in analysis. To use the mechanism method, it was necessary to assume equivalent member lengths so that joint rotation could be considered to act at a point.

Three choices were made for effective member lengths.

One approximation assumed member lengths to be determined by the location of the neutral axis. A beam length of 105.33 inches and a column length of 92.67 inches were derived by considering the neutral axis to lie one third of the section depth from the compression face.

A second choice followed the provision of the Code (3) which recommended using clear spans. This yielded a beam length of 100 inches and a column length of 90 inches.

A third means of defining effective member lengths was to use the clear span plus the depth of the section for the beam, and plus half the depth of the section for the columns. This provided a beam length of 108 inches and a column length of 94 inches. These longer spans were intended to take into account rotation within the corner sections.

7.2.3. Results

The upper bound theorem provided a solution by satisfying equilibrium and the formation of the collapse mechanism. By investigating all possible mechanisms, the lowest upper bound solution was found thereby obtaining the true mechanism and the collapse load.

Possible mechanisms for the rectangular portal frame loaded as in figure 7.2. were:

(1) beam

(2) sway

(3) combination beam and sway.

The combination mechanism gave the lowest collapse load:

$$Pu = 0.0316\ Mp$$

The units of Mp and Pu were inch-kips and kips respectively. This result was for effective member lengths based on the clear span. Using member lengths based on the neutral axis, Pu = 0.0303 Mp. For a beam span increased by the section depth, and column lengths increased by half the section depth, Pu = 0.0297 Mp.

The moment capacity of the section was determined using conventional ultimate strength design with a Whitney stress block, and was found to be 308 inch-kips for a concrete cylinder strength of 4850 psi with no axial load. Using the assumption of ideal elastic - plastic behaviour, the plastic collapse moment Mp was equated to the ultimate moment capacity Mu. Figure 7.3. indicates the shear force and bending moment diagrams for this analysis.

Since the moment capacity of a reinforced concrete section is dependent on the axial force, the ultimate moment computed above was realized to be in error. Based on an estimate of axial forces in the members, and using the moment-curvature relationships described in Section 7.5.2., the moment capacity of the members was found to be in the range 320 to 350 inch-kips. The variation in ultimate moment at each hinge location indicated a discrepancy in the computation of Pu. However, on the basis of the plastic analysis, Pu was estimated at between 10.0 and 11.0 kips.

7.2.4. Discussion

Although acceptable for general design work, the mechanism method did not accurately account for the behaviour of reinforced concrete, and was not readily adaptable to long-term studies.

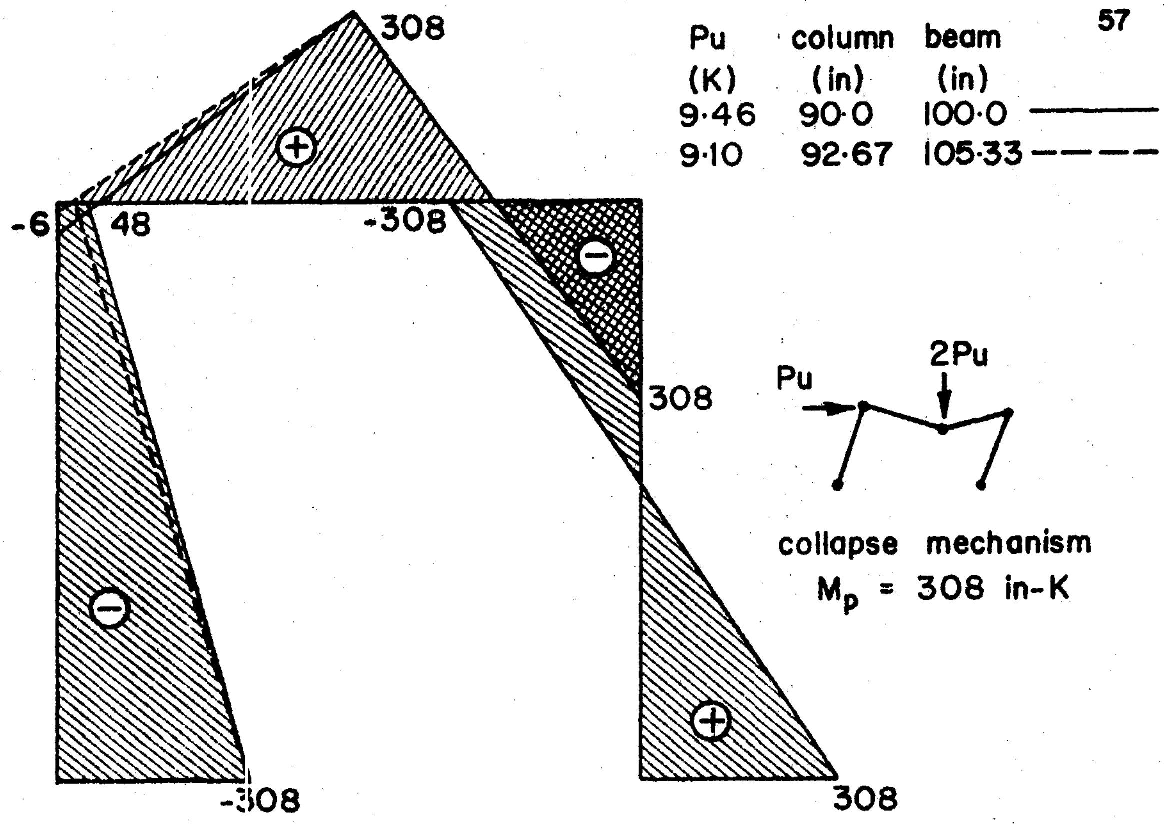

Bending moments (in-K)

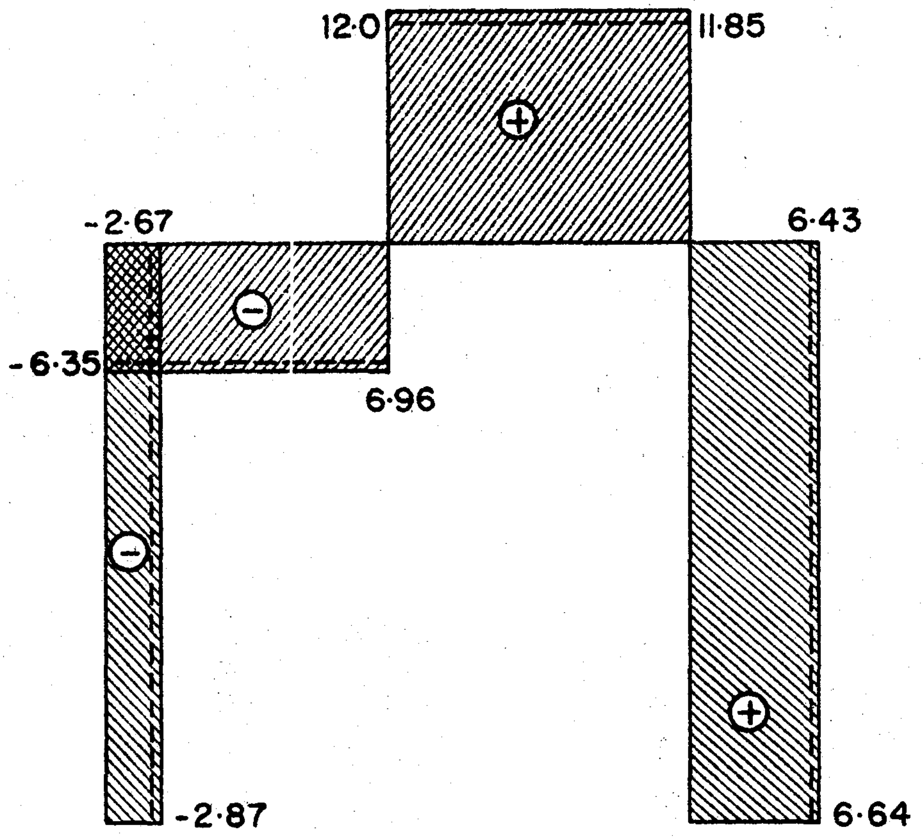

Shear force (K)

FIGURE 7·3 Shear force and bending moment

Since this method did not consider the effects of axial forces, it tended to underestimate ultimate moment for low axial loads and overestimate ultimate moment for high axial loads. In the frames studied, it underestimated the moment capacities of the members by not including the influence of axial forces.

By considering the affect of axial force on the moment, it was possible to estimate more accurately the capacity of each section. However, since the member capacities were different, the original assumption that each hinge was similar was violated. An iterative procedure could be used to successively recalculate the mechanism, the moment and shear force distributions, and the section capacities. This would be necessary in using this method as a design procedure, particularly if there were high axial loads on the columns.

There was no realistic provision in the plastic analysis for creep and shrinkage, and hence moment redistribution due to sustained load could not be determined.

Because this procedure was unable to account for the effects of secondary moments or buckling, it was not adaptable to frames with very slender columns.

Movement of the supports was another important factor not included.

7.2.5. Conclusion

In conclusion, great care must be taken in examining the assumptions involved before using the mechanism method for the design of reinforced concrete structures. In the present study, this procedure was used only to obtain an estimate of the anticipated short-term collapse load for the frames. This was used in establishing equipment requirements such as the capacity of jacks, loading mechanisms, supports, and instrumentation. The mechanism method also indicated the mode of failure of the structure.

7.3. Elastic Slope-Deflection Equations

7.3.1. Assumptions

This method was generally limited to working load levels since it contained the basic assumptions of elastic theory. The section was considered to behave in a linear-elastic manner for all load levels. Plane sections were assumed to remain plane, and deflection was considered small enough that secondary moments could be neglected.

7.3.2. Procedure

Using slope-deflection equations, it was possible to trace the formation of hinges in the frame in a step-by-step procedure. This was accomplished by first performing analysis on the rigid frame, then locating the point of highest moment, and declaring this the location of the first hinge. The moment at this point was set equal to Mp and all other moments and forces were adjusted accordingly. Next, unit loads were applied, and the frame was analyzed with a hinge at the previously located point. Once again, the highest moment was declared the plastic moment increment. A factor, obtained by taking the amount by which the previously determined moment at this point should be increased to reach the plastic moment and dividing by the incremental moment, was multiplied by all the incremental moments and forces. These were then added to their previous values. Should any moment thus obtained exceed Mp, its location was declared the true hinge and the procedure was repeated. These steps were iterated until the collapse mechanism was obtained.

The concrete modulus of elasticity was computed using the Code formula (3).

$$Ec = w^{1.5}\ 33\sqrt{f^1c}$$

for w = 145 pcf and f^1c = 4000 psi

To include creep, a reduced modulus Ec^1 was computed assuming creep strain equal to 80% of the elastic strain. The reduced modulus expression was

$$Ec^1 = \frac{Ec}{1.8}$$

Using the broad assumption that Ec^1 and the moment of inertia could be considered constant for all sections of a member, the member stiffnesses were calculated. These were based on a cracked section.

7.3.3. Use of Slope-Deflection Equations to Determine the Effects of Base Movements

Slope-deflection analysis was used to determine the effects of base deflection and rotation. Since the elemental procedure described in Section 7.5. resulted in erroneous boundary conditions at the right base, it was necessary to re-adjust the moment distribution and repeat the calculations until geometrical compatibility was obtained. One means used to obtain convergence was to re-adjust the boundary conditions at the left base by amounts indicated by slope-deflection analysis for the error at the right base. Also, the effect of residual deflections and rotations at the right base, on moments and reactions in the frame, as determined by slope-deflection equations, was used to determine acceptable limits for convergence. The results of this analysis were as indicated in Figure 7.5. and Table 9.1.

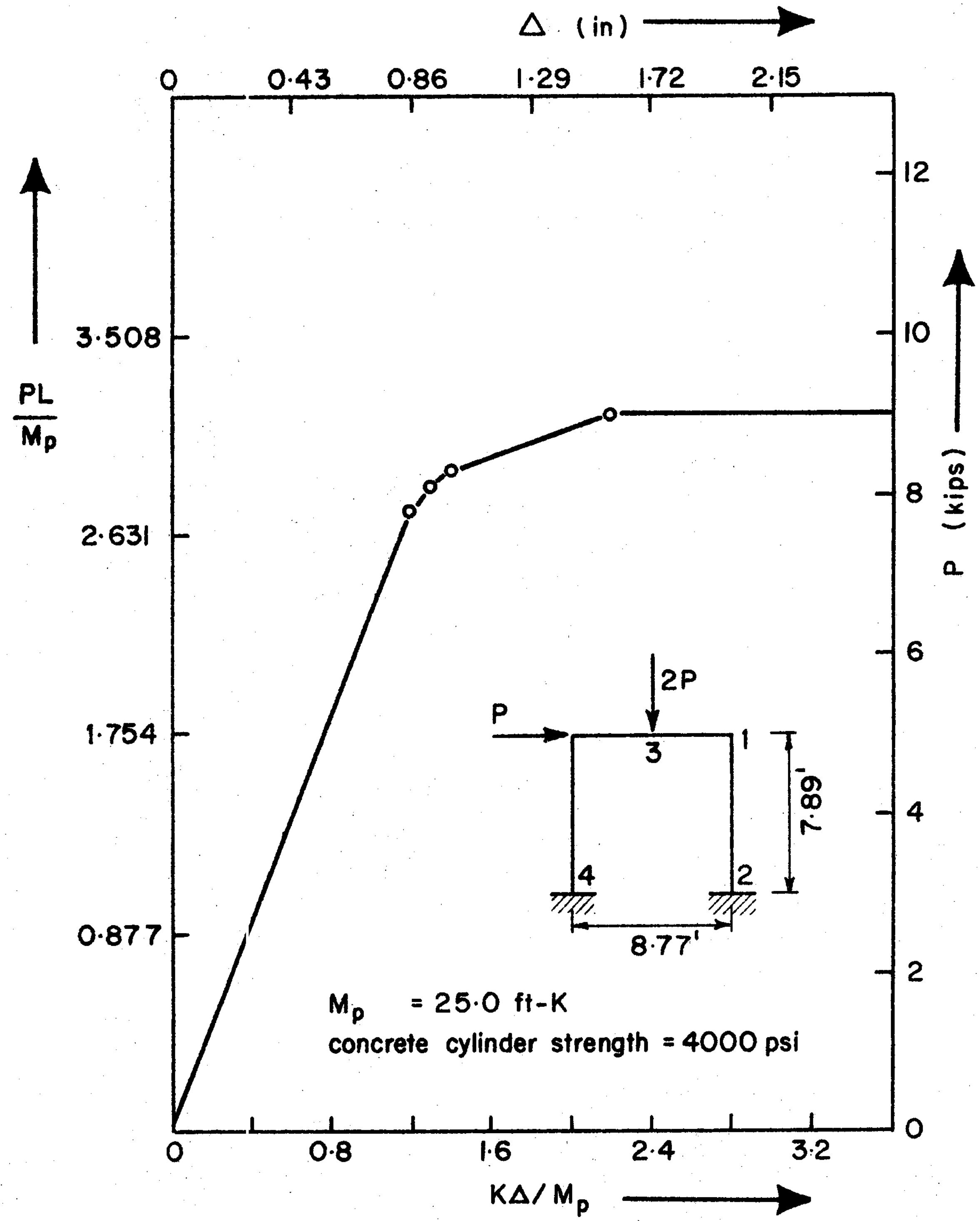

K = column stiffness
Δ = sidesway (inches)
L = beam length

E' (reduced modulus) = 2020 Ksi

FIGURE 7·4 Formation of plastic hinges.

7.3.4. Results

Using slope-deflection equations with assumed member lengths to the neutral axes, for Mu = 308 inch-kips, the ultimate load was found to be 9.0 kips. As indicated in Figure 7.4. the order of formation of hinges was as follows:

(1) upper right hand corner

(2) right base

(3) midspan of the beam

(4) left base

Deflections were computed by this method as a comparison with other procedures. However, it was realized that the assumptions of constant moment of inertia and reduced modulus were not very realistic and hence these deflections were not considered accurate. The calculated sidesway was included in Figure 7.4.

Moments and shear forces for boundary conditions compatible with test frame L1, were as shown in Figure 7.6. This analysis considered the effect of movements in the bases to act entirely at the right base. Since the rotation of the right base was considerably greater than that of the left base, this was not considered a severe source of error.

7.3.5. Discussion

For elastic circumstances, slope-deflection equations may be used to determine the deflection of a frame, but since this requires a knowledge of member stiffnesses, its applicability to concrete structures is limited. Because of cracking, a concrete member may exhibit a different stiffness at every section along its length for every different load.

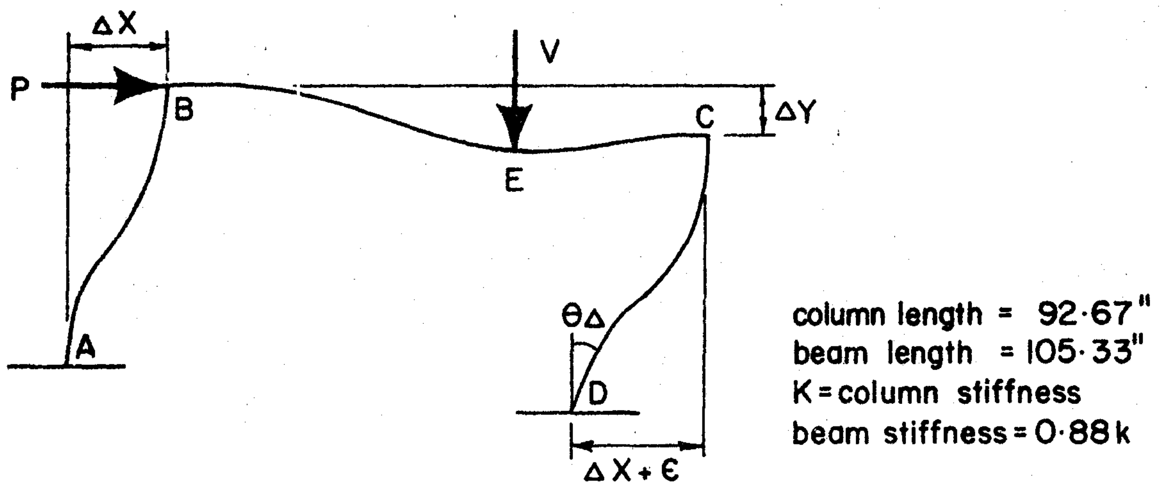

FIGURE 7·5 Frame model for slope - deflection analysis

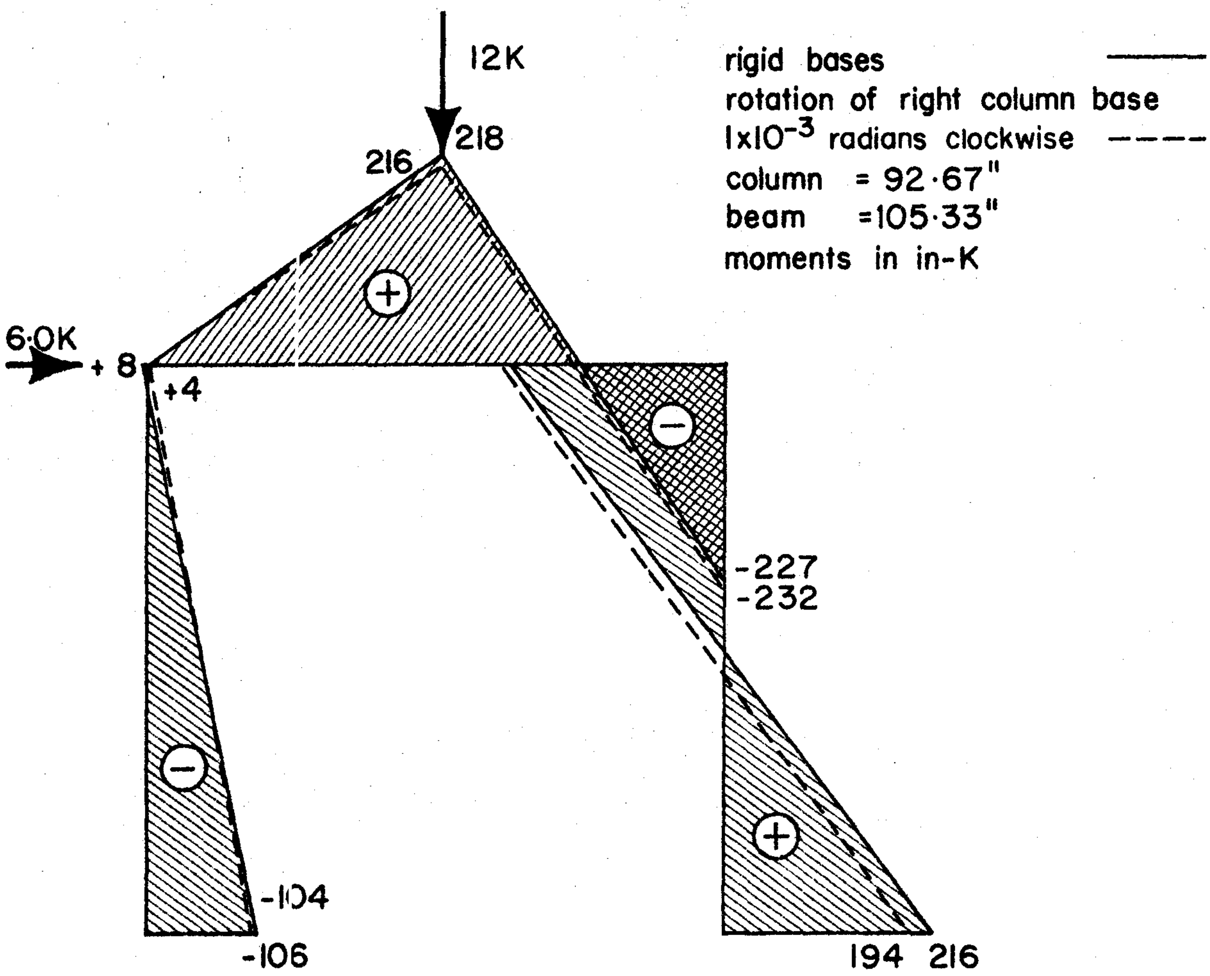

FIGURE 7·6 Frame moments by slope deflection.

Another limitation is the fact that reinforced concrete does not have a linear-elastic stress-strain relationship. Although this does not greatly restrict the use of slope-deflection equations in determining moments, since here only relative stiffnesses are required, it does prevent accurate calculations of deflections.

This procedure is subject to the same limitations as plastic analysis. It does not contain provisions for the inclusion of the effects of axial forces on moment capacity. The ultimate moment could be adjusted to give a more realistic approximation, but the problem of different relative stiffnesses and changes in section capacity would produce severe errors in analysis of the moment distribution on the frame.

Slope-deflection equations also cannot accurately account for the influence of secondary moments or creep.

7.3.6. Conclusions

The slope-deflection equations were considered inadequate for accurate analysis of the short-term or sustained load behaviour of reinforced concrete frames. However, they were used in the numerical integration procedures described in Sections 7.5. and 7.6. to correct the moment distribution for errors in geometric boundary conditions.

When used as a plastic analysis this method satisfied equilibrium, the collapse mechanism, and the requirement that yield nowhere be exceeded. Therefore, it complied with both the upper bound and lower bound theorems, and hence automatically provided the collapse load. Within the limitations imposed on the mechanism methods, the slope-deflection equations were considered adequate for the design of frames similar to those studied in this research.

7.4. Plastic-Slope Deflection Equations

7.4.1. Introduction

This procedure was similar to elastic slope-deflection equations and is not presented in detail here. Neal [18] gives a comprehensive description of the method and its application.

The primary feature of the plastic slope-deflection analysis was that it took into account inelastic rotation at assumed plastic hinges, whereas, the elastic method assumed that corners remained right angles during deformation.

7.4.2. Procedure

Basically, plastic slope-deflection analysis involved the selection of a mechanism, and formulation of inelastic rotation equations at each hinge in terms of the moment capacity and unknown deflection. Just prior to collapse, one of the plastic hinges would have zero "inelastic" rotation. A suitable hinge was selected and its inelastic rotation expression was equated to zero. This gave deflection in terms of moment capacity. This deflection was substituted into the rotation expressions for the other hinges and they were solved. Thus obtained, the inelastic rotations were tested for correct sign, and if they were all acceptable, the displacement was assumed correct as calculated. Otherwise, it was concluded that the hinge selected as last was not the true final hinge and others were tried until the correct answer was obtained.

7.4.3. Results

Although also limited by the necessity of estimating a stiffness for an entire concrete member, this procedure gave a reasonably realistic value of deflection for the test frame. Using a reduced modulus of 2.02 x 10^6 psi and a moment of inertia of 235 in.^{4} at ultimate load based on a cracked section, the predicted sidesway just prior to formation of the collapse mechanism was 1.97 inches. This analysis did not include provision for boundary condition variations. The bases were considered fixed.

7.4.4. Conclusions

The plastic slope-deflection equations provided a more realistic approximation of the inelastic behaviour of hinges. However, like the mechanism method, and elastic slope-deflection equations, they did not take account of the variation of moment capacity with axial force, the non-ideal properties of concrete, secondary moments due to deflections, and the influence of creep. Hence, it was concluded that the plastic slope-deflection equations were not adequate for accurate analysis of frame behaviour under sustained loads.

7.5. Numerical Procedure Using the Moment-Curvature Relationships for Short-Term Loads.

7.5.1. Introduction

This was the first of two procedures developed to study the behaviour of the reinforced concrete test frames, although they could be adapted in principle for use on other structures. This method, also referred to as the first stage element method, or the element method using moment-curvature, was used to predict response of the frame to short-term loading.

7.5.2. Assumptions

It was assumed throughout that the concrete stress-strain relationship was consistent, that plane sections prior to loading remained plane, that all deformation was in the plane of loading which was defined by the centroidal longitudinal axis of the members, and that buckling of individual members did not occur.

The primary objective was to devise a computer model which would closely approximate the behaviour of the actual test frame. Hence, assumptions had to be evaluated on the basis of how they would affect the precision in obtaining this goal.

The effect of ties was ignored. Other investigators have shown that ties do not appreciably affect the strength of a section before initial failure. As mentioned previously, the corners and bases were stiffened with additional reinforcing. In the bases, this steel extended to the edge of the wideflange flanges. Hence, it was assumed in the frame model that the effective column length was from the extremity of the upper flanges of the base to the top inside corner of the frame and the effective length of the beam was taken as the distance between the inside surfaces of the columns.

The concrete stress-strain relationship used was an expression developed by Drysdale(5) for concrete cylinder strengths of approximately 4400 psi. It was developed by a least squares fit of test results from a large number of standard 6 inch diameter cylinders.

For strengths other than 4400 psi, it was assumed that linear proportioning was applicable. The concrete strength used in this research was determined by cylinder tests performed at designated times. A comparison was also made between the stress-strain characteristics of the concrete and the analytic expression. This relationship was shown in Appendix A, Figure A1.

The reinforcing steel was considered as an elastic-plastic material. Tensile tests were performed in order to determine the elastic modulus and yield strength for use in the analysis. Results of these tests were presented in Appendix C. The stress-strain was linear up to 59,000 psi. The modulus of elasticity was 29.6 x 10^6 psi. Up to a strain of 0.005, fully plastic deformation occurred. For greater strains, strain hardening occurred at a relatively constant rate of 4000 psi per 1000 microstrain. Since the analytic procedure did not make allowance for strain hardening of the steel, the precision of this aspect of the method decreased for high strains beyond yielding.

The self-weight of the frame was not included in the analysis. This caused significant error at low load levels, but the effect at high loads was small. The maximum dead load moment was about one percent of the ultimate moment capacity. To improve precision of this method, particularly in the treatment of secondary moments, the dead load should be included.

7.5.3. The Frame Model

7.5.3.1. Introduction

The computer model of the frame consisted of a number of elements of equal length which made up the columns and beam. The columns were taken as 90" long and the beam as 100". Although a thorough quantitative study of the effect of element size on accuracy was not made, several configurations were tried in order to determine trends. Based on a consideration of computer time required against accuracy gained, twenty-eight elements, each ten inches long, gave satisfactory results.

The lateral load was assumed to be applied at the top of the column and the vertical load at mid-span of the beam.

The model cross-section and longitudinal reinforcing were identical to those of the actual frame.

The column bases consisted of a lower section, four inches long, which was capable of rotation similar to the lower flanges of the wideflange section, and an upper stiff section, 4 inches long, which represented the upper flanges of the wideflange and the heavily reinforced concrete between them. This upper portion of the base was considered completely rigid. No rotation took place along its length. The origin of coordinates was taken as the bottom centre of the left column base.

Deflections, curvatures, and strains were calculated from a line running through the centre line of each member. Since the member lengths were to the inside upper corners, this eliminated the stiffened corner sections from analysis.

7.5.3.2. Procedure

The following steps were used in developing the frame model to solve for the moment distribution and deflected shape of the frames.

(1) Based on the elastic analysis, assumptions were made for the reactions and moment at the left base.

(2) The rotation and displacement of the left base were calculated.

(3) From the moment-curvature relationship and the assumed moment, the curvature acting over the first element was calculated.

N.B. Frame elements were numbered from 1 to 28 starting at the left base. The interfaces between the elements were numbered similarly starting with 0 at the left base and proceeding to 28 at the right base. The moments acting at the interfaces were numbered from 1 at the left base to 29 at the right base. Hence the moment at the top of the left base was M_1, and that at the top of the first element was M_2.

(4) Using the curvature for M_1, considered to act over element one, M_2 was calculated from equilibrium. This computation included the secondary moment caused by the deflection and axial forces.

(5) The curvature for M_2 was averaged with that for M_1. Using this new curvature, a new M_2 was calculated. This step was iterated until the change in curvature was less than 1% or 1×10^{-6} radians.

(6) Starting with the moment at the upper end of the preceding element, steps (3), (4) and (5) were performed successively on all the elements of the frame. At the corners and the load point on the beam, equilibrium was used to determine the appropriate changes in shear and axial forces.

(7) Upon completion of the last element, the rotation and displacement of the right base were calculated.

The above procedure provided a solution for the forces and moments acting in the frame which satisfied static equilibrium. However, this method did not assure geometric continuity. Unless the solution obtained was correct, the boundary conditions at the right base were erroneous. Hence, it was necessary to iterate the procedure until both equilibrium and geometry were satisfied. The following steps were used to systematically alter the moment distribution in order to find the correct geometry.

(8) Based on the errors in displacements and rotation at the right base, slope-deflection equations were used to estimate new moments at the left base.

(9) Steps (1) to (7) were repeated until the geometric errors at the right base converged on an acceptable residual. If changing the reactions at the left base using slope-deflection equations did not produce convergence after a reasonable number of cycles, they were altered by fixed amounts.

A fortran program was written using the moment-curvature element method. The program was used to solve for the short-term behaviour of reinforced concrete frames with allowance for base movements, shrinkage, and secondary moments, but without the inclusion of creep. It was applicable in the present form only up to formation of the first hinge.

7.5.4. Moment-Curvature Computation

7.5.4.1. Introduction

An important requirement of the element method described above was an expression relating moment, curvature and axial force for the cross-section.

A fortran program was written to determine the relationship between moment and curvature for various axial loads on the section. This procedure adhered to the assumptions used in the numerical integration procedure. Input consisted of the section geometry, elastic modulus and yield strength of the reinforcing steel, concrete cylinder strength, and the shrinkage recorded from casting to the time of loading.

7.5.4.2. Shrinkage

The recorded shrinkage to the time of loading was used to obtain the compressive force in the steel. This was equated to the tensile force in the concrete. Using a constant elastic modulus, which was sufficiently accurate because of the low strains involved, the tensile strain in the concrete equivalent to the shrinkage was calculated.

7.5.4.3. Procedure

For a given axial load, the strain at the compression fibre was set at 0.003 and a neutral axis was assumed. Then the forces acting on the section including the effects of shrinkage for these conditions were calculated. The neutral axis was varied in an iterative procedure until equilibrium was obtained. Tension in the concrete was assumed to be effective up to a tensile strain of 0.00015 using a stress strain curve which mirrored that for compression. Figure 7.7. indicates the free body diagram for a section used to determine the moments and curvatures which were determined for axial forces from zero to 14 kips.

Using a least-squares technique, functions of curvature in terms of moment for each axial force were derived. Then, in a similar manner, using a separate program, the coefficients of the independent variable (moment) in the moment-curvature expressions were used to obtain a function relating them to axial force. In this way curvature was obtained as a function of moment and axial force.

Although not included in this study, an estimate of creep behaviour could have been made using the moment-curvature method by deriving a concrete stress-strain relation which included creep deformation. This would have been an effective modulus type of procedure and would be limited by its disregard for stress history as mentioned previously in Section 6.

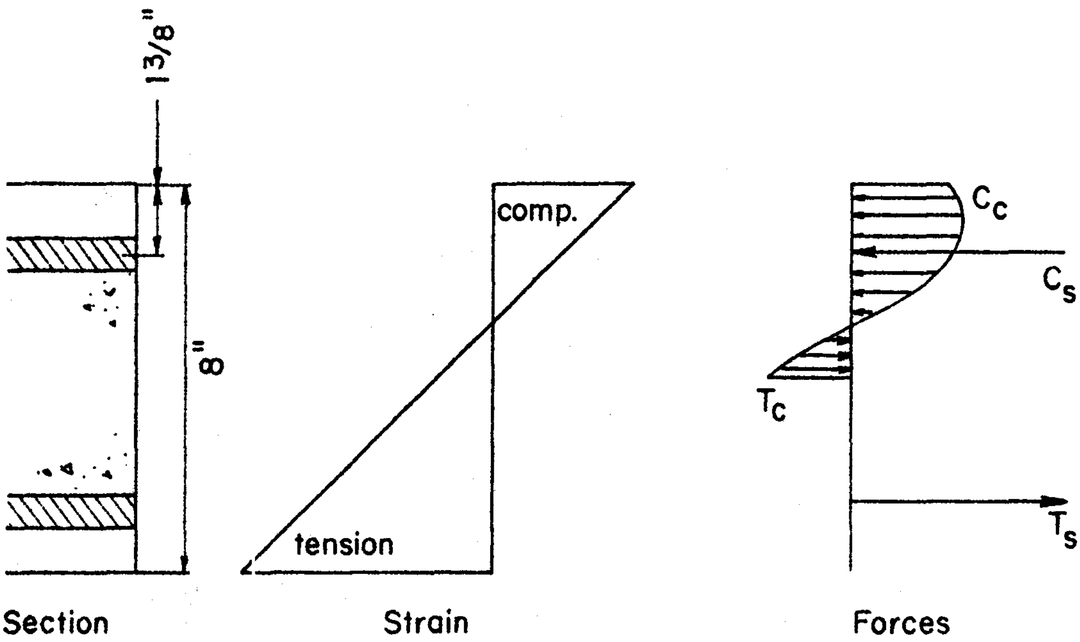

FIGURE 7·7 Free body diagram for member section.

7.5.4.4. Results

Moment-curvature curves were developed for different values of axial force and shrinkage. Some of these curves were presented in Figures 7.9., 7.10. and 7.12.

As shown in Figure 7.11, the variation in the moment-curvature relationship with axial force for moments greater than one hundred inch-kips, for the range of axial forces encountered in the analysis, ultimate moment increased with axial force.

As indicated in Figure 7. 8., the importance of considering the tensile strength of the concrete was significant for the variation of moment-curvature with axial force at moments less than 110 inch-kips.

With no concrete tension included, the moment-curvature relationship was linear above the low strains where shrinkage has a significant effect. When tension was included, the curves had a constant slope about three times as great as that without tension, up to a moment of approximately 25% of ultimate. Then there was a downward sweep with decreasing slope to a minimum point, followed by an upward curve which gradually approached that without tension considered.

7.5.4.5. Tensile Stress in the Concrete

The tension phenomenon may be explained as follows:

When the strain at the extreme tension fibre of the section was less than that required to produce cracking, the entire section acted to resist moment and the moment-curvature relationship was linear.

When the critical strain, in this case assumed to be 0.00015, was reached, a cracking moment capacity for the concrete section was reached. Further loading caused cracks to run from the tension face. Movement of these cracks produced unstable equilibrium points indicated by the downward and then upward curves of Figure 7.8. These points could not be obtained experimentally by a system which stored energy. What was observed was that, when tensile failure was reached at the extreme fibre, cracks shot across the section almost instantaneously until the next stable equilibrium position was reached. This occurred as shown in Figure 7. 9 . At both stable equilibrium positions, the moment was the same, but the curvature of the cracked section was two to four times greater, with the curvature change varying inversely as the axial force.

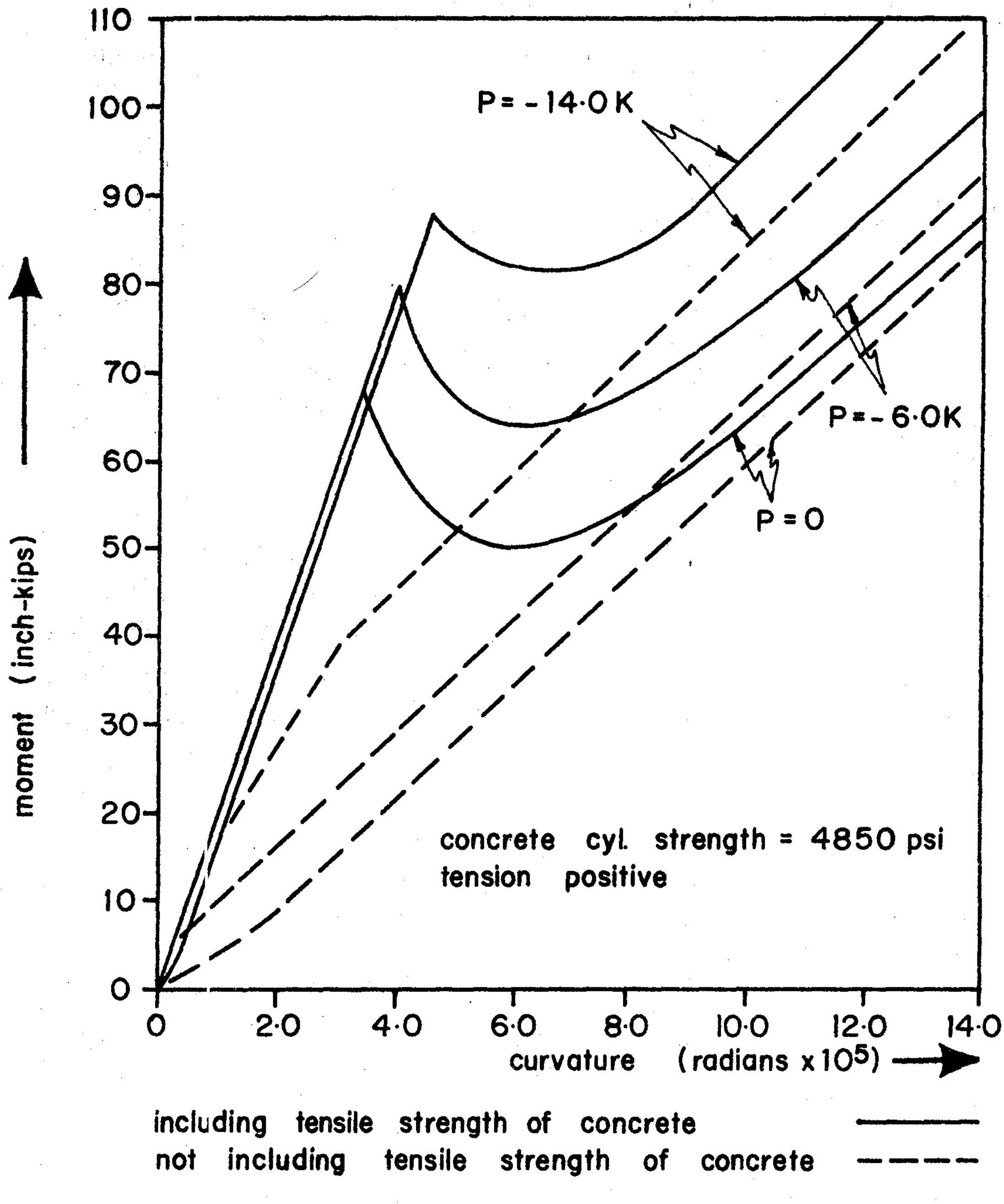

FIGURE 7·8 Moment - curvature relationship for low moments, for shrinkage 0·000050 in/in.

Once the cracked equilibrium position was reached, the influence of tension in the concrete was greatly reduced, since, because of the greater curvature, it affected a much smaller area of the section; and, because of the greater proximity of its centroid to the centre of the section, it contributed less to the moment. The curves with and without concrete tension gradually approached each other as the moment was increased further. At two thirds of ultimate moment, the influence of concrete tension was negligible.

7.5.4.6. The Influence of Shrinkage

The influence of shrinkage on the moment-curvature curves was as shown in Figure 7.10. Before cracking occurred, with concrete tension considered, shrinkage had very little effect.

With no external axial force on the section, the neutral axis was in the centre of the section. Since the concrete stress-strain curve for tension was assumed to be a mirror image of that for compression the forces in the concrete on either side of the neutral axis were equal and opposite, as were the forces in the steel. Because shrinkage caused equal compressive stresses in all the bars and equal tensile stresses in the concrete throughout the section, it decreased the moment contribution of the tension steel and compression concrete and increased the moment contribution of the compression steel and tension concrete by almost equal amounts. Hence, the total moment changed only slightly.

As the applied axial force was increased, the neutral axis deviated from the centre of the section and there was no longer a balance between opposite forces in the steel and opposite forces in the concrete. Hence, the influence of shrinkage was more evident for high axial loads.

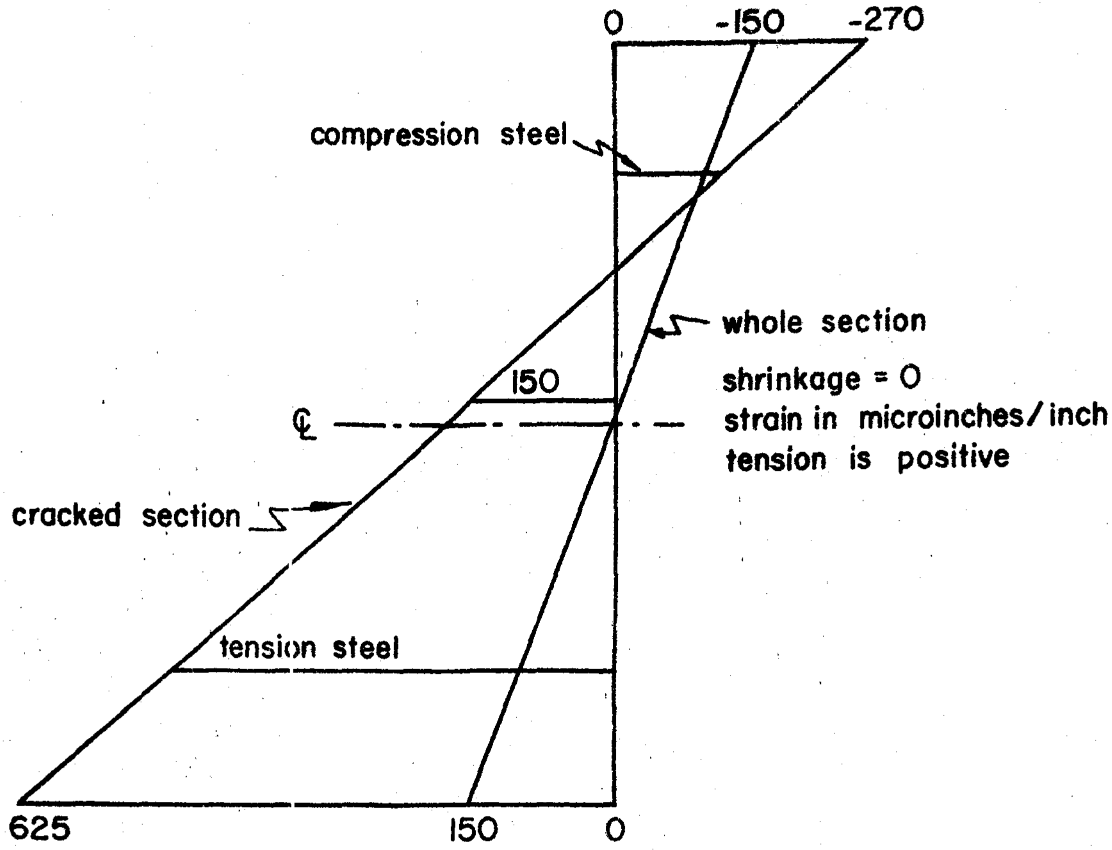

	FORCES (K) whole	FORCES (K) cracked	MOMENTS (IN-K) whole	MOMENTS (IN-K) cracked
T_c	11·70	4·11	31·15	-2·72
T_s	2·48	11·44	6·51	30·20
C_s	-2·17	-2·65	5·69	6·96
C_c	-11·92	-12·96	31·80	41·40
	0·08	-0·08	76·15	75·84

axial force = 0·0

allowed residual force for iterative solution = ± 0·1 K

T_c = tension in concrete

T_s = tension in steel

C_s = compression in steel

C_c = compression in concrete

FIGURE 7·9 Strain distribution for whole and cracked adjacent equilibrium configurations.

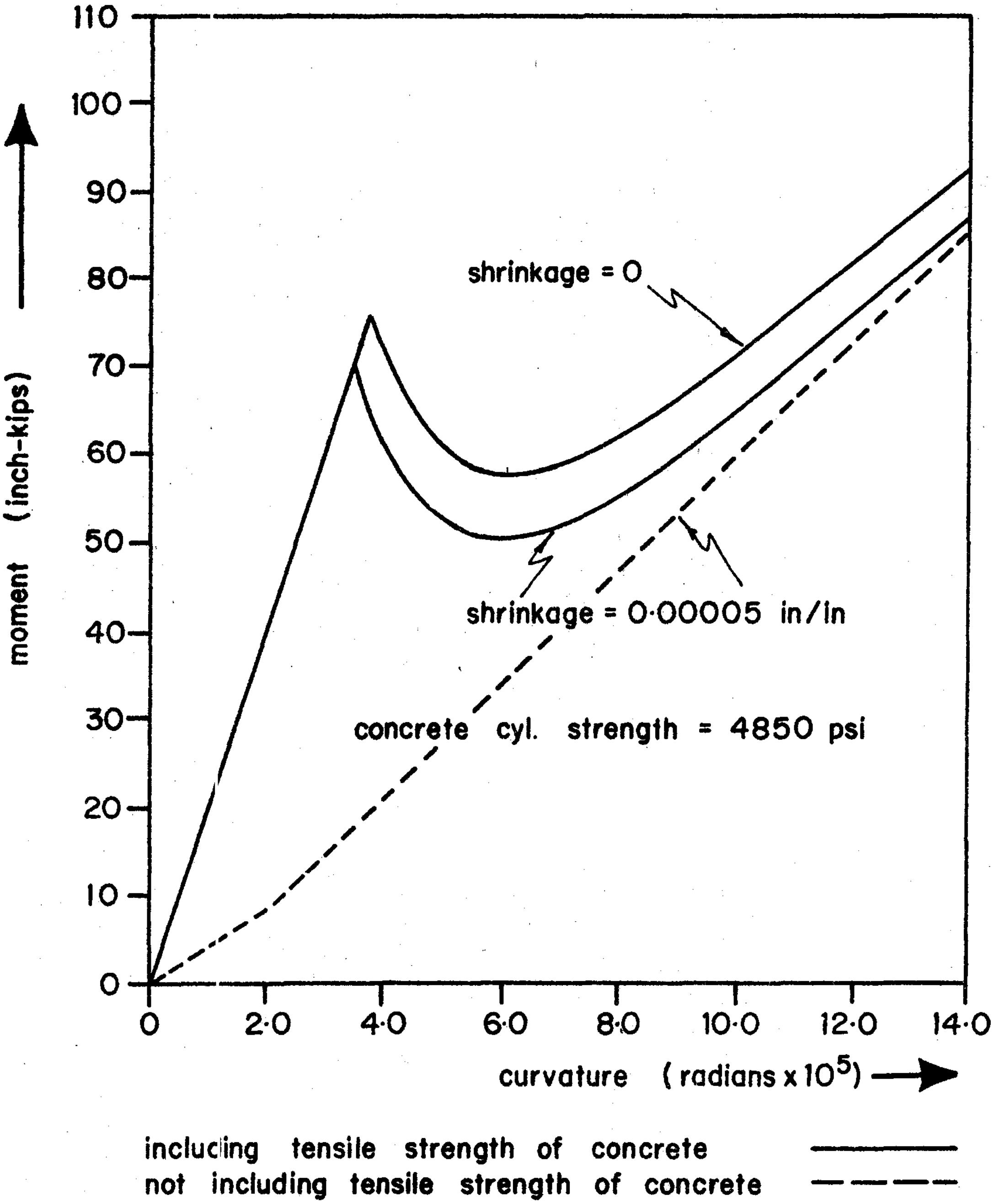

FIGURE 7·10 Moment-curvature relationship for low moments for zero axial force.

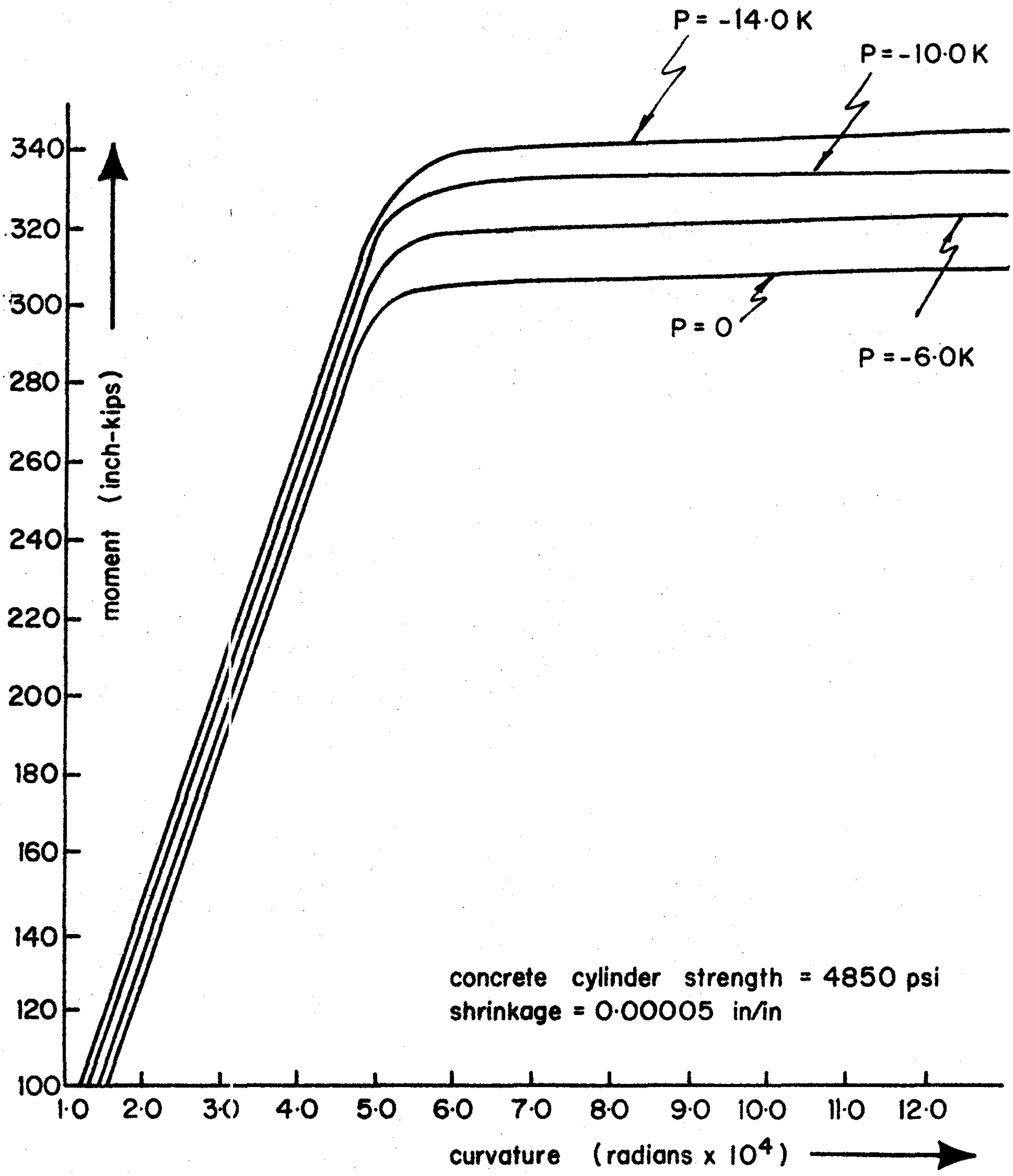

FIGURE 7·11 Moment/curvature relationship for high moments.

Once cracking had occurred, the influence of shrinkage was more important. The greater the shrinkage, the higher was the tensile stress in the concrete at any point on the section. Hence, an increase in shrinkage caused a reduction in the moment at which cracking strain was reached at the extreme fibre.

This effect was carried through the unstable equilibrium positions and did not lose significance until the stresses over most of the section were much greater than the equivalent shrinkage stress. Once stable equilibrium of the cracked section had been obtained, the influence of shrinkage decreased with increasing moment and could not normally be observed beyond two thirds of the ultimate moment.

7.5.4.7. Model for the Moment-Curvature Curves

For computer analysis of the test frames a model for the moment-curvature curves was devised.

For moments up to first cracking, a linear expression independent of axial force or shrinkage was used. It was assumed that for the range of axial forces encountered this would not lead to significant error. The moment and curvature at which first cracking occurred, and the curvature at which the lowest cracked equilibrium position was reached, were expressed as functions of shrinkage and axial force. It was assumed that a line of constant moment joined the two equilibrium states. Above two thirds of ultimate moment, and below 90% of ultimate moment, the slope of the moment-curvature curve for a given axial force was constant and independent of shrinkage.

This line was produced to meet a horizontal line at the level of the ultimate moment for each force considered. The points thus obtained were expressed as a function of axial force. From these points straight lines were extended to the lowest cracked equilibrium position. These lines were formulated in terms of axial force and shrinkage. Ultimate moment was expressed as a function of axial force.

The moment-curvature expressions thus developed were incorporated in the program for analysis of the short-term behaviour of the test frames by the element method.

7.5.5. The Influence of Concrete Tensile Strength on Frame Behaviour

Two expressions were used for moment-curvature in the first stage element program. The first, as described above, included the discontinuity caused by concrete tensile strength; the second used the moment-curvature curves without concrete tension. The effect of concrete tensile strength on the moment distribution of the frame was as indicated in Figure 7.12. Since including tension gave greater stiffness to the section, there was a tendency for moments to distribute more to the loaded side of the frame. This caused lower moments on the unloaded column and higher moments on the loaded column. Since the first hinge formed at the top of the unloaded column, including concrete tension resulted in the prediction of a slightly higher load for formation of the first hinge. However, since the influence of concrete tension became insignificant at two thirds of ultimate moment, it did not affect the overall capacity of the frame.

The most significant influence of concrete tension was in frame deflections particularly at low load levels. Frame deflections predicted by the moment-curvature element method with and without concrete tension were as shown in Figure 7.13. At a horizontal load of 1.5 kips and a vertical load of 3.0 kips, the frame sidesway deflection with concrete tension included was about one quarter the

location	horizontal load kips	moment (concrete tension inc.) inch/kip	moment (concrete tension omitted) inch/kip	deflection H ≡ horizontal V ≡ vertical (inches)	
				tension	no tension
left base (1)		-26·66	-24·48		
upper left cor. (2)		9·83	3·96	·035 H	·175 H
beam centre (3)	1·5	51·37	47·90	·01 V	·06 V
upper right cor. (4)		-57·12	-58·28	·035 H	·175 H
right base (5)		41·50	48·81		
left base (1)		-128·83	-118·17		
upper left cor. (2)		6·67	16·02	·419 H	·452 H
beam centre (3)	6·0	195·47	198·29	·15 V	·15 V
upper right cor. (4)		-217·05	-220·83	·418 H	·452 H
right base (5)		192·53	190·34		

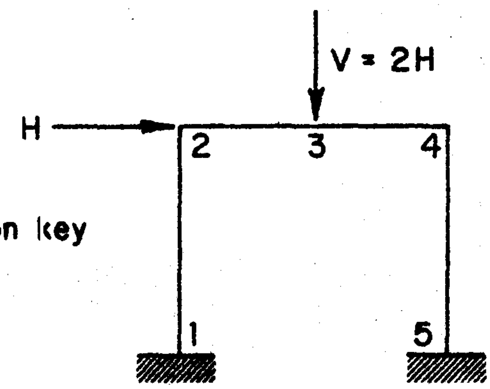

location key

FIGURE 7·12 Influence of concrete tensile strength on frame moments.

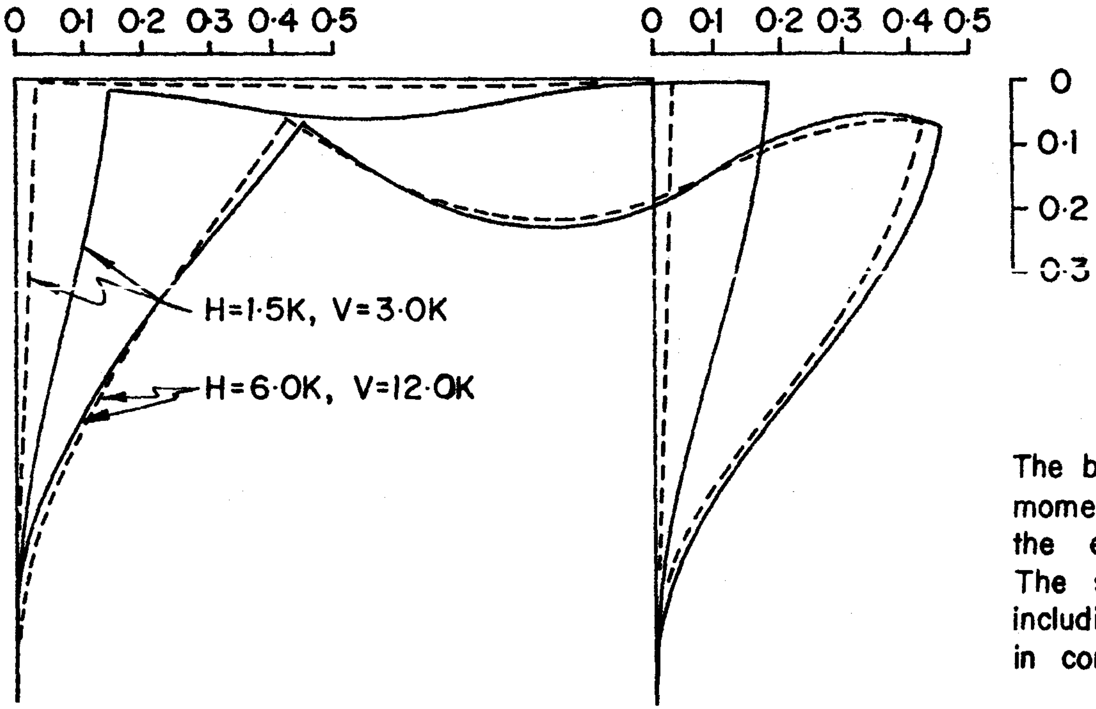

The broken line was derived using a moment/curvature relationship which included the effect of tensile stresses in concrete. The solid curve was computed without including the effect of tensile stresses in concrete.

For this example no base rotation was considered
Load for first hinge = 9·0 K
Ultimate load = 11·5 K
Deflection in inches

FIGURE 7·13 The influence of tension in concrete on frame deflection.

sidesway predicted with concrete tension omitted. At a horizontal load of 6.0 kips and vertical load 12.0 kips (about 52% of ultimate load) the difference was only 7%. Hence, it was apparent that the tensile strength of the concrete had a significant effect on frame behaviour prior to cracking, but once cracking has occurred at regions of higher moment, concrete tension had little influence.

7.5.6. Comparison Between the Moment-Curvature Element Method and Slope-Deflection Equations

Frame R2 was analyzed by elastic slope-deflection and the moment-curvature element method. The slope deflection analysis assumed all base movement and rotation to be concentrated at the right base. The error in this assumption was reduced by the fact that only relative displacements were important and the rotation at the right base was much greater than the rotation at the left base. The moment diagrams obtained by both methods for H = 8.0 kips and V = 16.0 kips were as shown in Figure 7.14. Good correlation was obtained, particularly in the beam and right column.

The major difference in the results of the two methods was in the calculation of sidesway.

The slope-deflection analysis used a cracked section at ultimate load to determine the moment of inertia and the A.C.I. Code formula[3] to determine a secant modulus of elasticity. Horizontal sidesway predicted by slope-deflection equations for H = 8.0 kips and V = 16.0 kips was 0.463 inches.

The moment-curvature element method predicted sidesway of 0.880 inches. The deflection observed at the inside corner during the test was not recorded, but from observed dial gauge readings

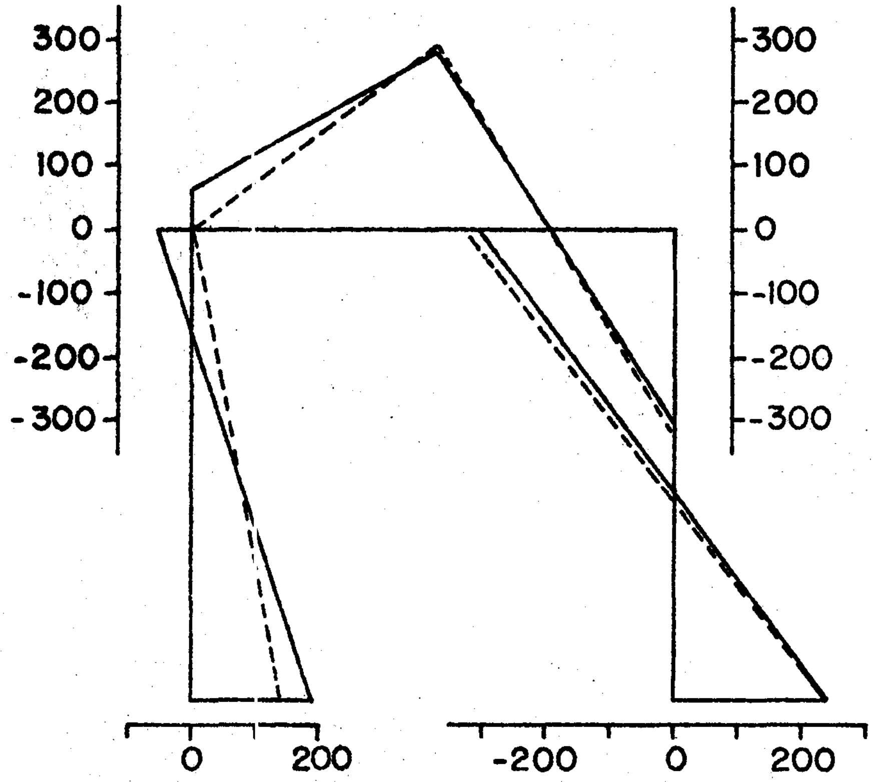

moments in inch-kips for a horizontal load of 8·0 K, vertical load = 16·0 K (8·0K is 89% of the load required to form the first hinge and 70% of the ultimate load.)

From slope deflection analysis - - - - - - -
From moment/curvature relationship ————————

Horizontal displacement of upper right hand corner –
from slope deflection = 0·463"
from moment/curvature = 0·880"

FIGURE 7·14 Frame R2 - predicted moments from moment/curvature proceedure and from elastic slope/deflection analysis.

40 inches and 80 inches above the column base, it was estimated that sidesway was 0.75 ± 0.05 inches.

Hence, the moment-curvature method overestimated deflection by about 17%, while slope-deflection underestimated deflection by about 39%.

Because axial forces in the frame were not large, secondary moments were not significant. However, in frames subjected to high column loads, the influence of secondary moments would be significant particularly where sidesway occurred. Hence, the moment-curvature method had definite preference over the slope-deflection analysis.

7.6. Numerical Integration Using Element Slices and Creep Data for Sustained loads.

7.6.1. Introduction

This procedure had many similarities to the moment-curvature element method. The frame model, and method of convergence to obtain geometric compatibility were the same for both analyses. The primary difference was that while the moment-curvature element method used the curvature of each element to determine the internal moment directly, the sustained load analysis used the strain distribution across each section.

The numerical procedure with element slicing and creep data was used to analyze both the short-term and sustained load behaviour of the test frames. It was also referred to as the second stage element method or sustained load element method. Since the procedures for summing the effects of the elements and changing the boundary conditions to obtain convergence were the same as for the moment-curvature element method, they are not described in detail in this Section.

7.6.2. The Solution of Forces, Moments, Rotation and Displacement for Each Element

7.6.2.1. Introduction

In the sustained load element method, the basic concept was that each element would be subject to strains due to "elastic" loading and strains due to creep. The forces and coordinates at the lower end of the element were known (by assumption for the first element, and by calculation for the others). The objective of this procedure was to compute the change in moment which occurred over the element length, and the displacement of the upper end relative to the lower end.

7.6.2.2. General Procedure

The following steps were used for the solution of the moment and displacement for each element:

(1) For initial loading, before creep had taken place, an "elastic" strain distribution was assumed across the upper section of the element

(2) The element was divided into a number of slices perpendicular to the plane of loading.

(3) The internal force (that due to stress) acting at the centroid of each slice was calculated from the "elastic" strain distribution. The total internal force was computed by summing the contributions of the slices.

(4) The calculated internal force was compared with the external force (the external force was the axial force in the member due to the applied loads). If these forces differed by more than 1%, the strain distribution was shifted by a constant amount based on the difference in them.

(5) Using this new strain distribution, the internal moment at the centroid of each slice was calculated. The total internal moment was obtained by summing these contributions.

(6) The external moment including that due to deflection was computed using equilibrium of the external forces and the moment at the lower end.

(7) The external and internal moments were compared. If they differed by more than 1%, the slope of the strain distribution was changed so as to correct the internal moment.

Steps (3) to (7) were then repeated until the internal force and moment differed from the external force and moment by less than 1%.

7.6.2.3. The Inclusion of Creep Strains

For time after initial loading, creep strains were present. Using the expression developed by Drysdale(5) for creep as a function of "elastic" strain, the creep strain on each slice was computed. For the first time interval, creep strain was calculated directly using the "elastic" strain and the time under load. For subsequent time intervals, the modified superposition method was used to include the effect of stress history. As used in the analysis the modified method of superposition may be explained as follows:

Consider the present "elastic" strain as ε_2 and the elastic strain at the end of the previous time interval as ε_1. The present time is T_2 and the time at the end of the last interval was T_1. The first part of the creep is that which existed at T_1 under strain ε_1 (computed by direct substitution if T_1 was the end of the first interval or by superposition for other intervals). The second part is the creep which would occur for an elastic strain equal to $\varepsilon_2 - \varepsilon_1$, for the period

$T_2 - T_1$ for loading at T_1. The third part is the creep which would occur for an "elastic" strain ε_2 for the period $T_2 - T_1$ considering this condition to exist since the beginning of loading. For increased stresses, these components are added directly to obtain the total creep. For decreasing stresses, that is for ε_2 less than ε_1, allowance is made for the irreversible portion of creep recovery. In this case the second part of the creep is reduced by one third and is substracted from the first and third parts. Creep recovery of two thirds was derived from the experimental results of Ross[20].

To solve for an element with creep present, the total strain distribution was assumed. The rotation of the element and the displacement of the upper end relative to the lower were calculated from the total strain at the top. The "elastic" strain was obtained by subtracting the computed creep strain from the total. Some error was introduced by the fact that creep was based on the "elastic" strain at one end of the element rather than at its centroid. This also applied to the deflection and rotation. However, because the iterative procedure averaged strains on the section, this error was small, and the amount of additional computer time required to correct it was not justified.

Once the "elastic" strain distribution had been obtained, the internal moment and force were calculated as described previously, in Section 7.6.2.2. The total strains were adjusted to equalize the internal force and moment with the external force and moment. After several cycles convergence was obtained and the total, elastic and creep strains for the element were stored. These were used as the starting point for the next element, and the procedure was continued around the frame as in the moment-curvature method of Section 7.5.

7.6.3. Concrete Strength

The influence of time on concrete strength was included in the sustained load analysis. The concrete strength was assumed to vary linearly from the time of loading for 120 days and then remain constant. The increase in strength was determined by cylinder tests the results of which were included in Appendix A.

7.6.4. Shrinkage

Shrinkage strains prior to loading and during the sustained load period were required.

Shrinkage strain at the time of loading was determined from the reinforced prism cast with the test frame. The stress in the concrete was calculated by the method described in Section 7.5.4.2.

During the sustained load test, shrinkage strains were based on an expression developed by Drysdale [5] from the results of a number of tests on plain concrete prisms. This analytic function, which had time as the dependent variable, was compared with data obtained from plain concrete prisms cast with test frame L1. The results of this comparison were presented in Figure 7.15. The scatter in experimental data for the two prisms was very severe, mainly because of difficulty encountered in obtaining adhesion between the Demec points and the concrete during curing. However, it was evident that the expression overestimated shrinkage somewhat. This was not unexpected, since the section used by Drysdale was smaller than that of the frames used in this investigation. The error associated with shrinkage is discussed in more detail in Section 9.3.4.

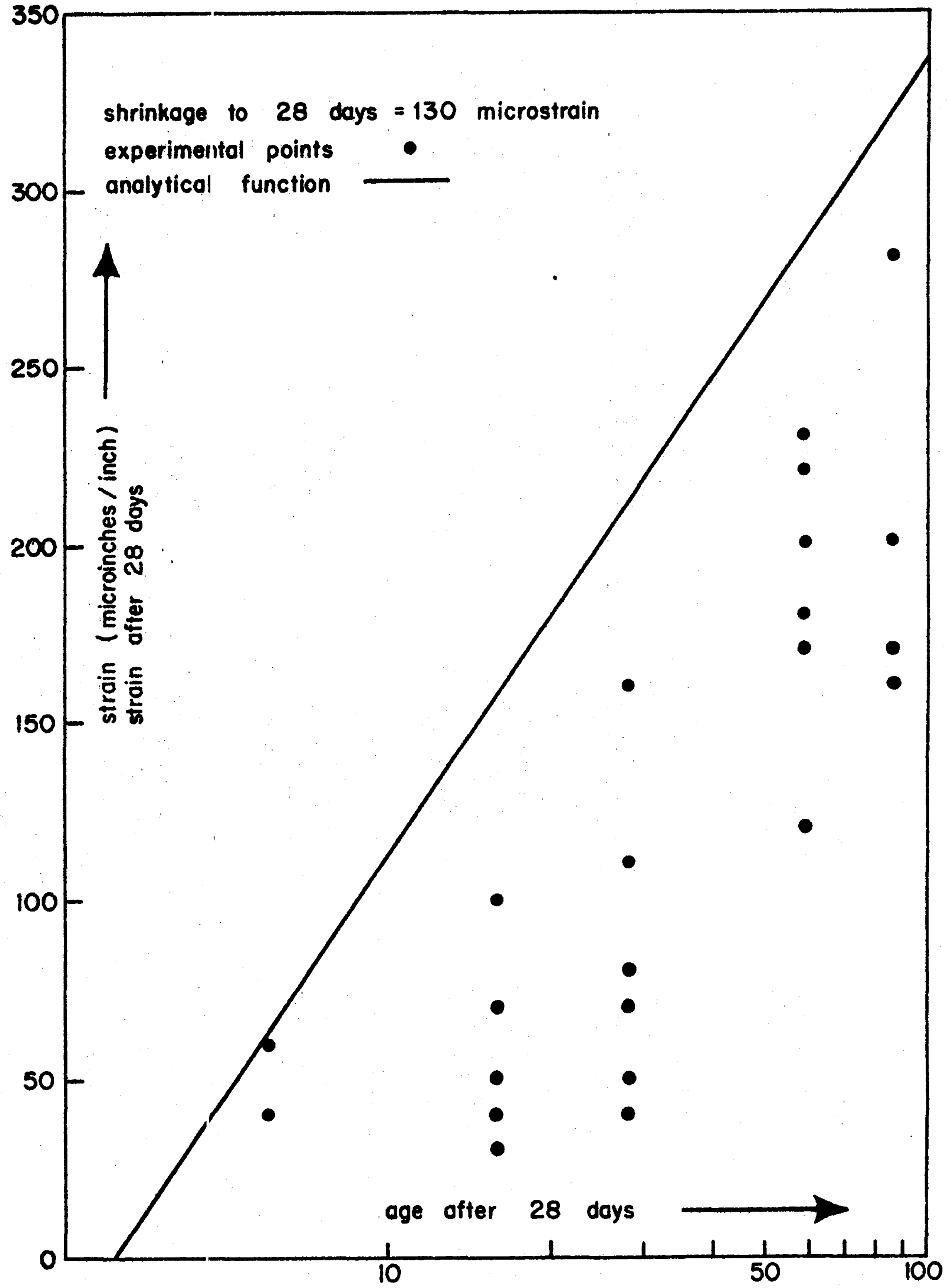

FIGURE 7·15 Shrinkage strain for frame L1

7.6.5. Changes in Load

There were four load conditions possible:

(1) short-term load to a sustained load level

(2) sustained load for a period of time

(3) short-term load from one sustained load to another sustained load

(4) short-term load to failure

The method was developed in such a way that the loads could be varied to coincide with the test conditions. For sustained load test L1, the loading program consisted of a short-term load phase to sustained loads H = 6.0 kips and V = 12.0 kips, followed by a sustained load period of 53 days. This was followed by a short-term increase to H = 7.5 kips and V = 15.0 kips. These loads were maintained for an additional 28 days. Then the frame was loaded to failure.

By varying the input data, this loading program or almost any other could be accomodated.

For frame L1, a solution was first obtained for short-term loading to H = 6.0 kips and V = 12.0 kips. Sustained load calculations were made for times of 11, 18, 30 and 53 days after loading. Then the frame was analyzed for short-term loading to H = 7.5 kips and V = 15.0 kips. This was followed by sustained load solutions at 66 and 81 days. At 81 days, short-term calculations were performed for horizontal forces 8.0, 8.5 and 9.0 kips with vertical forces twice these magnitudes. The first plastic hinge was obtained at H = 9.0 kips and V = 18.0 kips.

The main limitation of the analysis as developed for this investigation was that it did not apply beyond formation of the first hinge.

Chapter 8

COMPARISON AND EVALUATION OF RESULTS

8.1. Introduction

The data recorded from all frames tested was in the form of concrete strains from Demec readings and deflections obtained from dial gauges. For initial short-term tests prior to sustained loading, the strains were converted to moments using a similar procedure as that used in determining the moment-curvature relationship. Concrete strains obtained from sustained loading and subsequent quick loading to failure were used to obtain extreme fibre strains. These formed the basis for comparison between the test and theory. In all cases, the deflected shape of the frame was predicted for various loading conditions, and was compared with the dial gauge readings.

Some sources of error which directly effected the presented results are discussed in this Chapter. A further study of the precision in results obtained is contained in Chapter 9.

8.2. Moments Calculated from Demec Readings

The procedure for calculating moment from strains obtained from Demec readings used a strain distribution across the section based on the gauge points in the compression zone. As in the analytic moment-curvature method, stress-strain relations for concrete and steel were assumed. Using these relations and the developed strain distribution, the axial force and moment were computed at each gauge location for each loading condition.

Shrinkage measurements on reinforced prisms from the time of casting to testing were used to compute the unloaded condition at each section.

Shrinkage measurements from the reinforced prism were considered as compressive strain in the steel. From this strain, the total compressive force in the steel was computed and set equal to the tensile force in the concrete, from which an equivalent tensile strain in the concrete was calculated. This shrinkage strain was considered constant throughout the test. This procedure was the same as that described in Section 7.5.4.2.

A fortran program was written to convert Demec readings to moments by this process. Input consisted of the section properties, steel yield stress, concrete cylinder strength, shrinkage strain and the Demec readings with their locations for all sections and loadings. Moment, curvature, location of neutral axis and axial force were output. Since the axial force at each section could be approximated from an elastic solution, the values calculated in the program provided a means of evaluating the relative accuracy of the strain distributions from Demec readings. The precision of this procedure is discussed in detail in Section 9.4. A listing of this computer program is included in Appendix B.

8.3. Extreme Fibre Strains from Demec Readings

Because of the influence of creep, moments could not be computed from Demec readings obtained from sustained load testing. Hence, under these conditions, predicted extreme fibre strains were compared with those obtained from the Demec gauge points. Using readings from the compression zone, a linear strain distribution across the section was computed. Although it was not used directly, the strain at the level of the tension steel was obtained from Demec measurements and was compared with the computed strain at this point.

In order to process the large quantity of data obtained from the test, a short fortran program was written. This is included in Appendix B.

The precision of this procedure is discussed in Section 9.6.

8.4. Frame R2

8.4.1. Introduction

For the short term test, predicted moments were compared with those obtained from Demec readings, and the predicted deflected shape was compared with member displacements at dial gauge locations.

8.4.2. Moments from Testing and Analysis

The moment distribution on the frame from Demec readings and as computed using the moment-curvature relationships and elemental procedure was as shown in Figure 8.1. It should be noted that Demec gauge points were located only at critical sections (i.e., the column ends, corners and beam centre). Experimental curves were derived by passing straight lines through the calculated points; hence, over the large spans between critical sections, a linear moment variation was postulated. Another important factor in evaluating results was the fact that the error in reading the Demec was generally within ± 5 micro strain. Hence, the error in moment calculated from strains of 50 microstrain was 10 times that for strains of 500 microstrain.

A third source of error concerned the column ends. The lowest Demec point was located just above the wideflange base and was therefore vulnerable to any unusual cracking or other influences produced by the behaviour of this base.

Comparison of moments acting on the loaded column indicated the effect of the various sources of error. The Demec reading four inches above the bottom showed a sharp increase in moment. This sharp increase was probably caused by the wideflange base. There was generally close agreement between the prediction and experimental value for the gauge location twelve inches above the steel base. The deviation present at the top of the column was probably due to the error in Demec reading which had considerable influence in this low moment region.

Predicted values were computed up to the formation of the first plastic hinge, since this was the limit of the analytic method. Beyond the first hinge only experimental results were presented.

Because the analytic frame model could be made to closely approximate the actual structure of the upper part of the frame, and because the strains were large enough to reduce Demec error, the correlation between predicted and experimentally derived moments in the beam was fairly close. Some of the discontinuous appearance of the curves was attributed to true non-linear behaviour of the structure, particularly as plastic deformation was produced, but much of this was more likely caused by Demec errors. The results were represented by drawing lines through points determined directly from the experimental data. There was no attempt to adjust the data or to produce smooth curves.

The difference between predicted and experimental moments was greatest in the unloaded column. A possible reason could be due to the steel base both as it effected the bottom Demec reading and caused uncertainty in determining accurately the magnitude and influence of its rotation. Also, since plastic deformation occurred first at the upper right corner (unloaded column), inelastic strains there developed at relatively low loads. The influence of cracking on Demec errors could be observed at this corner. Even at the working load level there appeared to be a decrease in moment very near the corner where moment would be expected to be a maximum. This could be attributed to the development of a crack pattern at the corner which produced apparent strain between the Demec points which was not indicative of the true configuration. As shown in Figure 8.1., this condition worsened as load increased and cracking became more intensive.

8.4.3. Deflections - Predicted and Experimental

The relationship between deflection and load at the dial gauge locations as determined by the moment-curvature element method and by the test was as indicated in Figure 8.2. Predicted deflections were obtained only up to formation of the first hinge which occurred at H = 9.0 kips and V = 18.0 kips according to the analysis (because of the beam deflection, the deflection at the top of the loaded column, had to exceed that at the top of the unloaded column). However, the deflection at location E, 80 inches above the base of the unloaded column, was greater than the deflection at B, 80 inches above the base of the loaded column. This condition was explained by the greater reverse curvature of the unloaded column. Good correlation was obtained between theoretical and observed deflection of the loaded column. The moment-curvature method underestimated the vertical displacement at the centre of the beam particularly at higher loads. This could probably be attributed to the condition imposed that corners of the frame remain right angles during loading which caused a negative curvature at the right corner. This negative curvature reduced the positive curvature

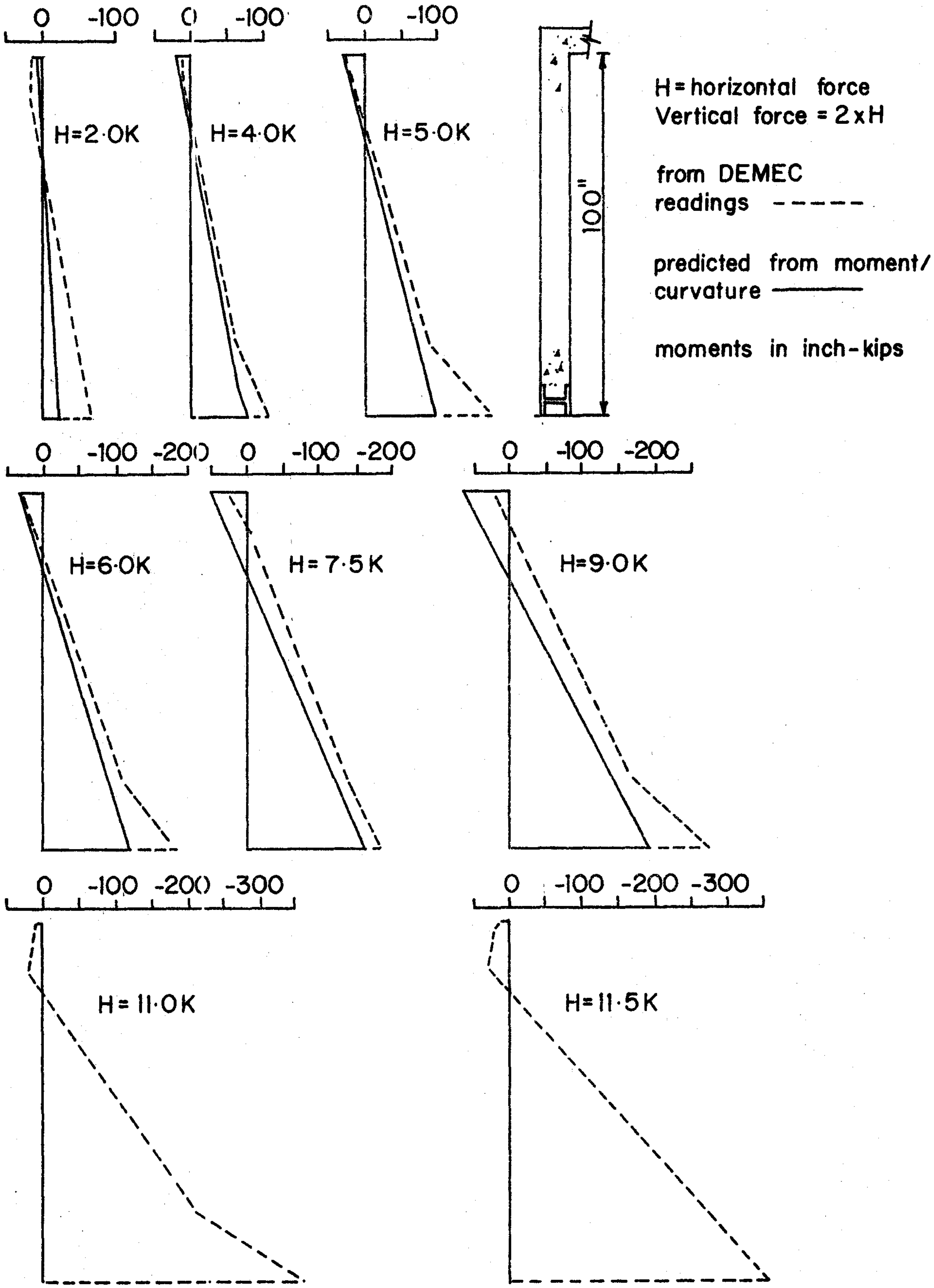

FIGURE 8·1(a) Frame R2 - moments. Loaded column.

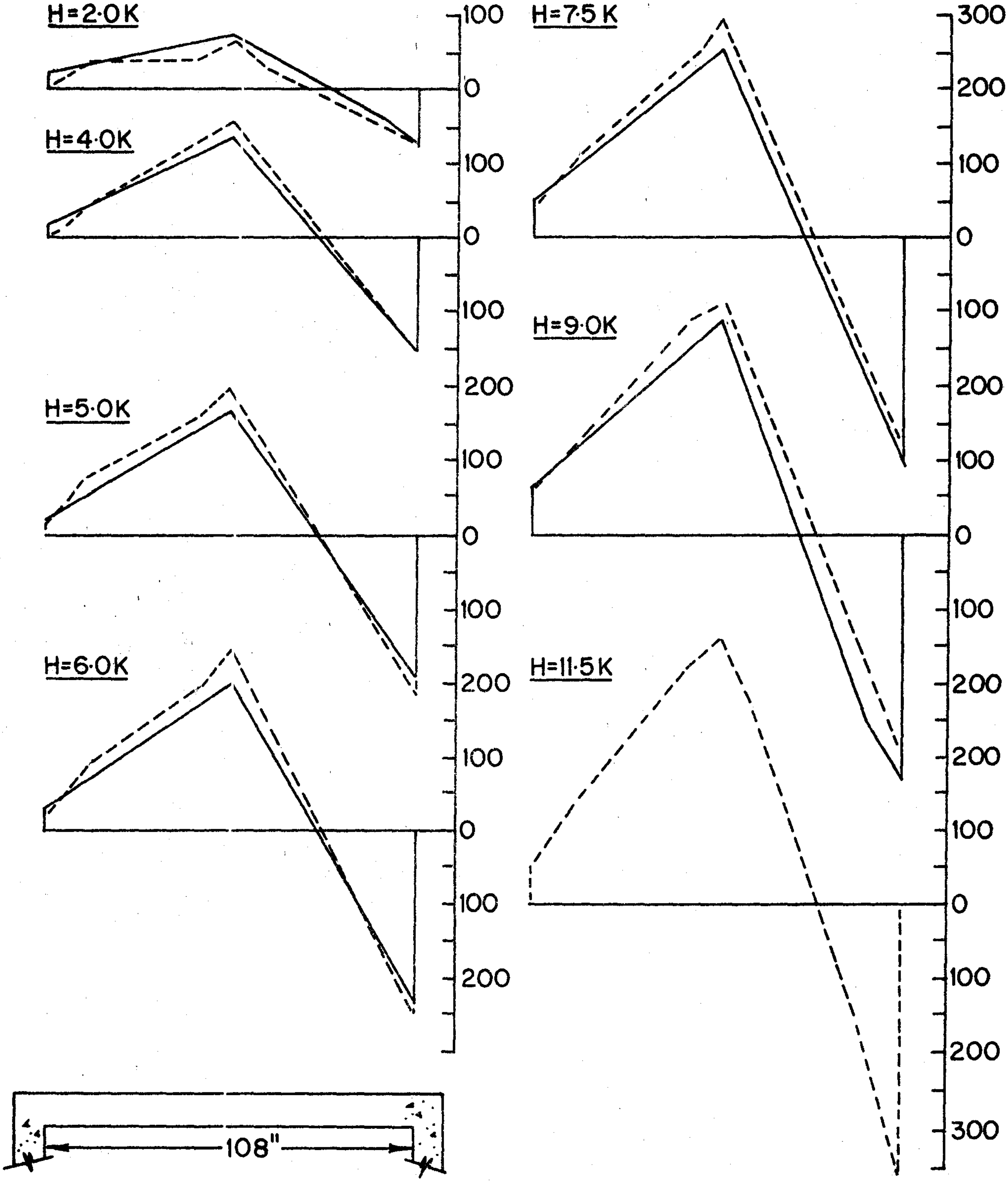

H = horizontal force
Vertical force = 2 x H
From DEMEC readings ----
predicted from moment/curvature ——

FIGURE 8·1(b) Frame R2 - moments. Beam.

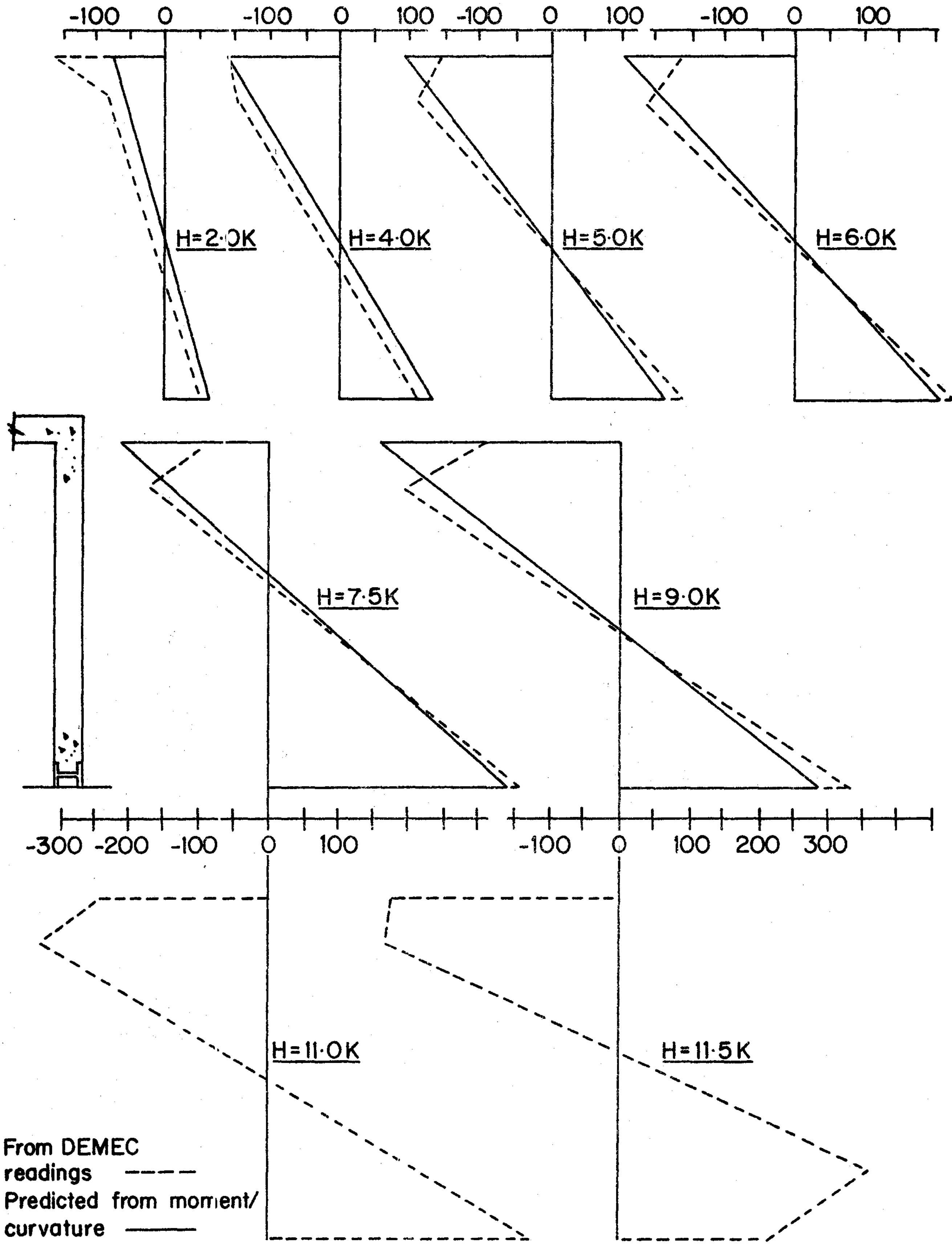

FIGURE 8·1 (c) Frame R2 - moments. Unloaded column.

McMASTER UNIVERSITY LIBRARY

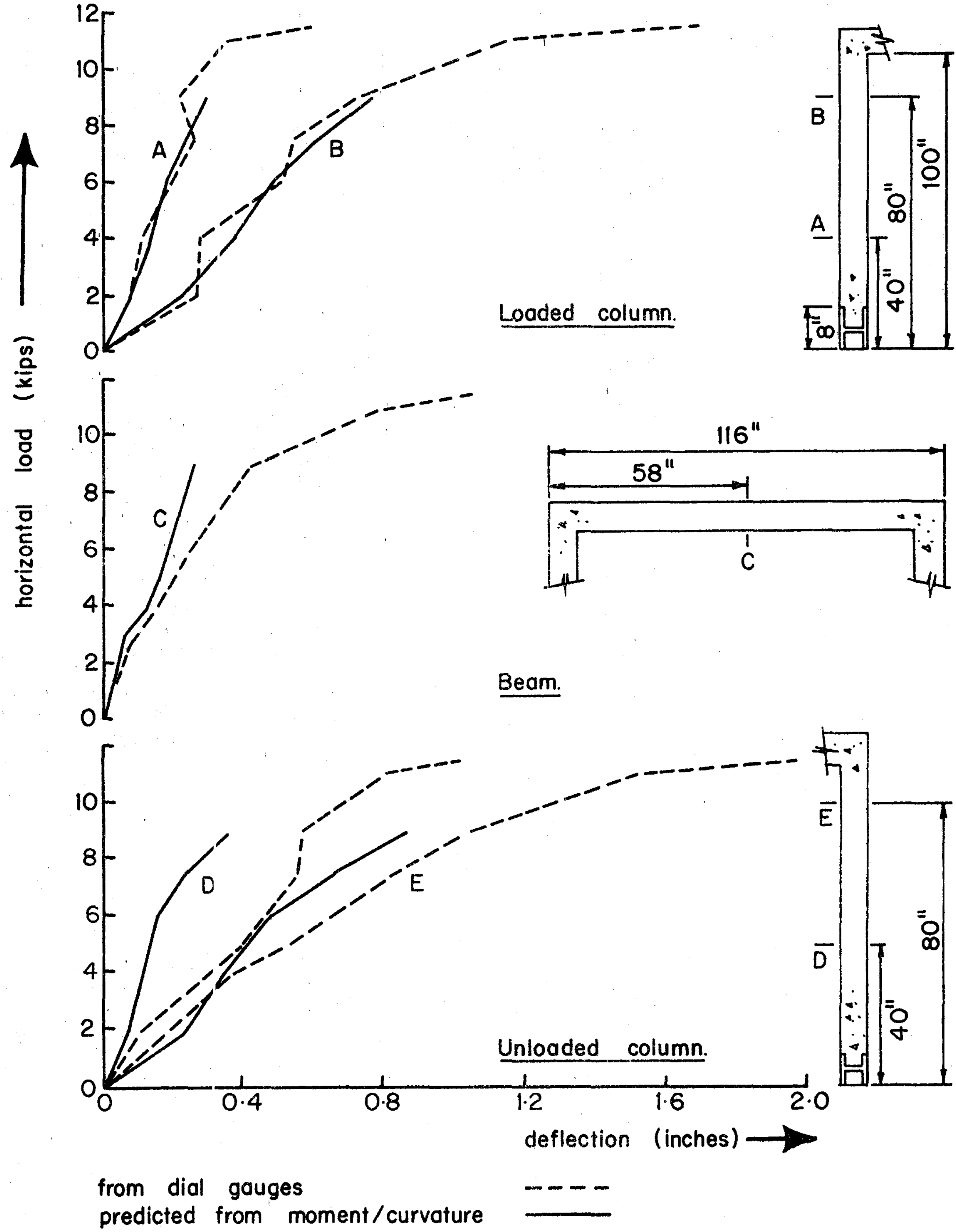

FIGURE 8·2 Frame R2 - deflection.

at midspan thus reducing the beam deflection. During the test it was observed that some inelastic deformation of the right corner occurred at relatively low loads (about H = 5.0 kips and V = 10.0 kips) so that the corner did in fact undergo rotation which increased with load. This rotation had the effect of reducing the negative curvature at the corner which allowed greater deflection of the beam. It was concluded that the difference between theory and experiment in this case was caused by deviation of the real frame from the analytic model, a condition which could be improved by further stiffening the corner.

Fairly good correlation was obtained for the upper deflection point of the unloaded column. However, it appeared that the deflection recorded at D, 40" above the base of the unloaded column was in error.

Figure 8.3. shows the predicted deflected shape of frame R2 for various load levels. As in all analyses, the midspan vertical load was double the horizontal load.

Reversal in curvature was almost negligible for the loaded column but was significant in the beam and unloaded column particularly at higher loads. Maintenance of 90° corners by the analysis may have been unrealistic at high loads since the actual test frame, even with heavily reinforced corners, did not adhere to this condition. The error in this assumption was not severe up to the formation of the first hinge, but following hinge development, the corner rotation became significant and the moment capacity dropped considerably. The fact that the deflection of the top of the unloaded column was almost identical to that at the top of the loaded column, which indicated almost no decrease in beam span, was as indicated in Figure 8.3.

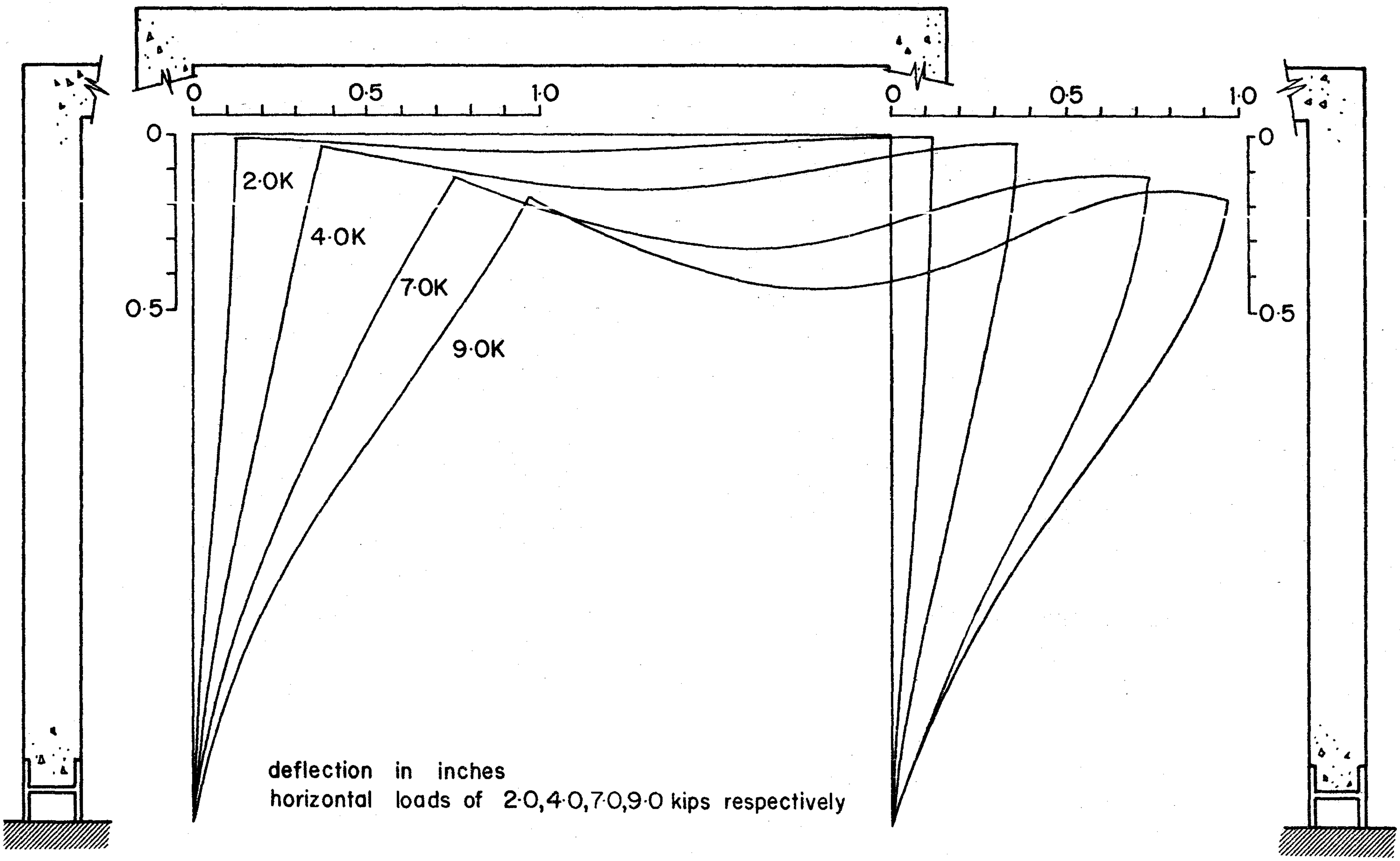

FIGURE 8.3 Frame R2 - predicted deflected shape from moment/curvature.

8.5. Frame L1

8.5.1. Introduction

For frame L1, both an initial short-term test and a sustained load program were provided.

The predicted moments and deflected shape for the short-term test were compared with experimental results as was done with frame R2.

For the sustained load test, the predicted extreme fibre strains and deflected shape were compared with the experimental results.

8.5.2. Short-Term Test

8.5.2.1. Introduction

The results of the short-term test on Frame L1 were compared with both analytic procedures, the moment-curvature method and the sustained load element method. Experimental moments were calculated from Demec gauge readings as described in Section 8.1.

A comparison between moments and deflections obtained by the two methods of analysis was made as shown in Figure 8.4. The moment curvature procedure predicted slightly greater member flexibility than the sustained load method since the former indicated greater changes in member curvature. There was very close correlation between deflections calculated by the two methods. Because of the greater predicted stiffness, the sustained load method yielded slightly lower deflections than the moment-curvature analysis.

8.5.2.2. Moments from Demec Readings and Predicted by Moment-Curvature Method

The short-term moment distribution on frame L1 was as shown in Figure 8.5. for H = 6.0 kips and V = 12.0 kips. Good correlation was

LOCATION		MOMENT-CURVATURE METHOD		SUSTAINED LOAD ELEMENT METHOD	
		MOMENT(IN-K)	DEFL'N (IN)	MOMENT	DEFLECTION
LEFT BASE	(1)	-123·35		-120·06	
UPPER LEFT COR.	(2)	18·83	0·486 →	25·70	0·472 →
BEAM CENTRE	(3)	198·16	0·173 ↓	204·34	0·157 ↓
UPPER RIGHT COR.	(4)	-223·86	0·485 →	-218·22	0·450 →
RIGHT BASE	(5)	179·71		174·06	

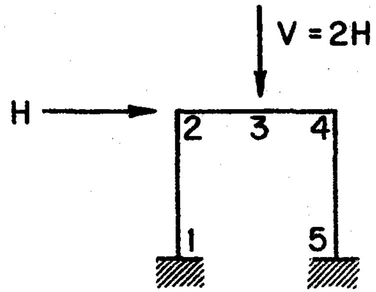

location key

Horizontal force = 6·0 kips
Vertical force = 12·0 kips
arrow denotes direction of deflection

FIGURE 8·4 Frame L1 – short term moments and deflections.

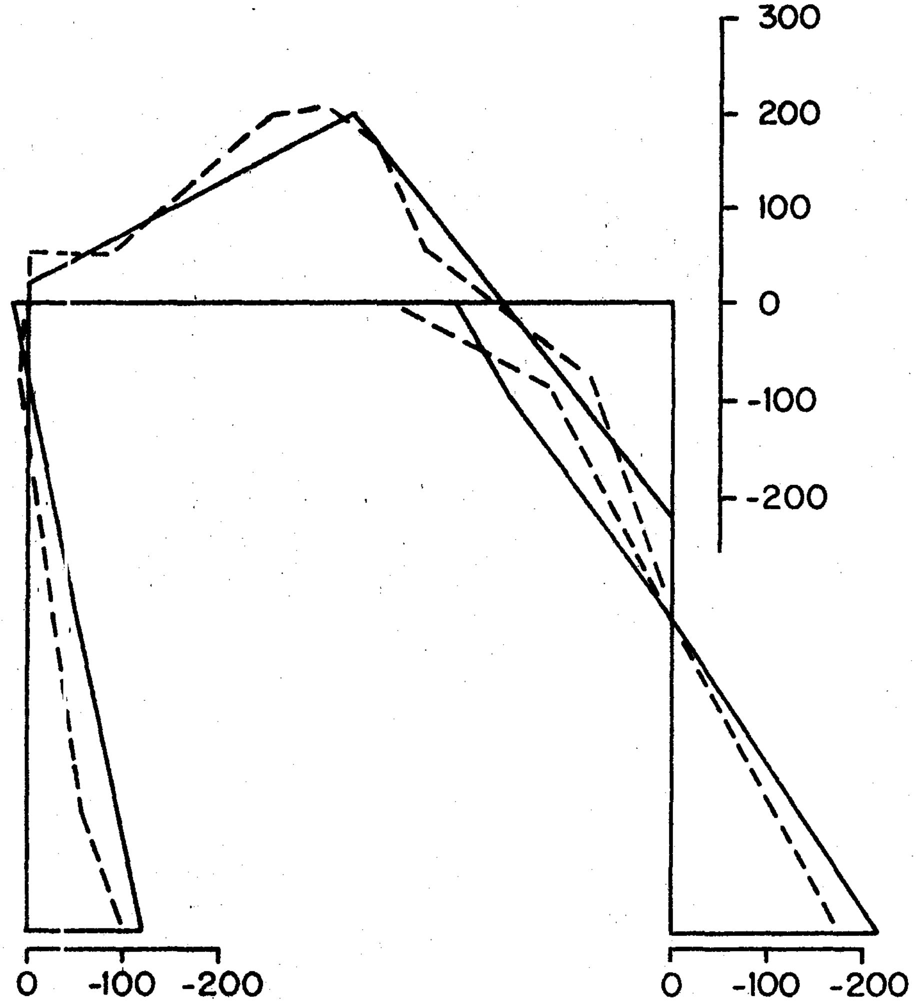

— — — — from DEMEC readings
——— from moment-curvature method
short term load H = 6·0 K, V = 12·0 K
moment in inch-kips

FIGURE 8·5 Frame L1 – moments.

obtained between the prediction from the moment-curvature procedure and the experimentally derived moments. It appeared that the analysis slightly underestimated the moment at the upper right corner and overestimated the moments in the bases. The effect of crack patterns on the Demec readings may have caused an experimental overestimate of moment at the upper right corner. The error in determining base rotation from the two dial gauges on each base could have contributed significantly to the difference in base moments.

8.5.2.3. Deflected Shape Predicted by the Moment-Curvature Method and Recorded by Dial Gauges

The deflected shape for the short-term test on frame L1 was as shown in Figure 8.6. The prediction was very good for the loaded column and the beam; and was fairly good for the unloaded column.

8.5.3. Sustained Load Test

Since, under sustained load, there was no way of computing "elastic" strains from the total strains obtained from the Demec readings, without knowing the creep, moments could not be used as a means of comparison. Instead, total strains obtained experimentally were compared with total strains calculated by the sustained load element method. The point taken for comparison was the extreme compression fibre. Member deflections from dial gauge readings and the predicted deflected shape were also investigated. Frame moments predicted by analysis for the load sequence performed on frame L1 were computed and evaluated on the basis of the correlation between experiment and theory for total strains and deflections.

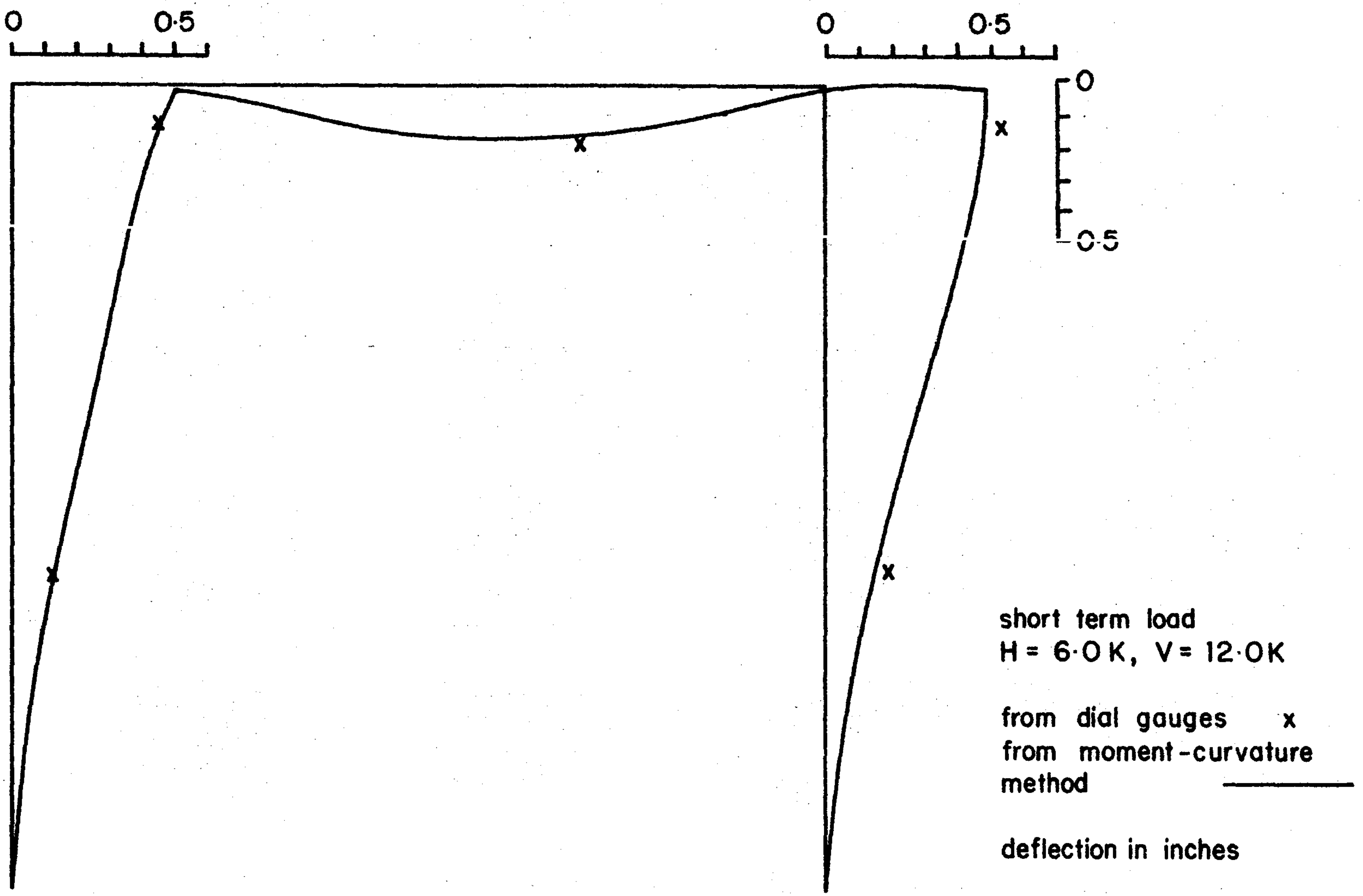

FIGURE 8·6 Frame L1 - short term deflected shape.

8.5.3.1. Moments by the Sustained Load Element Method

The moment distribution on frame L1 was as indicated in Figure 8.7. for the sustained load test. The moment diagram for the loaded column indicated a decrease in moment at the base with time for the sustained loads H = 6.0 kips and V = 12.0 kips. The rate of change in moment decreased rapidly with time. Similar behaviour was observed for moment at the second sustained load level of H = 7.5 kips and V = 15.0 kips.

Under sustained load of H = 6.0 kips and V = 12.0 kips from the start of testing to 53 days, the base moment at the left column decreased by 9%. For sustained loads of H = 7.5 kips and V = 15.0 kips, from 53 days to 81 days, the moment at the left column base decreased by 4%. The figure also included moments calculated for H = 8.0 kips and V = 16.0 kips as well as H = 9.0 kips and V = 18.0 kips.

There was very little change in moments in the beam during the two sustained load periods. However, a very slight increase (about 1%) in both the positive and negative moments was noted with time.

Moments in the unloaded column also changed very little during the periods of sustained loading. Ultimate moment was reached at the top of the unloaded column at H = 9.0 kips and V = 18.0 kips. The loads at which the first hinge occurred were in agreement with those predicted.

8.5.3.2. Extreme Fibre Commpressive Strains from Demec Readings and from the Sustained Load Element Method

The strains at the extreme compression fibre computed from

FIGURE 8·7(a) Frame L1 - predicted moments including creep. Loaded column.

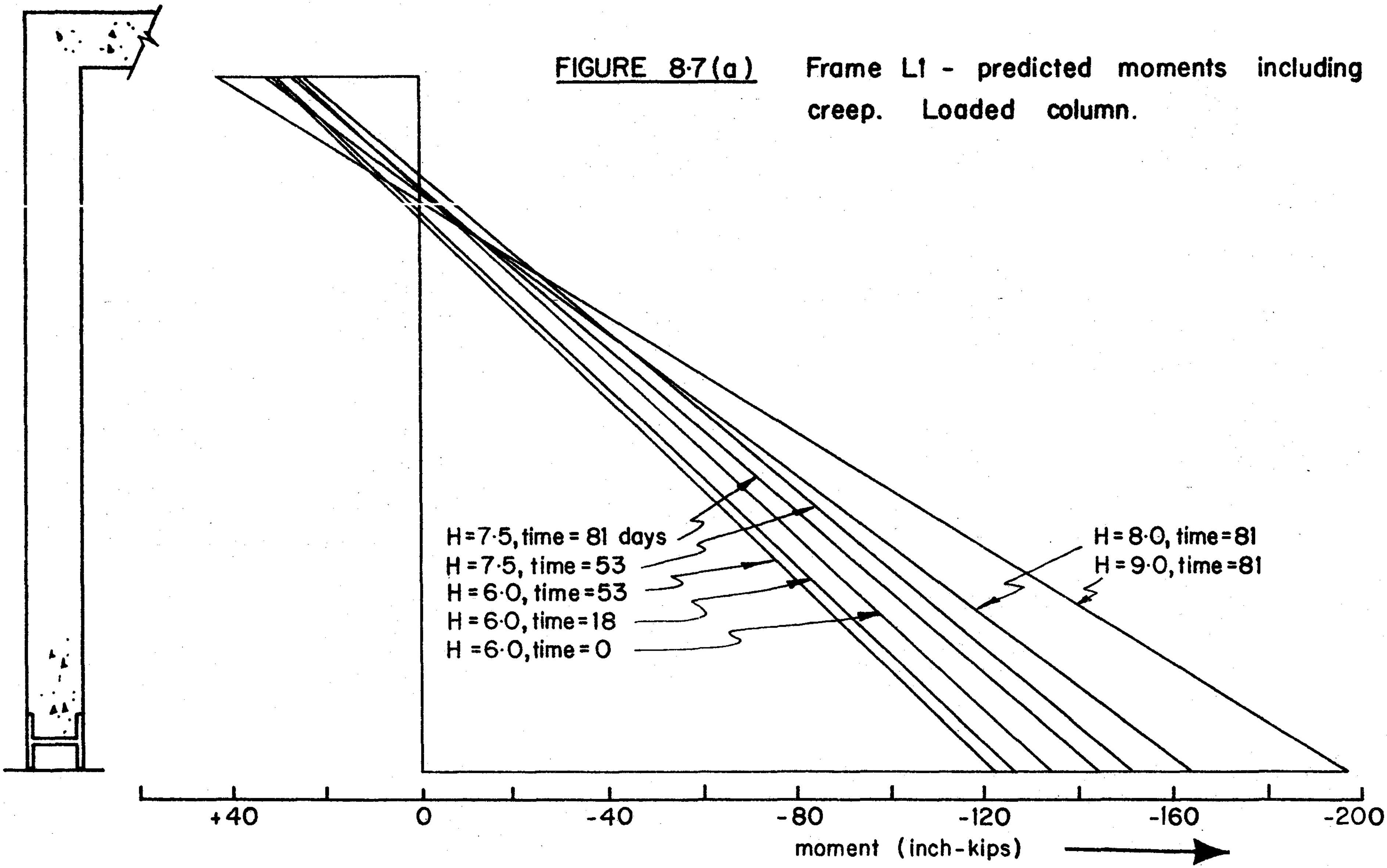

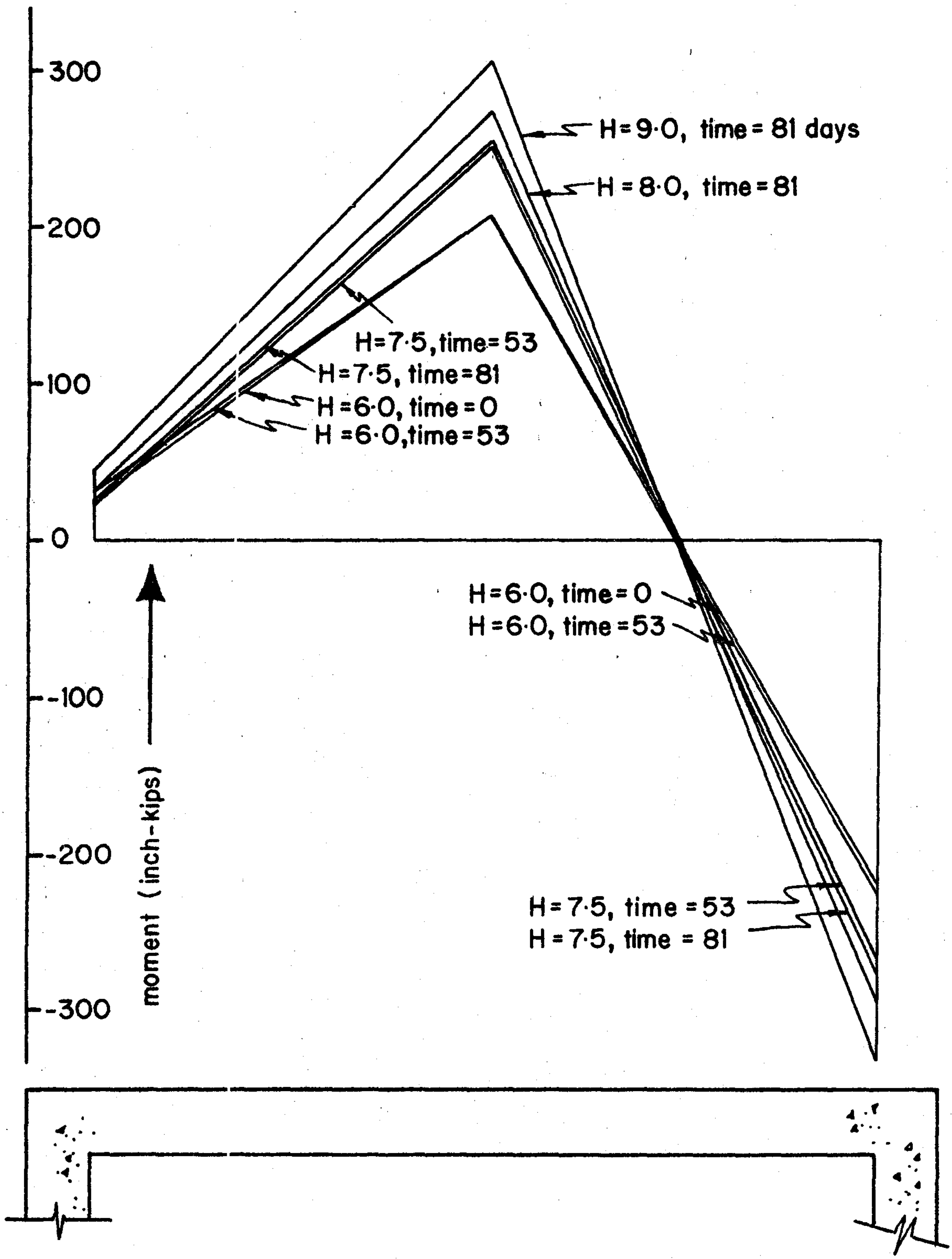

FIGURE 8·7(b) Frame L1 - predicted moments and creep. Beam.

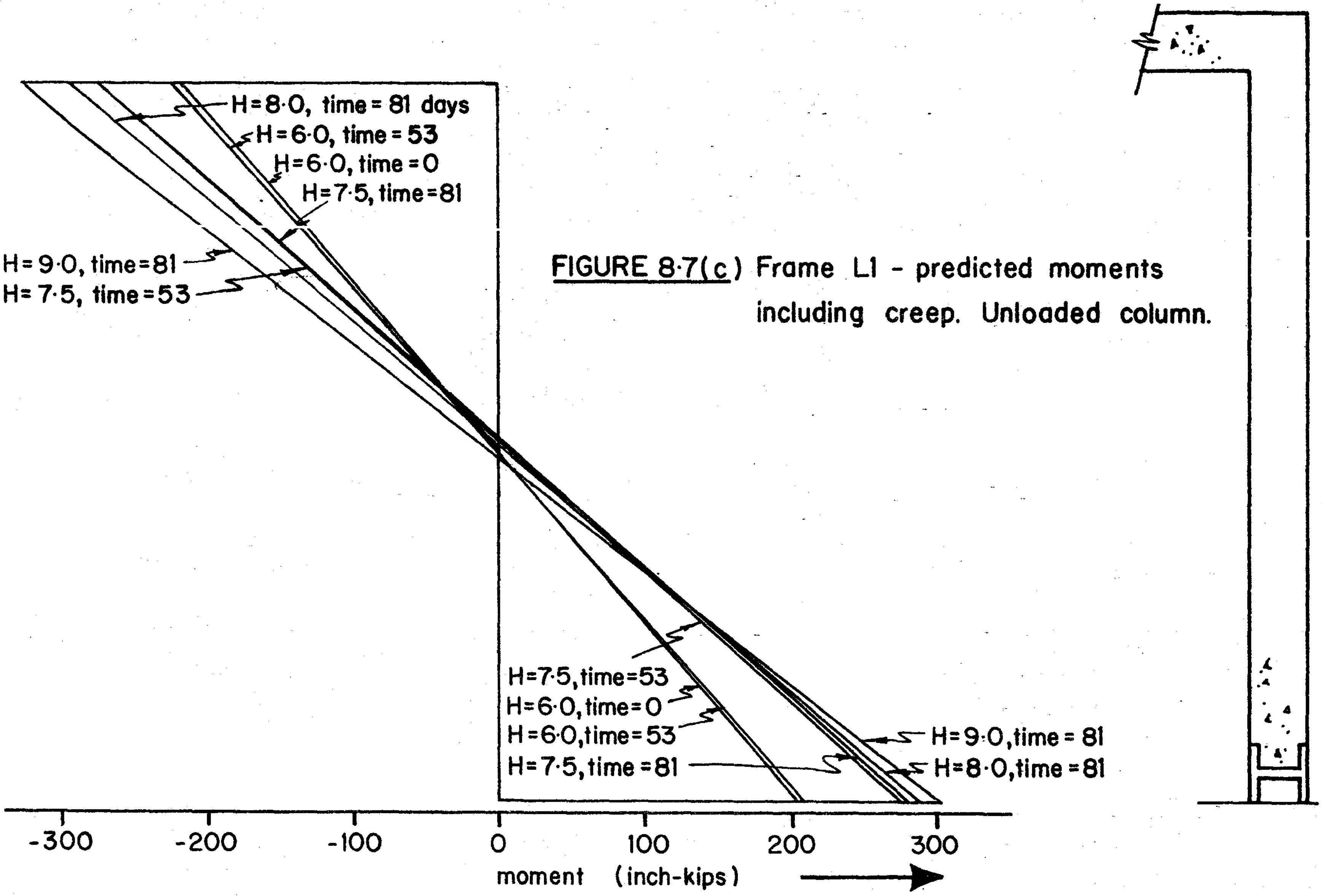

FIGURE 8·7(c) Frame L1 - predicted moments including creep. Unloaded column.

Demec readings by the method described in Section 8.2. and as determined analytically were as shown in Figure 8.8. The best agreement was expected at high strain regions since the error in Demec readings was of relatively constant magnitude except where cracking occurred.

Good correlation was obtained for strains at the base of the loaded column and at all points in the unloaded column. Fairly good agreement occurred in the beam. Because of the large error associated with Demec readings for small strains, the correlation at the top of the loaded column was not good. Part of the reason for this difference was due to the method of computing extreme fibre strains from the Demec readings. The Demec points indicated compression at both sides of the section as shown by the analytic procedure, but the computer program for processing Demec data could calculate the condition at one surface only.

Under a sustained load of H = 6.0 kips and V = 12.0 kips for the first 53 days of the test, the strain predicted at the compression fibre of the left base increased 200%. During the same period the predicted compressive strain at the top of the beam increased 186%. Other increases in predicted compressive extreme fibre strains were: 200% at the right end of the beam, 193% at the top of the right column and 223% at the right column base.

The predicted percentage increases were consistent with experimental results. In almost all areas, the predicted strains were greater than the strains obtained from Demec readings. The maximum differences between predicted strains and experimental strains for the first sustained load period were: 28%*at the left column base, 18% at midspan of the beam, 38% at the right end of the beam, 2% at the top of the right column and less than 1% at the bottom of the right column. These were the worst correlations; most of the results gave better agreement between the theory and experiment.

The increases in predicted extreme fibre strain for a sustained load of H - 7.5 kips and V = 15.0 kips for the period 53 days to 81 days were: zero at the left column base, 7% at midspan of the beam, less than 1% at the right end of the beam and the top of the column, and 8% at the base of the right column. Maximum difference between predicted strains and experimental strains for the second sustained load period were 6% at the left column base, 36% at midspan of the beam, 30% at the right end of the beam, 15% at the top of the right column, and 12% at the right column base.

The compressive strains for the short-term load to failure at 81 days after the start of the test were as indicated in Figure 8.8. The ultimate load capacity of frame L1 at 81 days was H = 12.6 kips and V = 25.2 kips. This was 8.7% higher than the ultimate load for the short-term test frame R2. It was felt that this increase in capacity was partly due to the increase in concrete strength with time and the fact that, with the low secondary moments, creep did not have adverse effects on frame behaviour.

8.5.3.3. Frame Deflections from Dial Gauges and Sustained Load Element Method.

Deflections at dial gauge locations from the theory and experiment for the sustained load periods were as shown in figure

---

* Percentages were obtained by taking the differences in strain over the lesser of the two strains.

8.9. The deflections at E, 88" above the base of the right column, exceeded the deflections at B, 89" above the base of the left column, because of the greater curvature of the right column.

The experimental results were always greater than the prediction except at the top of the left column up to 25 days after the start of the test. The difference was particularly noticeable during the second sustained load period from 53 to 81 days. Very slight increases in deflection were predicted for this time interval. Since there appeared to be very little change in strains over this period, this would seem to be a consistent result. It was concluded that inelastic rotations at the forming hinge locations, particularly the beam centre, right column top and right base, were responsible for the larger observed deflections.

Both the analysis and test results indicated a considerable increase in deflection for the first sustained load period, particularly up to 30 days after the start of loading. From the starting point to 53 days, the deflection 89 inches above the base of the left column increased from 0.45 to 0.60 inches - a change of 33%. During this period, observed midspan deflection of the beam increased 40% from 0.29 to 0.41 inches and observed sway 88 inches above the base of the right column increased 55% from 0.45 to 0.70 inches. For the period from 53 to 81 days, observed deflection increases were 6% near the top of the left column, 13% at midspan of the beam and 7% near the top of the right column.

The deflections for the short-term load to failure test following sustained load were as shown in Figure 8.10. The sustained load element method predicted deflections less than those which were observed probably because the frame was subject to considerable inelastic deformation prior to the formation of the first hinge.

The predicted deflected shape of frame L1 for the sustained load test was as shown in Figure 8.11. The point of formation of the first hinge was at the upper right corner. Although a significant increase in deflection took place during the sustained load period from 0 to 53 days, there was no change during the higher load interval from 53 to 81 days.

Most creep activity took place during the first month under load. The rate of creep decreased with time as indicated by Figure 8.9. After 53 days very little change was taking place. Increasing the loads at 53 days by 25% did not appear to cause significant change. Even with the higher stress level, it would appear that the rate of creep was so low from 53 to 81 days that the creep strain did not increase as quickly as the growth in concrete strength.

8.5.3.4. Creep Collapse

A solution was obtained for the sustained load behaviour of the frame with H = 8.5 kips and V = 17.0 kips for times of 20, 60, 120, 240, 480 and 960 days. The applied load was 94.5% of the load predicted to form the first hinge, and 67.5% of the experimental ultimate load for frame L1. The predicted horizontal sway increased from 0.585 inches initially to 1.108 inches after 960 days. During the sustained load period there was no significant redistribution of moment, and no trend toward formation of the hinge.

8.5.3.5. Summary of Sustained Load Test L1

As predicted by the analytic method, there was very little change in moment distribution for a load of 47.5% of ultimate* sustained for 53 days followed by a load of 59.5% of ultimate sustained for an additional 28 days. However, during the first sustained load period compressive strains at high moment regions increased about 200% and sidesway increased by one third. During the second sustained load period, compressive strains at high moment areas increased less than 8% and sidesway increased by 7%.

8.6. Resume

Data from the frame tests was in the form of Demec readings used to determine strains and moments, and dial gauge readings for member deflections.

It was felt that the most valid comparison for evaluation of the analysis was provided by the deflections. The following reasons were given for this.

(1) The errors in reading dial gauges were much less than those associated with Demec readings.

(2) Data from dial gauges could be used directly, whereas Demec information had to be converted to strain distributions or moments by calculations which introduced further sources of error.

(3) The analytic computation of deflection was accomplished with the same accuracy as the calculation of strains and moments.

(4) Even with low secondary moments, and very little redistribution, creep had a significant influence on deflections.

---

* The ultimate load referred to was the capacity of the frame at 81 days.

(5) Since the prediction of deflections normally required calculation of the member stiffnesses, the use of deflections provided a realistic evaluation of conventional methods such as slope-deflection equations.

For loads 11 % less than required for formation of the first plastic hinge, using member stiffnesses based on the provisions of the Code (3), slope-deflection equations predicted sidesway for short-term loading about one half the observed deflection. For the same case, the moment-curvature element procedure provided an accurate prediction.

The sustained load element method provided the only prediction of deflection due to creep. It slightly underestimated member displacements due to creep and changes in the level of sustained loads. This was probably caused by the inability of the method to account for inelastic rotation within the "joints" which in this study were at the corners, bases and midspan of the beam.

For short-term loads, the moment distributions on the frames were predicted by both the moment-curvature and sustained load element programs. Good agreement was obtained by both methods with the experimental results from Demec readings.

Extreme fibre strains computed by the sustained load element method were generally in accord with those derived from Demec readings within the precision of the tests. The analytic procedure for the investigation of the influence of creep also indicated the following conclusions for the particular frame and sustained load program studied:

(1) Redistribution of moments due to creep was not significant.

(2) Member displacements increased substantially (as much as 40%) during sustained loading.

(3) Strains produced in the concrete by creep were of the same order of magnitude as the strains caused by the applied stresses.

These conclusions were substantiated by the test results. Hence, it was concluded that the element procedures provided realistic approximations for frame behaviour under short-term and sustained loads, within the limitations imposed by the precision of testing and analysis.

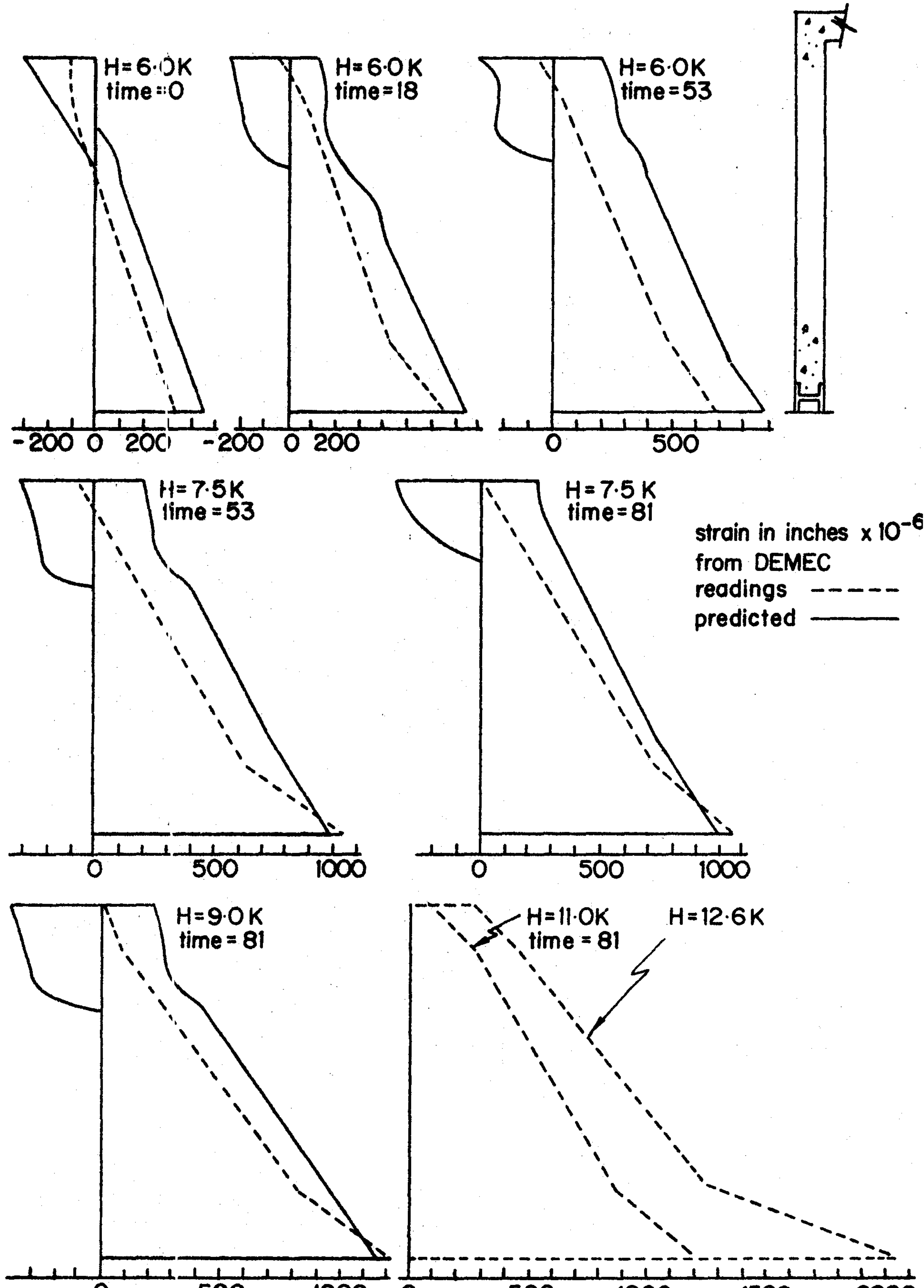

FIGURE 8·8(a) Frame L1 - compressive strain at extreme fibre.

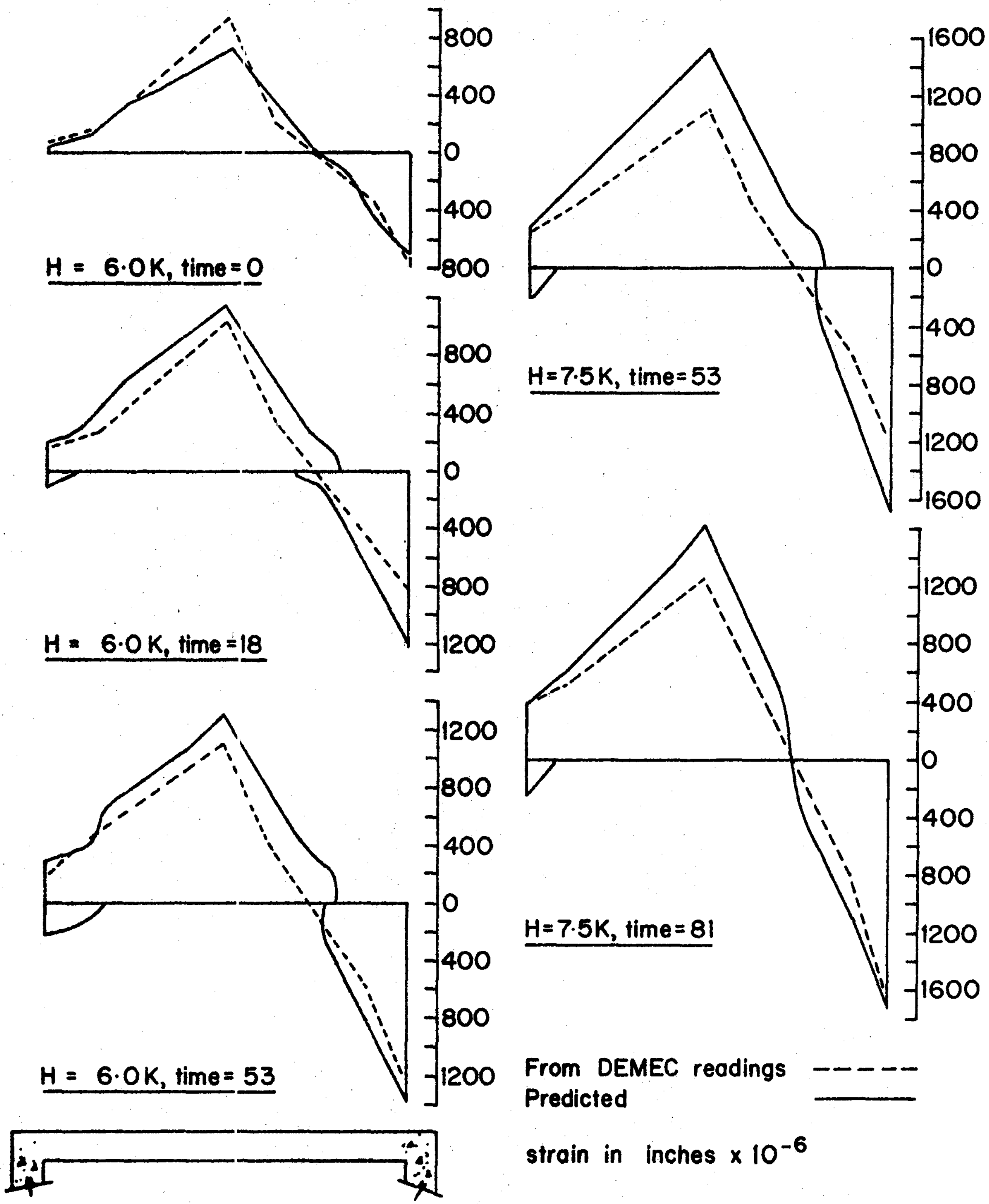

FIGURE 8·8(b) Frame L1 - compressive strain at extreme fibre. Beam.

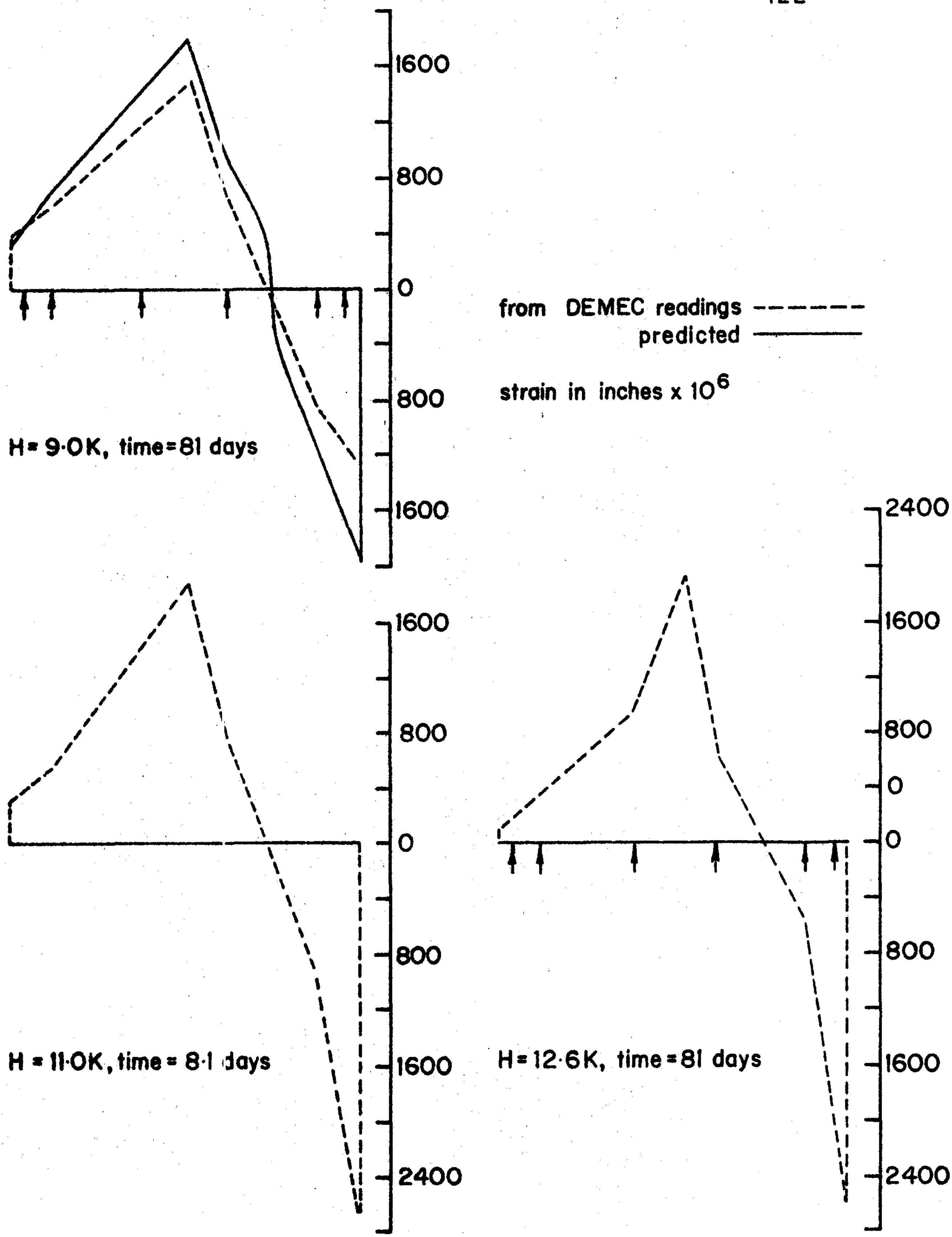

FIGURE 8·8(c) Frame L1 - compressive strain at extreme fibre. Beam.

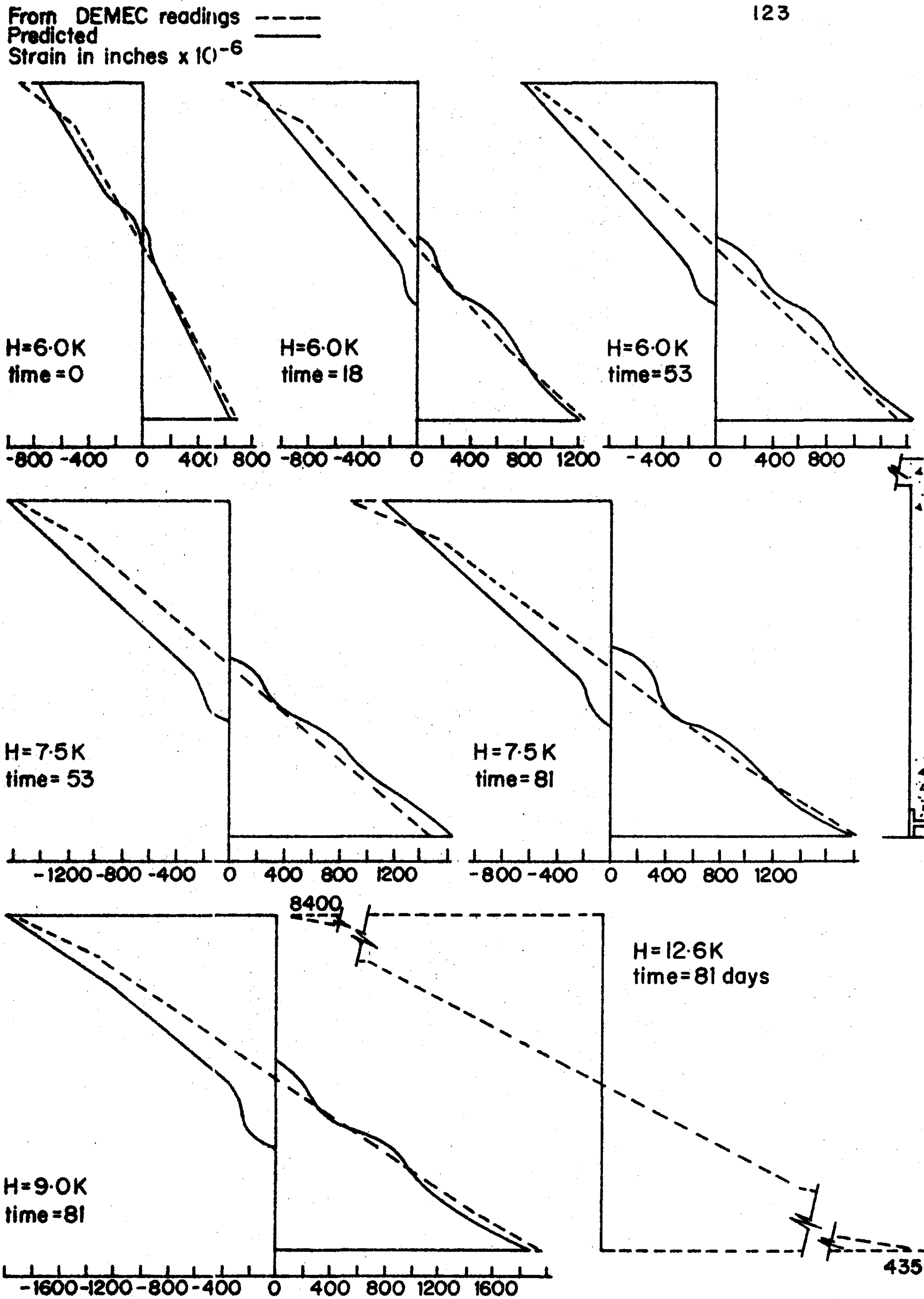

FIGURE 8·8(d) Frame L1 - compressive strain at extreme fibre.

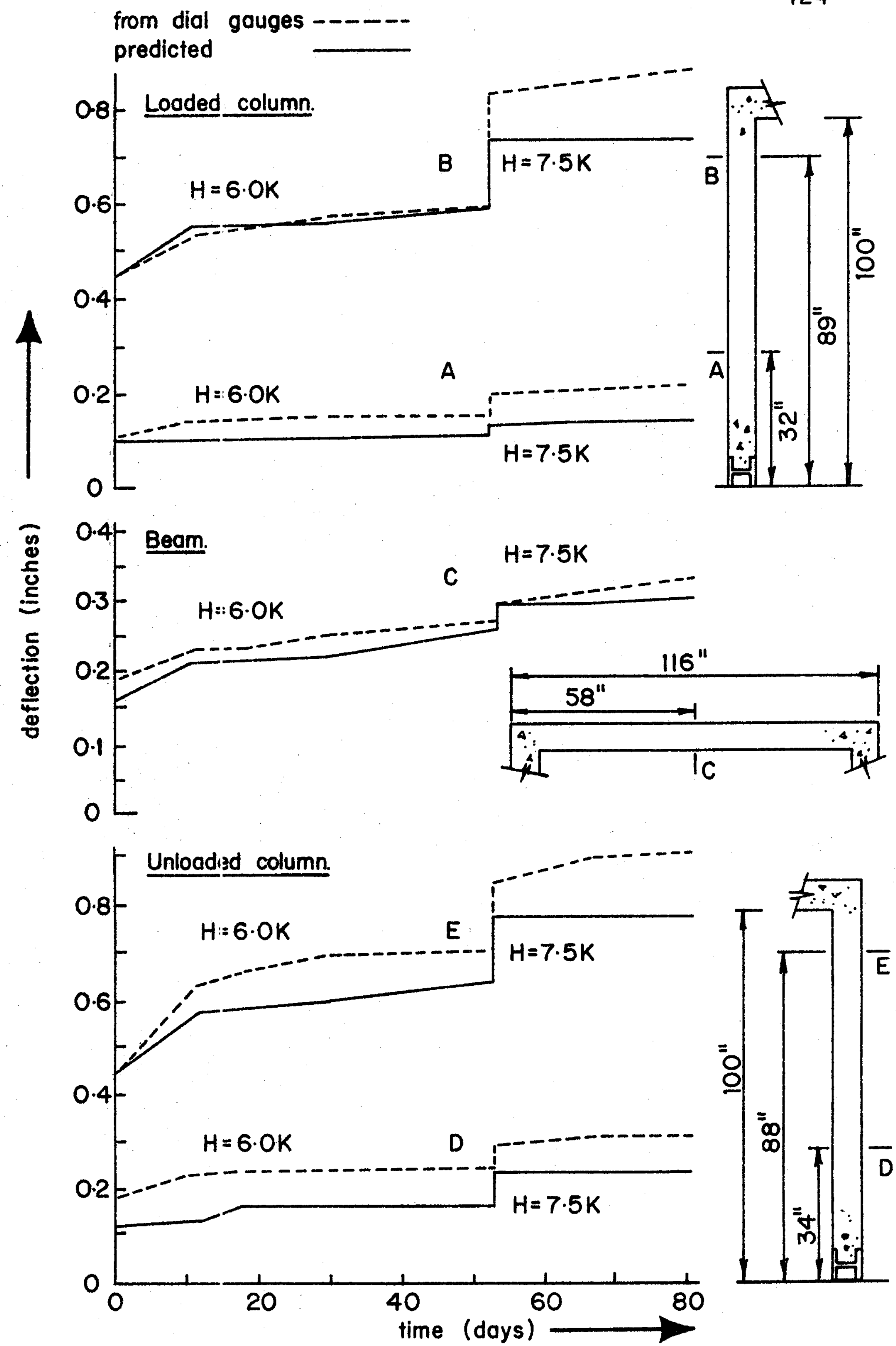

FIGURE 8·9 Frame L1 - deflection.

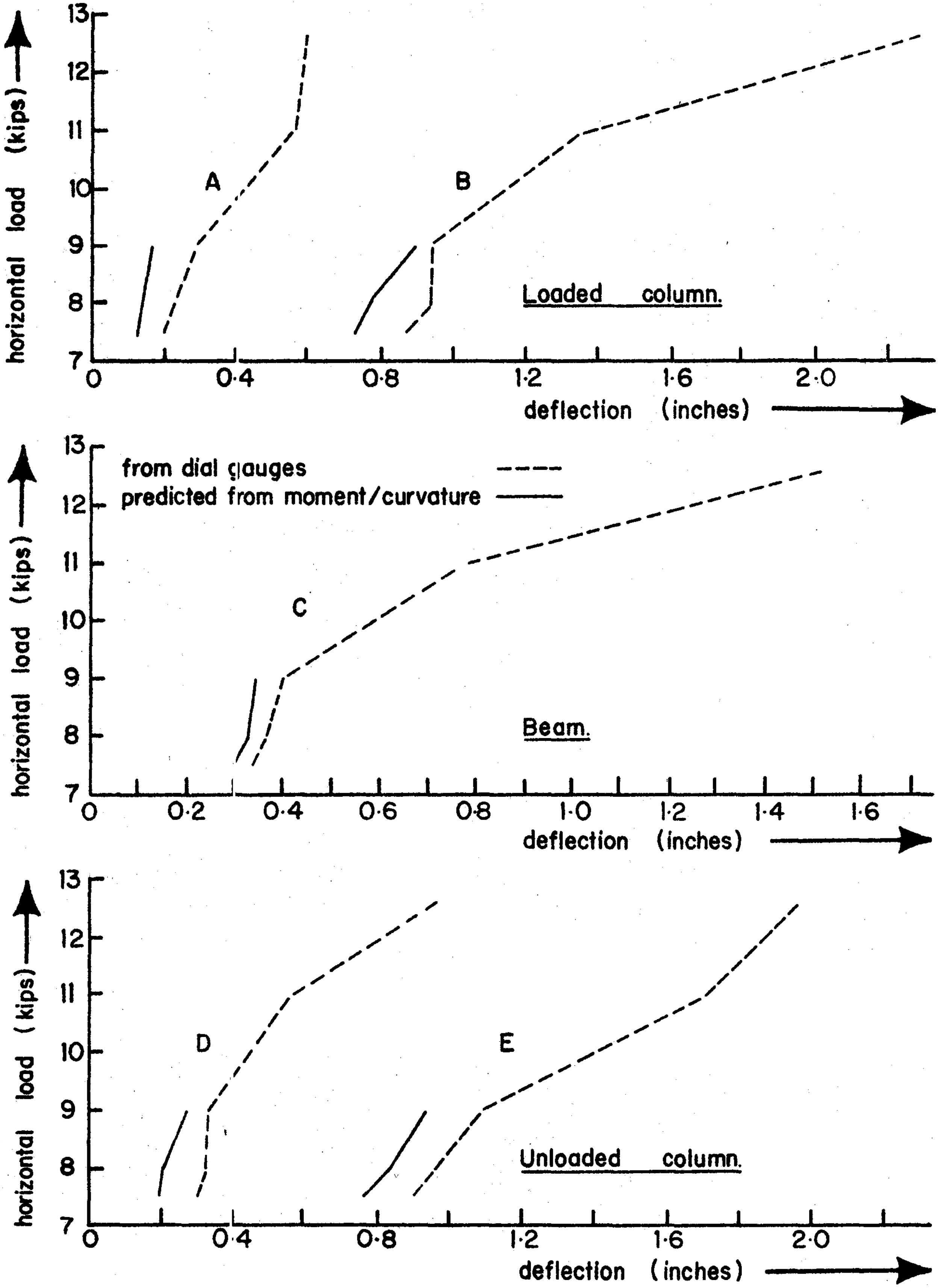

<u>FIGURE 8·10</u> Frame L1 - predicted deflection after sustained load. (For location of dial gauges see figure 8·9)

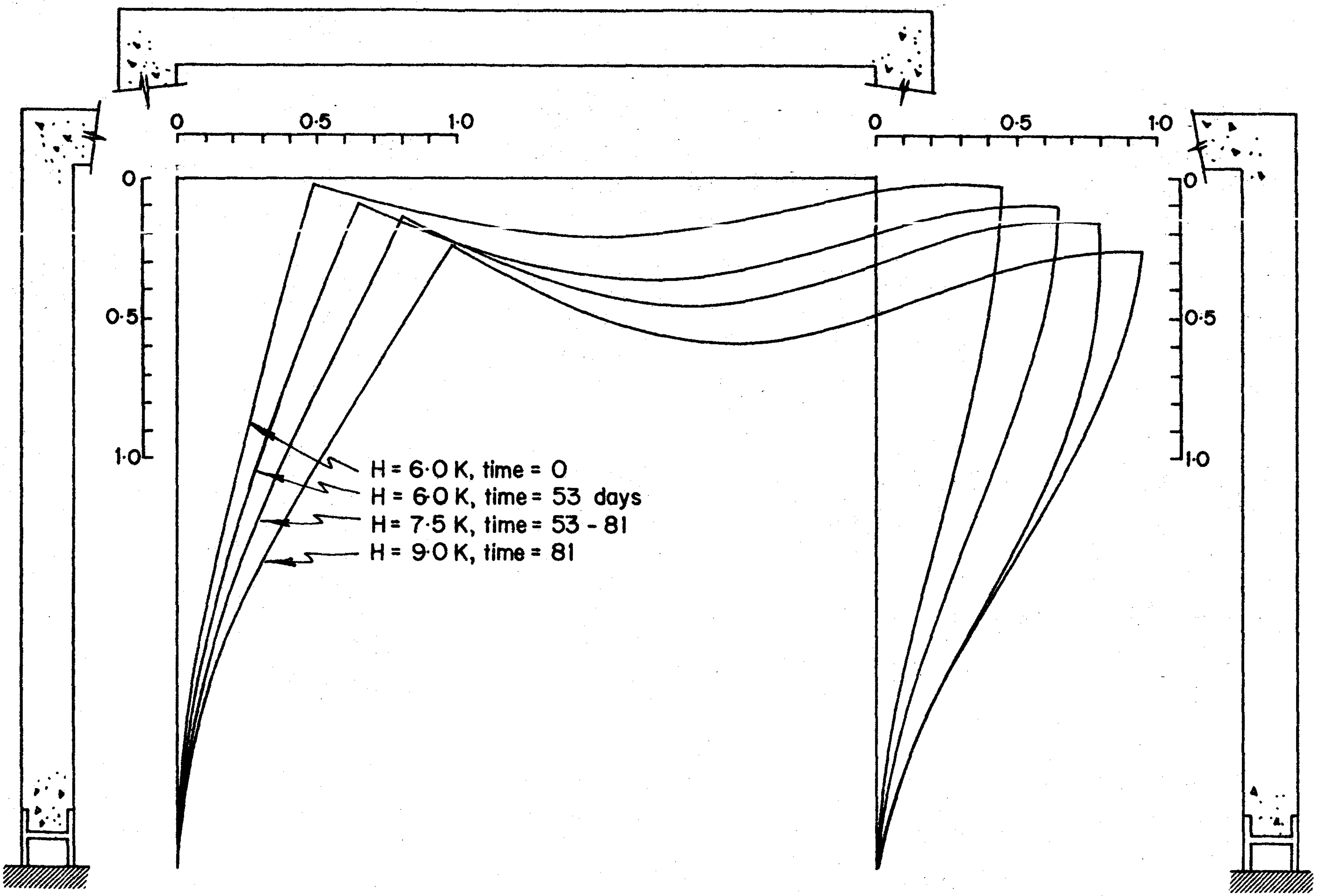

FIGURE 8.11 Frame L1 - predicted deflected shape.

Chapter 9

SOURCES OF ERROR

9.1. Introduction

In this chapter, the sources of error affecting the results of the tests and analyses are discussed. These included errors associated with material properties, measurement and calculation of creep and shrinkage, Demec readings, convergence of iterative procedures, and the influence of differences between the computer model and the actual frames.

Along with the test precision described in Section 5.5., the errors discussed in this chapter provided a basis for evaluating the validity of the methods of analysis and test procedures.

9.2. Errors in Conventional Methods of Analysis

The conventional methods of analysis, such as slope-deflection and the mechanism method, could be used as design procedures for the short-term case. They provided a reasonable solution for frame moments because the relative stiffnesses of members could be determined fairly accurately. However, because of cracking, the reinforced concrete did not exhibit a constant moment of inertia. Also, the non-linear nature of the concrete stress-strain curve above very low stresses made the use of a constant elastic modulus very inaccurate. Since the conventional methods required a constant member stiffness, a cracked section moment of inertia and secant modulus of elasticity were used, but with somewhat erroneous results for frame deflections.

Also, the conventional methods did not provide for the effects of axial loads on the moment capacity, or the influence of secondary moments produced by deflections.

For sustained load analysis, a reduced modulus was used.

However, this solution did not take account of previous stress history as well as secondary moments and the non-linear behaviour of the concrete.

Hence, the conventional methods did not provide sufficiently accurate results for deflections of the frame and moments under sustained load conditions.

9.3. Errors Common to the Element Methods

9.3.1. Introduction

Because the conventional methods could not accurately solve either the short-term or sustained load behaviour of reinforced concrete frames, the moment-curvature element method and sustained load element method were developed. Since these procedures, particularly the latter, relied to some extent on experimental results, they could accomodate differences in material properties and other factors, but they were also subject to experimental errors.

9.3.2. Concrete Stress-Strain Relationship

Drysdale[(5)] showed that the assumption that the stress-strain relationship was linearly dependent on the concrete strength provided a reasonable fit of test results for unloaded specimen. Some error was introduced because the effect of high sustained stresses was not included in the stress-strain relationship. Although it provided higher stresses than usually accepted, the allowable tensile strain of 0.00015 was used for concrete in an attempt to compensate for bond between steel and concrete in the region between cracks. Reference should be made to Drysdale's work and Appendix A for details on concrete strength.

The results of two cylinder tests were compared with the analytic expression as indicated in Figure A1. Good agreement was obtained up to 60% of ultimate strength, and at the peak of the curves. Between these levels, the function overestimated stresses by a maximum of 8%. On the basis of these results, the concrete stress-strain relationship was considered adequate.

9.3.3. Reinforcing Steel

Of the fourteen heat treated tensile specimen, six indicated a well defined yield point. The average yield for these samples was 59,800 psi with a standard deviation of 420 psi. The average yield for the three tensile tests on non-heat treated bars was 59,000 psi with a standard deviation of 390 psi. For analysis, a yield strength of 60,000 psi was used.

The error in the modulus of elasticity based on the three "cold" tensile specimen was 1.5%.

Most of the error associated with the steel was due to the assumption of ideal elastic-plastic behaviour. This was valid up to a strain of 0.005, but for further deformation, strain hardening occurred. At a strain of 0.01, the increase in stress above yield was 16.7%. Because the present analysis was applicable only to formation of the first hinge which occurred at yielding of the steel, this error was not severe. Also, tensile strains much beyond yield were accompanied by crushing of the concrete at the compression fibre which reduced the section capacity to a greater extent than the increase due to strain hardening. However, it was decided to include the effects of strain hardening, based on tensile test results, in future analyses.

9.3.4. Shrinkage

An important source of error in the analytic procedures was the use of the expression for shrinkage developed by Drysdale. Because the concrete mix and curing conditions were similar for this investigation and the University of Toronto column tests, there was negligible error in these factors. However, the sections used were considerably different.

The shrinkage function and prism data for frame L1 were as indicated in Figure 7.16. The scatter in results from the two prisms was very severe. This was caused by difficulties encountered in attempting to obtain firm adhesion between the Demec points and moist concrete during curing. Sealing wax and several types of epoxy had been used without success in previous tests. For the L1 prisms, the Demec points were implanted in the freshly poured concrete. Due to the accumulation of moisture around the brass discs, the embedment was not completely rigid. However, it was felt that much better results could be obtained through further practice with this technique.

Despite the test scatter, the shrinkage measurements did indicate two trends. First, the slope of the analytic expression appeared in reasonable agreement with the experimental data, and, second, the shrinkage for frame L1 was considerably less than that predicted by the function. This latter result was expected because of the larger section for the test frames. However, it was not felt that the experimental results were sufficiently accurate to develop a new expression.

Before loading, shrinkage from the reinforced prisms was used. After load was applied, results were taken from the plain prisms. This was valid because the loaded concrete was free to shrink without any influence from the reinforcing. In this case, shrinkage caused the concrete to lose some compressive stress.

9.4. Errors in Moment-Curvature Computation

9.4.1. Introduction

Errors due to the use of the shrinkage data and the concrete stress-strain expression were present in this procedure. Since this method used iteration to obtain a solution, there was also an error introduced by the convergence criterion. Equilibrium of forces on the section within an allowable residual of 0.1 kips was the requirement imposed. This meant that precision was determined by a fixed value rather than a percentage. The maximum error in force based on the absolute values of the various contributions for the lowest moment considered was 0.5%.

9.4.2. Tension in the Concrete

In Chapter 7, the effect of omitting the tensile strength of the concrete was indicated. For moments less than 25% of ultimate this omission would lead to a completely erroneous moment-curvature relationship. The error from ignoring concrete tension diminished rapidly once cracking had occurred. Concrete tension had great significance on the section stiffness and on frame behaviour only prior to cracking of the concrete; it had practically no effect on ultimate capacity.

9.4.3. Moment-Curvature Expressions

Some error was introduced by the mathematical model for the moment-curvature curves. It was assumed that, once cracking had occurred, there would be an instantaneous increase in curvature without a change in moment. This assumption ignored the unstable equilibrium states which occurred during cracking, but was more realistic since the unstable positions could never be obtained for the energy storing type of system used in loading the frames.

The relationships between curves for different values of load and shrinkage were assumed linear or exponential depending on the best fit of selected data. The largest difference between the mathematical model and the actual moment-curvature relationship, with the exception of the unstable equilibrium positions, was 4%.

Because it was only significant at relatively low moments, the error due to shrinkage in formulating the moment-curvature relationship was not severe.

9.5. Moment Calculation from Demec Readings

9.5.1. Data from Demec Points

As mentioned in section 8.2., considerable error was possible in obtaining strain distributions from the Demec gauge points because of the influence of cracking and through mis-location of the gauge points. Curvature over the 8 inch section had to be determined from two gauges only 1 5/8 inches apart because the large moments developed reduced the compression area of concrete to a narrow band with the neutral axis only about 2 inches from the compression face. The error in distance between Demec gauges was ± 1/16". This could cause an error in curvature in the order of 7%.

9.5.2. Calculations

The method for processing strains from Demec readings was basically the same as the analytic solution used to obtain the moment-curvature curves. However, in this case since the strain distribution for equilibrium was known, no iterative procedure was required. The forces and moments on the section were computed using the concrete and steel stress-strain relationship applied to the experimental strain distribution. An estimate of the precision of a particular section computation was obtained by comparing the axial force calculated by this method with that expected. Because of the minimum Demec error of ± 5 microstrain, the precision for low moments was not good. The axial capacity of the cross-section was very large. For example, an axial compressive strain of 10 microstrain represented a force of about 0.3 kips with zero moment, or 0.1 kips at ultimate moment. A 5% error in a strain distribution ranging from 1000 microstrain in compression to 3000 microstrain in compression could cause an error in "axial" strain of 200 microstrain, enough to indicate an error in axial force of 2 kips. Hence, it was not expected that this method would yield accurate results for forces, its main use was to determine the moment on a section for a given strain distribution.

Because the method of processing test data to obtain moments was the same as used in determining the moment-curvature relationship used in the frame analysis, it was concluded that a realistic comparison was provided by this method. As with the sustained load procedure, strains could have been used directly as the means of comparing the theory and experiments. However, it was felt that variation in the moment distribution on the frame provided a more useful result and a clearer picture of frame behaviour. Also, the applicability of the traditional methods such as plastic analysis or slope-deflection could best be considered on the basis of moments produced in the frame.

9.6. Extreme Fibre Strains from Demec Readings

Comparison of extreme fibre strains was used to correlate test results and analysis for the sustained load program. The errors associated with Demec readings were described in Sections 8.1. and 9.3.

This procedure used the Demec gauge results from the compression zone to determine the curvature and extreme fibre strains. A comparison was made between the calculated strain (at the level of tension steel) and the experimental strain. The difference was generally in the order of 10 to 30 percent and increased with load. Based on accepted theory and on these results, there was considered adequate justification for assuming that the strain distribution was linear. At high loads severe cracking caused Demec points in the tension zone to be shifted and dislodged in an unpredictable manner so that extreme deviation from the calculated strain distribution was common. Breakdown of bond between the concrete and steel also caused severe inaccuracies in strain readings from Demec gauge points in the tension zone.

9.7. Frame Analysis Using the Moment-Curvature Element Method

9.7.1. Calculations for each Element

The iterative procedure as described in Section 7.5.3. was used to obtain equilibrium for each element. Calculations were repeated until the average curvature converged on an allowable residual of 1% or 1×10^{-6} radians. Since some error was inherent in assuming an average moment to act over a finite element, accuracy depended on the number of elements in the frame. Based on the results of errors presented by Drysdale[5], it was decided that elements ten inches long would be subject to very small errors due to their finite length.

Because quite large changes in moment occurred over each element, the number of cycles required for convergence was sometimes considerable, particularly in the regions where reversal of curvature occurred. Iterations ranged from three to about fifteen cycles. An average of seven cycles per element meant 196 cycles per frame solution. Since as many as 125 frame solutions were required to obtain an accurate result, as many as 25,000 element iterations could be

ΔX = X-COORDINATE ERROR AT RIGHT BASE

ΔY = Y-COORDINATE ERROR AT RIGHT BASE

θ_D = ROTATION ERROR AT RIGHT BASE

	LOCATION	$\Delta X = 0.01''$		$\Delta Y = 0.01''$		$\theta_D = 0.001$	
		MAGNITUDE	%*	MAGNITUDE	%*	MAGNITUDE	%*
MOMENTS (IN-K)	LEFT BASE	1.25	1.14	-0.47	0.43	0.19	0.17
	TOP LEFT COL.	-0.68	3.78	-0.47	2.61	-0.38	2.11
	TOP RT. COL.	-0.57	0.25	0.47	0.21	-0.58	0.26
	RIGHT BASE	-1.25	0.66	-0.47	0.25	2.18	1.15
REACTIONS (K)	HOR. FORCE AT LEFT BASE	0.021	1.50	0.000	0.00	0.005	0.35
	VERTICAL FORCE AT LEFT BASE	-0.001	0.03	0.010	0.28	-0.010	0.71

TABLE 9.1. MOMENTS AND REACTIONS FOR GEOMETRIC ERRORS AT THE RIGHT BASE

* Percentage of total moment for horizontal force of 6.0 kips and vertical force of 12.0 kips.

required at each load level. For 18 load levels this figure could be multiplied to 450,000 cycles. Careful choice of initial conditions reduced this figure by a factor of at least ten in the actual computer runs. On the McMaster University CDC 6400 computer, the computation time for 18 load levels was about 60 seconds.

9.7.2. Solution for the Frame

Summation of the contributions of each element in the frame resulted in an error in geometry at the right base. The error in coordinates and rotation was expressed as a sum, and was compared with an allowable residual. For the moment-curvature element method, the allowable frame error was 0.03 and was made up of the sum of the absolute coordinate errors plus one hundred times the absolute error in rotation. Table 9.1. indicates the significance of these errors based on an elastic solution. A constant allowable error, which meant that accuracy increased with load, was used in order to reduce computer time by attempting to keep iterative cycles within reasonable limits. Because a large portion of the contributing error was relatively constant throughout loading, a percentage residual would have lead to an increase in the number of cycles required at low load levels.

In Table 9.1. it was revealed that the residual allowed almost any combination of effects so that the real error could vary considerably. For instance, a residual of 0.03 could be obtained from an error in coordinates of 0.01 inches in both x and y directions combined with a rotational error of 0.0001 radians. The resulting errors in moments would be 1.74% at the left base, 8.50% at the top of the left column, 0.72% at the top of the right column, and 2.06% at the right base.

The maximum possible errors in moments obtained independently for each location were 3.75% for the left base, 11.34% for the top of the left column, 0.78% for the top of the right column, and 6.54% for the right base. Actually, such severe errors could never occur together. It should be noted that the error in moment was independent of the magnitude of the moment so that the precision obtained was best at regions of high moments. The figures presented above were obtained for a horizontal load of 6.0 kips and a vertical load of 12.0 kips. The probability of obtaining errors in maximum moment greater than 2% was quite low. Table 9.2. indicates the actual error obtained in the moment at the right base for various loads. This may be considered as representative of the average precisions for the frame solution

HORIZONTAL LOAD LEVEL (KIPS)	ERROR IN MOMENT AT RT. BASE (%)	PERCENT OF RESIDUAL (0.03)
2.0	3.33	98.6
4.0	0.71	53.3
6.0	1.51	56.6
8.0	1.14	93.3

TABLE 9.2. Error in Moment for Frame R2

Better precision could be obtained by considering each coordinate and the rotation separately since their effects on moments were quite different. However, the increased accuracy would be gained at the expense of considerable computer time. The residual allowed severe errors only at very low load levels which were not of major importance in this study.

FRAME NUMBER	TIME AFTER LOAD (DAYS)	HOR. LOAD (K)	LEFT BASE (LOADED COL.) X-DISP. (IN)	Y-DISP. (IN)	ROTATION (RAD)	RIGHT BASE X-DISP.	Y-DISP.	ROTATION
R1	0	3.0	N.R.	-0.002	-0.00118	N.R.	-0.007	-0.00183
		6.0	N.R.	0.001	-0.00336	N.R.	0.001	-0.00336
		9.0	N.R.	0.010	-0.01100	N.R.	0.025	0.00780
R2	0	3.0	0.006	0.001	-0.0012	0.013	0.001	-0.0010
		6.0	0.014	0.011	-0.0023	0.028	0.008	-0.0026
		9.0	0.024	0.016	-0.0037	0.048	0.021	-0.0075
		11.5	0.043	0.017	-0.0047	0.069	0.030	-0.0105
L1	0	6.0	N.R.	-0.0030	-0.0010	N.R.	-0.0020	-0.0010
	53	6.0	N.R.	-0.0030	-0.0010	N.R.	-0.0020	-0.0010
	53	7.5	N.R.	-0.0033	-0.00138	N.R.	-0.0025	-0.0011
	81	7.5	N.R.	-0.0033	-0.00138	N.R.	-0.0025	-0.0011
	81	9.0	N.R.	-0.0020	-0.00185	N.R.	0.0016	-0.0022
	81	11.0	N.R.	-0.0035	-0.00192	N.R.	0.0062	-0.0035
	81	12.6	N.R.	+0.0016	-0.00323	N.R.	0.0109	-0.0048

TABLE 9.3. BASE MOVEMENTS DURING TESTING

9.7.3. Bases

Another source of error in the frame solution was the analytic model for the wideflange column bases. It was assumed that the rotation of the base could be approximated by considering the wideflange in two sections. The lower flanges were subjected to uniform strains compatible with the applied moments while the upper flanges were considered as part of a rigid unit because of the concrete and extra reinforcement between them. This model ignored shear deformation and any curvature of the flanges. The model for the bases used values for rotation and displacement obtained from test results to obtain the boundary conditions at the bottom of the wideflange. These boundary conditions were not more than 30 times the magnitude of the allowable residual.

Most of the error occurred because the real bases were observed to undergo curvature over both the upper and lower flanges. However, it was felt that, despite this error in the actual behaviour, the analytic model provided a realistic approximation of the effect of the bases on the end fixity of the columns. The base movements recorded during the tests were as indicated in Figure 9.3.

9.8. Frame Analysis Using Sustained Load Element Method

9.8.1. Introduction

The sustained load procedure was subject to the same errors as the short-term procedure except for those associated with the moment-curvature relationship and the solution for each element. In addition, there were errors in connection with the expression for creep, the iterative solution for each element (which differed considerably from that for the moment-curvature method) and the effect of time on shrinkage, and concrete strength.

9.8.2. Creep Expression

Reference should be made to Drysdale's work [5] for details on the precision of the creep curves. The use of superposition of creep results for constant stress levels to obtain creep under a stress gradient produced some error, but the modified superposition method used was an improvement over previous superposition procedures. The accuracy of this method was dependent on the magnitude of the stress gradient and the time intervals used.

Good precision was obtained for the creep curves by the use of maximum quality control and least squares fitting of all data to alleviate individual test differences. The curves yielded a linear relationship between creep and stress up to 35% of the concrete strength. Severe inaccuracy developed for "elastic" strains over 0.001 inches per inch, but the "elastic" portion of strain encountered in the frame rarely exceeded this level.

Because of the greater section used in the McMaster frames, the curves from the University of Toronto series would tend to somewhat overestimate creep.

9.8.3. Shrinkage

The general errors associated with the treatment of shrinkage were described in Section 9.3.4. Because of the addition of the time factor, the error was more significant in the sustained load method than in the moment-curvature method. Despite the rather poor precision in shrinkage data, because the strains produced were only in the order of one tenth those produced by creep, the error attributed to shrinkage was not considered severe.

9.8.4. Concrete Stress-Strain Relationship

The concrete stress-strain relationship varied linearly between cylinder test points at the time of loading and 120 days later, and was held constant above this time. Since the increase in strength was only 13.7% over the test period, the error in assuming a linear increase was not significant.

9.8.5. Solution for Each Element

The allowable error in convergence of the iterative solutions for force and for moment on the element was 1%. Convergence was dependent on the number of slices into which the section was divided, since the force and moment were made up of the sum of the contributions taken at the centroid of each slice. Hence, in order to obtain a solution, the total error due to the number of slices had to be less than 1%. The portion of the fortran program for the solution of each element was run separately for different numbers of slices in order to find a condition which would provide convergence after a reasonable number of cycles. The problem was amplified by the fact that the moment on an element in the frame could vary from zero to the ultimate moment. Because the axial forces were low compared to the axial capacity of the section, for high moments a very slight error in strain distribution could cause an error much greater than 1% of the force. For this reason, for high moments, the force part of the calculation was ommitted. For very low moments, the allowable residual of 1% represented a very small magnitude and could be less than the error from other sources. In this case a fixed residual of one tenth the difference between external and internal moment was used.

The number of slices on an element was fixed regardless of the magnitude of the moment. It was found that eight slices provided fairly quick convergence for high moments, but would not give any solution for very low moments. Sixteen slices gave a solution for each element, but the number of cycles required was excessive. It was decided to use twenty-four slices since this number yielded a solution in a reasonable number of cycles (usually less than ten) for all possible moments. The total number of individual calculations was considerably less for 24 slices than for 16.

9.8.6. Total Precision for the Frame Solution

Because of the effects of creep, it was felt that the "elastic" criterion for convergence of the solution for the entire frame was conservative. If solution could not be obtained in a reasonable number of cycles, the allowable residual as described in Section 9.5. was increased from 0.03.

After 75 cycles, the error factor was set at 0.05, and after 100 cycles it was increased to 0.1. Based on the moment-curvature method, this would mean an increase in estimated error for the frame solution from about 2% to 6%. However, it was realized that, under sustained loading, rotation occurred without changing the moment distribution on the frame significantly, and hence the relaxation of the convergence criterion would not increase the error to a large degree. It was concluded that, despite the relaxed convergence criterion, the overall error for the sustained load element method was 2 to 4%.

9.9. Summary of Errors in Analysis

Because of the large number of variables involved, it was not possible to establish a definite precision for each method. Where possible, an appraisal of the magnitude of the error caused by a particular factor was made, and in other cases the probable significance of discrepancies was investigated. Allowable residuals from iterative techniques were minimized with respect to accuracy obtained versus computer time and the influence of other errors on convergence. Generally, the error for each element was 1%. The error in geometric compatibility and moment distribution on the frame was variable, but was tabulated for each case. Results were evaluated on the basis of this error. They were not used in the comparisons with test data if the error exceeded about 2% for most cases with the exception of load levels less than H = 2.0 kips and V = 4.0 kips, the load level at the first hinge, or under conditions of extended sustained load. For low loads, the error definitely increased above 2%. At the first hinge, the method could not account for hinge rotation and precision decreased sharply. After a long time under sustained load, the convergence factor was allowed to increase, but it was condsidered that, because of the influence of creep, the precision did not decrease accordingly.

It was felt that the various sources of error in the solution did not act in a cumulative manner in most instances.

The comparison between test results and the analysis indicated that fairly good precision was obtained by both the moment-curvature element method and the sustained load element method. The errors in test results associated with dial and Demec readings, the size of the frames, bases, the location of steel and other sources were discussed in Section 5.5.

Chapter 10

CONCLUSIONS AND RECOMMENDATIONS

10.1 Introduction

The purpose of this investigation was to develop a means of analyzing reinforced concrete frames subjected to short-term and sustained loading. The procedures developed were to be sufficiently general that they could be applied to a variety of structures and loading systems. They were to require only data derived from relatively simple tests on cylinders, prisms and tensile specimen. Verification of the methods of analysis was to be provided by a testing program using a particular frame and loading system.

This investigation formed part of an extensive study on creep in concrete at McMaster University.

In this chapter, the degree to which the objective of this study was attained, as well as recommendations for further research, are discussed.

10.2. Methods of Analysis

10.2.1. Conventional Methods

The conventional methods of structural analysis such as slope-deflection equations and the collapse mechanism method were found to be inadequate for predicting accurately the behaviour of reinforced concrete frames. There were a number of reasons for this which included the following:

(1) The effect of axial force on the moment capacity of a section was not included.

(2) Secondary moments due to deflection were omitted.

(3) A constant modulus of elasticity and moment of inertia were required (a linearly varying moment of inertia could be accomodated but this only extended the methods to a specific case).

(4) Creep and previous stress history could not be accurately included.

(5) Unusual aspects of the structure (i.e., the bases) could not be accounted for.

Despite approximations such as the use of a reduced modulus for sustained loading, the conventional methods did not provide accurate predictions of deflections. This was a serious limitation where high column loads, and hence large secondary moments were expected.

10.2.2. The Element Methods

10.2.2.1. Introduction

These methods were developed in order to account for the limitations of the conventional methods described in the previous Section. The sustained load procedure was such that creep could be included using the accurate modified method of superposition.

10.2.2.2. Moment-Curvature Expression

Expressions were derived analytically to describe the moment-curvature relationship for the frame cross-section. It was shown that cracking of the section occurred at about 25% of ultimate load. Prior to cracking, tension in the concrete was found to contribute greatly to the section stiffness. Once the tensile fracture strain was reached at the extreme fibre, further attempts to increase the load led to unstable equilibrium positions until a stable state was reached. This indicated that cracking was an instantaneous phenomenon which increased the flexibility of the structure without any observable change in moment under conservative loading. The influence of tension in the concrete was not significant once cracking had occurred.

It was concluded that concrete tensile strength should not be omitted from the analysis of structures where cracking of the concrete had not occurred. In prestressed concrete this could be important up to more than 50% of ultimate capacity.

The moment-curvature element method used the moment-curvature curves to determine the frame geometry and secondary moments for an assumed primary moment condition. The solution was based on satisfying the equilibrium and geometry conditions with the use of successive corrections.

10.2.2.3. Moment-Curvature Element Method

This procedure was used to predict the moment distribution and deflected shape of the particular frame studied. Based on the good correlation of results from the analysis and experiments, and on an evaluation of the sources of error, it was concluded that this method provided a realistic solution for the short-term behaviour of the test frame.

The moment-curvature element method was general in its derivation, but the fortran program was written with specific limits. Without alteration, it could be applied to rectangular portal frames with a horizontal point load at the top of the column and a vertical point load at the centre of the beam. The cross-section, member lengths and load magnitudes could be varied. The procedure could be modified to analyze more complex structures without changing the basic concepts such as the use of small elements, moment-curvature relationships, summation of effects, and the convergence on geometric compatibility.

From the results of this investigation, it was concluded that the moment-curvature element method could be used as the basis for developing a procedure for the analysis of the short-term behaviour of reinforced concrete structures.

10.2.2.4. Sustained Load Element Method

This method was used to predict moments and deflections for the frame under sustained loading. The comparison between extreme fibre compressive strains and deflections from the analysis and tests was generally good. On this basis, and from an evaluation of the precision of the experiments and calculations, it was concluded that the sustained load element method provided an adequate prediction of the behaviour of the test frame under sustained loading.

Like the moment-curvature element method, this procedure was general in principle but was applied specifically only to a particular frame and loading configuration. From the results obtained and the comparison with experiment, it was concluded that the sustained load element method could be used to develop a technique for the sustained load analysis of more complex structures.

10.2.2.5. Recommended Improvements in the Methods of Analysis

(1) Convergence Criteria

The iterative procedure for achieving geometric compatibility at the right hand base was very time consuming. Also, the residuals allowed variations in the precision of the solution. It would be desirable to improve the convergence technique and the means of establishing residuals.

(2) Extension to Collapse

Both the short-term and sustained load procedures provided solutions only to formation of the first plastic hinge.

It is proposed to extend these methods to collapse of the frame. There are a number of problems associated with this extension. For instance, when each new hinge is formed a new structure is effectively created which requires an alteration in the iterative procedure for the frame. Also, a redistribution of moments could be caused by creep which could change the order of formation of hinges or the collapse mechanism. Hence, the analysis would have to be flexible enough to allow for variations in the order and location of hinge formation.

For analysis, the plastic hinge may be approximated by imposing two conditions: (a) the moment is held constant at the ultimate moment for the particular axial force, and (b) the rotation of either arm is allowed to assume any value.

Although not incorporated into the fortran programs, an iterative procedure was developed for analysis of the frame from formation of the first hinge at the upper right hand corner to formation of the second hinge. This method is described as follows:

Upon formation of a plastic hinge at the upper right hand corner, an assumption is made for new reactions at the right base. Then, using the element technique, the moments and deflected shape of the right column are calculated. If ultimate moment is not obtained at the top of the column, the base reactions are changed, and the moments and displacements for each element are again calculated for these new conditions. These steps are repeated until the ultimate moment is reached at the top of the column. The moments and displacements are stored for each element.

From equilibrium, the reactions and moment at the left base are computed. Again using the element technique and proceeding up the column and across the beam from left to right, the reactions, moment and coordinates at the right end of the beam are obtained. By this method, equilibrium at the right corner is obtained automatically but not geometric compatability.

Based on a comparison between the x and y coordinates at the right end of the beam and top of the right column, the reactions and moment at the base of the right column are changed. Then the entire procedure is repeated until geometric compatability is obtained at the upper right corner.

A similar procedure would be followed for the successive formation of other hinges in the frame.

The method proposed for the solution for the first hinge indicates a serious limitation. Since several different iterative stages are required, the amount of computer time required is increased greatly. Also, because the element procedure applies to specific structural conditions only, a different method for the frame iterations would have to be used for the development of each hinge. This is further complicated by the possibility that creep could cause a change in the order of hinge formation so that the method would have to be adaptable to various combinations. Despite the possibility of introducing some generalization, the procedure for extending the element methods to collapse would involve specific stepwise progression through the formation of all the necessary hinges.

Another problem associated with extending the element procedures to collapse is the calculation of rotations after the formation of hinges. It might be possible to resolve this difficulty by developing moment-curvature curves up to collapse of the section. These would have to be obtained, at least to some degree, by testing using a loading system which could not store energy. These curves could be incorporated into the moment-curvature element method to provide a solution for short-term loads.

The element methods could also incorporate a similar procedure as was used to analyze the frame up to collapse by the slope-deflection equations. This would involve considering each plastic hinge in turn as a real hinge and determining the increase in moments required to form the next hinge. This procedure would not account for the decrease in moment as the concrete at the compression fibre started to fail.

In conclusion, despite the limitations imposed by the amount of computer time required, and the difficulties in accounting for hinge behaviour, it is felt that the element methods could be extended to analyze the frames up to collapse.

(3) Changes in Frame Geometry and Loading

It is proposed to extend the element methods to analyze other structures. Provision for varying the section properties of the beam and columns independently would be advantageous.

With the system of loading used, there was a significant increase in deflections for sustained loads, but negligible redistribution of moments. It is felt that the influence of creep would be much more pronounced if axial forces, and hence secondary moments, were increased. This could be accomplished by adding axial loads to the columns.

Very little change in the element methods would be required to incorporate these provisions.

10.3. Test Apparatus and Procedures

10.3.1. Introduction

Large scale frames were used in order to minimize errors due to construction, dimensional tolerances, material properties, instrumentation and loading. The large size also eliminated the error which usually accompanies the use of data from small scale tests to predict the behaviour of practical structures.

10.3.2. Loading Systems

It was found that the hydraulic jacks and load cells provided accurate control over loads for the short-term test. The spring systems used to provide sustained loads also performed well. The daily corrections required rarely exceeded 1% of the total load, so it was not necessary to include fluctuations in load in the analysis.

10.3.3. Instrumentation

The load cells, Demec points and dial gauges generally provided accurate results within the limitations discussed in Chapter 9.

The performance of the column bases was the only unsatisfactory aspect of the tests which was not completely resolved. The intention to make the structure determinate by using strains in the steel bases to obtain moments and reactions seemed feasible, but could not be realized in practice. Despite modifications to the bases, the rotation was still unacceptable. Hence, the measurement of reactions had to be abandoned in favour of added rigidity. An additional factor in this decision was the consistently poor precision of readings from the electric resistance strain gauges on the bases. Despite adequate surface preparation, the use of several adhesives, and installation by two different experienced men, neither useful results nor an explanation for the inconsistency could be determined. The stiffened steel bases provided adequate rotation resistance.

10.3.4. Recommended Changes in Testing

Unless bases could be developed which would allow determination of reactions while restricting rotation, it would be preferable to use channel sections for the column bases and weld these directly to the lower base plates.

As discussed in Section 10.2.2.5., it would be advantageous to increase the axial loads on the columns considerably. This could be accomplished by applying point loads on the beam near the columns using a spreader, or by incorporating separate loading systems.

10.4. Additional Recommendations for Further Research

Along with the desirability of increasing the column loads, extending analyses to collapse, and improving the bases, a number of further investigations would be useful.

The effect of variations in relative stiffnesses of the members could be studied. Also, the tests and analyses could be extended to other framed structures.

Concerning the study of creep in general, a great deal more information is required on the effects of humidity, temperature, concrete strength, section dimensions, percentage and location of reinforcement, and the level of sustained load. Variations in creep due to these parameters would affect only the input for the moment curvature element method. Hence, it would be possible to study the effects of these factors on frame behaviour without the necessity of performing complex tests on frames.

10.5. Resume

Methods were developed to analyze the short-term and sustained load behaviour of rectangular reinforced concrete portal frames subjected to sidesway and vertical loads. These procedures accounted for the effects of base movements, secondary moments, variations in material properties, shrinkage and creep. Based on the results of tests on large-scale frames, it was concluded that these simplified "element" methods provided accurate analyses of the behaviour of the case studied.

It was further concluded that the techniques used to analyse the particular frame studied in this investigation could be used as the basis for developing methods of analysis for more complex structures. Variations in creep, shrinkage, and material properties could be determined from tests on relatively simple specimen such as prisms and cylinders. This data could be used with the methods of analysis to study the behaviour of various structures for short-term and sustained loading without the necessity of complex large-scale tests.

APPENDIX A - CONCRETE CYLINDER TESTS

TABLE A1 Variations in Concrete Strength from 6" Dia. x 12" Cylinders

FRAME NO.	NUMBER OF CYLINDERS	AGE (DAYS)	AVERAGE STRENGTH (Psi)	MEAN DEVIATION (Psi)	STANDARD DEVIATION (Psi)
R1	2	7	3375	15	15
	2	14	4125	115	115
	7	28	4887	197	235
L1	2	7	3635	5	5
	2	14	4460	60	60
	3	44	5040	140	168
	2	126	5490	170	170
R2	3	7	3210	6	8
	3	14	3760	67	75
	3	28	4493	42	49

$$\text{AVERAGE STRENGTH} = \bar{f}^1{}_c = \frac{\Sigma f^1{}_c}{n}$$

$$\text{MEAN DEVIATION} = \frac{\Sigma \left| f^1{}_c - \bar{f}^1{}_c \right|}{n}$$

$$\text{STANDARD DEVIATION} = \frac{\sqrt{\Sigma \left(f^1{}_c - \bar{f}^1{}_c \right)^2}}{n}$$

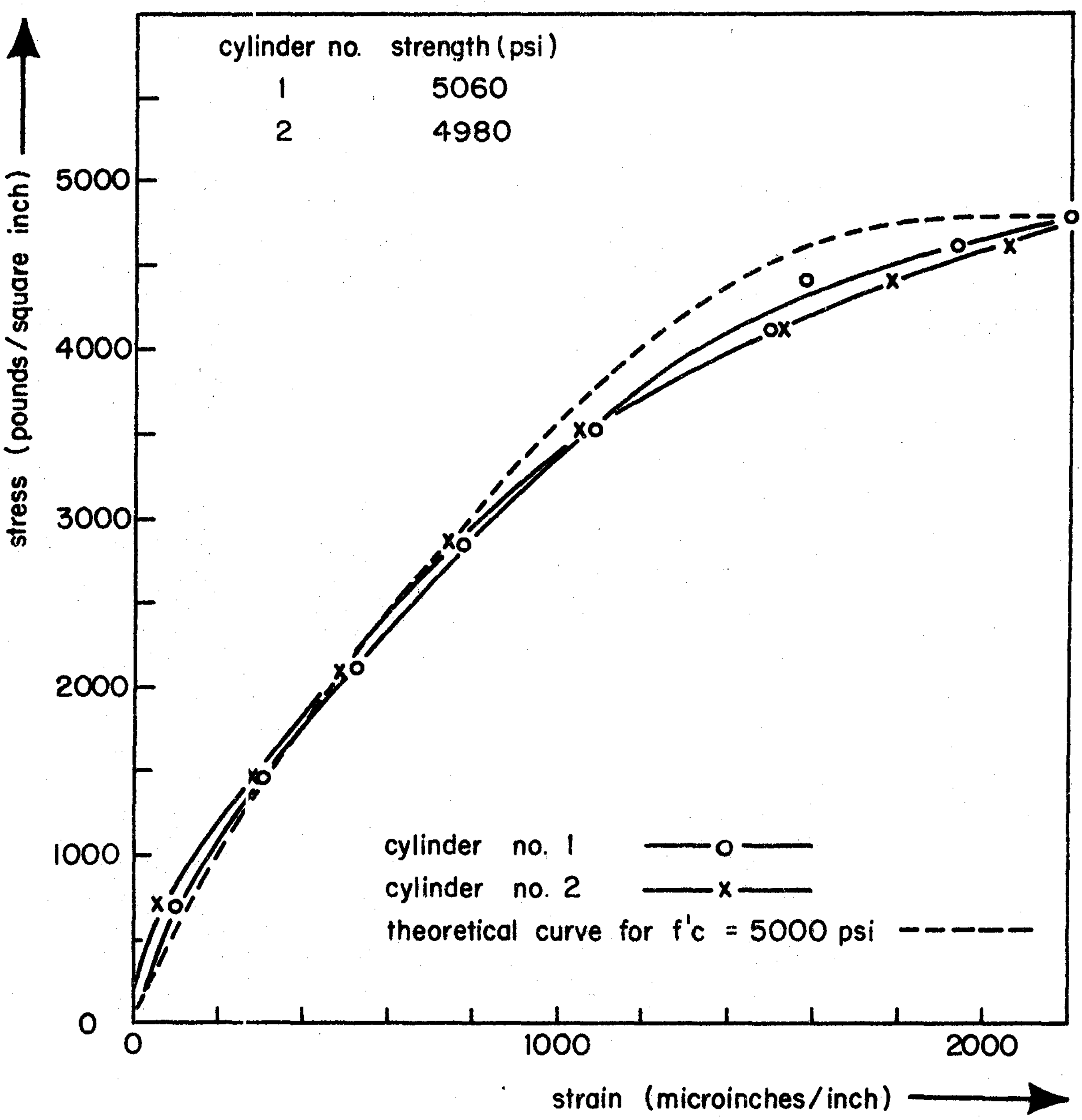

FIGURE A1 Concrete stress-strain relationship

APPENDIX B

Computer Programs

Nomenclature: The meanings of the important variables used in the programs are listed below. Those which do not appear here are defined by the context in which they are used. All dimensions are in inches, forces in kips, moments in inch-kips, rotations in radians and time in days.

ASC, AST	Area of steel in compression, tension
B	Section width
BAX	Applied bending moment at a section
BEAM	Beam length
BMXCAL	Calculated bending moment at a section
COL	Column length
COM	Compressive force in concrete
CS	Compressive force in steel
D	Distance from extreme compression fibre to the level of the tension reinforcement
DELP, DELV, DELM	Increments in reactions at the base of the loaded column
EPC	Strain at the extreme compression fibre
ES	Modulus of elasticity of the reinforcing steel
FPC or CYL	Concrete cylinder strength
FY or SFY	Steel yield strength
H	Steel strain due to concrete shrinkage prior to loading
P	Applied axial force

PCAL	Calculated axial force
PEEP (II,JJ)	Total creep and shrinkage on a particular section slice
PHI(I)	Curvature at a section
SLOER	Error in rotation at the base of the unloaded column
SSRR	Shrinkage strain during a time interval
TC	Tensile force in concrete
TCF	Increase in concrete strength after loading
THK	Section depth
TS	Force in tension steel
T_1, T_2	Times defining an increment of time under sustained load
UU (II, JJ)	Total strain on a particular cross-section slice
V	Applied shear force
X (I), Y (I)	Coordinates of the centroid of a cross-section
XERR, YERR	Errors in coordinates at the base of the unloaded column
XM (I)	Applied moment at a section
XMULT (I)	Applied moment capacity of a section
XN, YN	Coordinates of the base of the unloaded column

Subroutines:

AFORCE	Internal force at a section
AXSTR	Change in length of an element due to axial force
BASE	Rotation and displacement of the wideflange column bases
CREEP	Creep and shrinkage during a time interval
CURVA	Moment-curvature relationship for a section
STEEL	Forces in reinforcing bars

STRAIN	Concrete stress-strain relationship for short-term loading
TENCO	Tensile force in concrete
XBMX	Internal bending moment at a section

B1. MOMENT-CURVATURE RELATIONSHIPS FROM DEMEC READINGS

```
C      MOMENT-CURVATURE RELATIONSHIPS FROM DEMEC READINGS
C      IT IS ASSUMED THAT CAGE X-SECTION IS SYMMETRICAL.
C      SHRINK IS SHRINKAGE STRAIN IN IN/IN.
C      COMPRESSION IS TAKEN AS NEGATIVE IN THIS PROGRAM.
       DIMENSION TITLE(15),XX1(25),XX2(25),XX3(25),YO1(25),YO2(25),YO3(25
      1),K(25)
       COMMON/S1/A1,A2,A3
       COMMON/S2/B1,B2,B3
       READ(5,1)FY,FPC,B,D,ASC,AST,ES,THK,SHRINK
       WRITE(6,2)FY,FPC,B,D,ASC,AST,ES,THK,SHRINK
       READ(5,3)N,M
       WRITE(6,15)N,M
C      N IS THE NUMBER OF STRAIN GAUGE ZONES, M IS THE NUMBER OF LOAD
C      STAGES.
C      X IS THE DISTANCE FROM THE INSIDE FACE IN INCHES
C      YY IS STRAIN ORDINATE IN MICROSTRAIN
C      X1 IS THE POINT CLOSEST TO THE INSIDE FACE
C      L IS THE ZONE NUMBER.
       EPSY=FY/ES
       DO 30 J=1,N
       READ(5,4)XX1(J),YO1(J),XX2(J),YO2(J),XX3(J),YO3(J),K(J)
    30 CONTINUE
C       CALCULATE COMPRESSION IN STEEL DUE TO SHRINKAGE.
       CALL STEEL(SUN,FY,SHRINK,EPSY)
       STAR=SUN*(AST+ASC)
C      CALCULATE TENSILE STRESS IN CONCRETE DUE TO SHRINKAGE.
       XMOON=STAR/((B*THK)-(AST+ASC))
C      CALCULATE TENSILE STRAIN IN CONCRETE DUE TO SHRINKAGE-- SINCE
C      LOW STRAIN, USE SLOPE OF STRAIN CURVE FROM ZERO TO 100 MICROSTRAIN
C      THIS IS THE STRAIN IN THE CONCRETE EQUIVALENT TO THE COMPRESSIVE
C      FORCE IN THE STEEL
       EC=4.0E+03
       DOG=XMOON/EC
       DO 200 I=1,M
       WRITE(6,11)I
       READ(5,13)(TITLE(J),J=1,15)
       WRITE(6,14)(TITLE(J),J=1,15)
       DO 200 J=1,N
C      READ STRAIN COORDINATES FOR EACH ZONE.
       READ(5,40)YY1,YY2,YY3,L
C      IF THERE WAS NO READING, PUT ZERO VALUE INSTEAD STRAIN
       IF(YY1.LT.1.0)GO TO 157
       YY3=(YY3-YO3(J))*10.
       YY2=(YY2-YO2(J))*10.
       YY1=(YY1-YO1(J))*10.
       X1=XX1(J)
       X2=XX2(J)
       X3=XX3(J)
       Y1=YY1*1.0E-06
       Y2=YY2*1.0E-06
       Y3=YY3*1.0E-06
       SLOPE=(Y2-Y1)/(X2-X1)
       IF(SLOPE.EQ.0.0) GO TO 150
       EPC=(SLOPE*X1)-Y1-DOG
```

```
      XBAR=X1-(Y1/SLOPE)-(DOG/SLOPE)
C     CHECK LINEARITY OF STRAIN CURVE.
      FUN=Y3-(SLOPE*X3)+(SLOPE*X1)-Y1
      AX=1.3155E-03
      BX=1.3287E+08
      CX=9.5397E+05
      DX=1.4334E+03
      EX=3.7854
      B1=BX/4.
      B2=(-3.*BX*AX-CX)/3.
      B3=(3.*AX*AX*BX+2.*AX*CX+DX)/2.
      B4=-AX*DX+EX-AX*AX*AX*BX-AX*AX*CX
      A1=B1*(4./5.)
      A2=B2*(3./4.)
      A3=B3*(2./3.)
      GO TO 800
  137 WRITE(6,138)L
  138 FORMAT(10X,10HNO READING,75X,15H GAUGE ZONE NO.,I3)
      GO TO 200
  800 X4=THK-D
      Y4=(SLOPE*X4)-(SLOPE*X1)+Y1
      Y44=-Y4
      CALL STEEL(FSC,FY,Y44,EPSY)
      CS=-FSC*ASC-SUN*ASC
      Y5=(SLOPE*X3)-(SLOPE*X1)+Y1
      CALL STEEL(FST,FY,Y5,EPSY)
      TS=FST*AST-SUN*AST
      IF(EPC.GE.0.)GO TO  802
      XMU=0.0
      COM=0.0
      GO TO 801
  802 COM=-B*(PIKE(EPC))*(XBAR/EPC)*(FPC/4.4)
      XMU=(POLY(EPC)/POKE(EPC))*(XBAR/EPC)
  801 CONTINUE
      CALL TENCO(SLOPE,THK,EPC,DOG,XBAR,B,TC,ARM,FPC)
      P=CS+COM+TS+TC
      IF(EPC.LE.0.0) GO TO 810
      PHI=EPC/XBAR
      GO TO 812
  810 PHI=SLOPE
  812 CONTINUE
      XMOM=-COM*((THK/2.)-(XBAR-XMU))-(CS-TS)*((THK/2.)-(THK-D))+TC*(A
     1+XBAR-(THK/2.))
      WRITE(6,10)L,XMOM,PHI,XBAR,P,YY1,YY2,YY3
   10 FORMAT(1X,8H ZON NO.,I2,2X,8H MOMENT=,F10.1,1X,4HIN-K,8H  CURV.=
     110.3,1X,9H N. AXIS=,F10.3,3H IN,1X,9H AX.FORC=,F10.1,8H STRAIN ,
     27.0)
      GO TO 200
  130 WRITE(6,16)
   16 FORMAT(1X,10HSLOPE ZERO)
  200 CONTINUE
      STOP
    1 FORMAT(6F6.3,E12.3,F6.3,E12.3)
    2 FORMAT(1X,3H FY,F6.3,4H FPC,F6.3,2H B,F6.3,2H D,F6.3,4H ASC,F6.3
```

```
  14H AST,F6.3,3H ES,E12.3,4H THK,F6.3,7H SHRINK,E12.3)
15 FORMAT(1X,19H NO. OF GAUGE ZONES,I3,25H NO. OF LOAD INCREMENTS,I3)
 3 FORMAT(2I3)
 4 FORMAT(6F10.3,I3)
11 FORMAT(1X,11H LOAD STAGE,I2//)
13 FORMAT(13A6)
14 FORMAT(1X,13A6)
40 FORMAT(3F10.1,I5)
   END
   FUNCTION POLY(Z)
   COMMON/S1/A1,A2,A3
   POLY=A1*Z**4+A2*Z**3+A3*Z**2
   RETURN
   END
   FUNCTION PORE(Z)
   COMMON/S2/B1,B2,B3
   PORE=B1*Z**3+B2*Z**2+B3*Z
   RETURN
   END
   SUBROUTINE TENCO(SLOPE,THK,EPC,DOG,XBAR,B,TC,ARM,FPC)
C     THIS SUBROUTINE ASSUMES CONCRETE TENSION STRESS-STRAIN CURVE
C     FOLLOWS MIRROR IMAGE OF THAT FOR COMPRESSION UP TO 150 MIN/IN.
   COMMON/S2/B1,B2,B3
   BTMS=EPC-SLOPE*THK
   STRAW=150.0E-06
   WARTS=DOG-STRAW
   EX=STRAW/SLOPE
   IF(BTMS.GT.WARTS) GO TO 200
   ARM=2.0*EX/3.
   TC=B*(PIKE(STRAW))*(EX/STRAW)*(FPC/4.4)
   GO TO 100
200 IF(BTMS.GT.0.0) GO TO 300
   EX=THK-XBAR
   RUM=DOG-BTMS
   ARM=0.667*(THK-XBAR)
   TC=B*(PIKE(RUM))*(EX/RUM)*(FPC/4.4)
   GO TO 100
300 ARM=0.0
   TC=0.0
100 CONTINUE
   RETURN
   END
   SUBROUTINE STEEL(FS,FY,EPS,EPY)
   FS=FY*(((EPS-EPY)-ABS(EPY-EPS))/(2.*EPY))
   RETURN
   END
   FUNCTION PIKE(Z)
   COMMON/S2/B1,B2,B3
   PIKE=B1*Z**4+B2*Z**3+B3*Z**2
   RETURN
   END
```

B2. THEORETICAL MOMENT-CURVATURE RELATIONSHIPS

```
C     MOMENT CURVATURE INCLUDING AXIAL FORCE P.
C     IT IS ASSUMED THAT THE CAGE CROSS-SECTION IS SYMMETRICAL.
C     SHRINK IS SHRINKAGE STRAIN.
      COMMON/S1/A1,A2,A3
      COMMON/S2/B1,B2,B3
      DIMENSION PHI(300),XMOM(300),EXPO(300)
      READ(5,1)FY,FPC,B,D,ASC,AST,ES,THK,SHRINK
      WRITE(6,2)FY,FPC,B,D,ASC,AST,ES,THK,SHRINK
      EPSY=FY/ES
C     CALCULATE COMPRESSION IN STEEL DUE TO SHRINKAGE
      CALL STEEL(SUN,FY,SHRINK,EPSY)
      STAR=SUN*(AST+ASC)
C     CALCULATE TENSILE STRESS IN CONCRETE DUE TO SHRINKAGE
      XMOON=STAR/((B*THK)-(AST+ASC))
      WRITE(6,18)STAR,XMOON
   18 FORMAT(1X,4HSTAR,E12.3,4HMOON,E12.3)
C     CALCULATE TENSILE STRAIN IN CONCRETE DUE TO SHRINKAGE-- SINCE
C     LOW STRAIN, USE SLOPE OF STRAIN CURVE FROM 0 TO 100 MICROSTRAIN.
C     THIS IS THE STRAIN IN THE CONCRETE EQUIVALENT TO THE COMPRESSIVE
C     FORCE IN THE STEEL.
      EC=4.0E+03
      DOG=XMOON/EC
      WRITE(6,17)DOG
   17 FORMAT(1X,3HDOG,E12.3)
C     ITERATE P.
      P=0.
C     ITERATE STRAIN IN COMPRESSION FIBRE DOWN FROM 0.003.
  330 EPC=0.003
      ITCH=1
C     ASSUME A VALUE FOR THE NEUTRAL AXIS.
      DO 340 II=1,100
      JJ=II-1
      OX=0.333*THK
 2000 CONTINUE
      DO 310 J=1,200
      SLOPE=EPC/OX
      EPL=EPC-DOG
      IF(SLOPE.EQ.0.) GO TO 130
      XBAR=OX-DOG/SLOPE
      AX=1.3155E-03
      BX=1.5287E+08
      CX=9.5397E+05
      DX=1.4334E+03
      EX=3.7854
      B1=BX/4.
      B2=(-3.*BX*AX-CX)/3.
      B3=(3.*AX*AX*BX+2.*AX*CX+DX)/2.
      B4=-AX*DX+EX-AX*AX*AX*BX-AX*AX*CX
      A1=B1*0.8
      A2=B2*0.75
      A3=B3*(2./3.)
      X4=THK-D
      Y44=EPC*((OX-X4)/OX)
      YY4=Y44-DOG
      CALL STRAIN(FCON,YY4,B1,B2,B3,B4)
```

```
      CALL STEEL(FSC,FY,Y44,EPSY)
      CS=ASC*(-FSC+FCON-SUN)
      IF(OX.LT.X4) CS=ASC*(-FSC-SUN)
      Y5=EPC*((D-OX)/OX)
      YY=Y5+DOG
      YYY=Y5-DOG
      CALL STRAIN(FCON,YY,B1,B2,B3,B4)
      IF(YY.GT.0.00015) FCON=0.0
      CALL STEEL(FST,FY,Y5,EPSY)
      TS=AST*(FST-SUN+FCON)
      IF(OX.LT.D) TS=AST*(FST-SUN)
      IF(YYY.GE.EPSY) GO TO 200
      GO TO 201
  200 TS=AST*(FST+FCON)
      IF(OX.LT.D) TS=AST*FST
  201 CONTINUE
      IF(XBAR.GT.THK) GO TO 500
      IF(XBAR.GT.(THK/2.)) GO TO 400
      GO TO 410
  400 EPMID=EPC*(XBAR-THK/2.)/XBAR
      COM=-B*(PIKE(EPL)-PIKE(EPMID))*(XBAR/EPL)*(FPC/4.4)
      ANTICO=-B*(PIKE(EPMID))*(XBAR/EPL)*(FPC/4.4)
      XMU=((POLY(EPL)-POLY(EPMID))/(POKE(EPL)-POKE(EPMID)))*(XBAR/EPL)
      ANTX=(POLY(EPMID)/POKE(EPMID))*(XBAR/EPL)
      GO TO 420
  410 COM=-B*(PIKE(EPL))*(XBAR/EPL)*(FPC/4.4)
      ANTICO=0.0
      ANTX=0.0
  420 CONTINUE
      XMU=(POLY(EPL)/POKE(EPL))*(XBAR/EPL)
      CALL TENCO(SLOPE,THK,EPC,DOG,XBAR,B,TC,ARM,FPC)
      CHECK=CS+COM+TS+TC-P
      IF(ABS(CHECK).LE.0.1) GO TO 300
      DELOX=0.01
  310 OX=OX*(1.0+DELOX*CHECK)
      ITCH=ITCH+1
      IF(ITCH.GT.2) GO TO 313
      IF(ABS(CHECK).GE.0.3) GO TO 313
      IF(ABS(CHECK).GE.0.1) GO TO 2000
  300 PHI(II)=EPC/OX
      EXPO(II)=PHI(II)
      XMOM(II)=-COM*((THK/2.)-(XBAR-XMU))-(CS-TS)*((THK/2.)
     1-(THK-D))+TC*(ARM+XBAR-(THK/2.))+ANTICO*((THK/2.)-ANTX)
      WRITE(6,10)XMOM(II),PHI(II),P,CHECK
      WRITE(6,999)OX,SLOPE,EPL,XBAR,X4,Y44,FCON,FSC,CS,Y5
      WRITE(6,999)YY,FST,TS,EPMID,COM,ANTICO,XMU,ANTX,TC,ARM
  999 FORMAT(1X,10F10.6)
      WRITE(6,19)EPC
   19 FORMAT(1X,5HEPC,E12.3)
   10 FORMAT(1X,7H MOMENT,F12.3,5H IN-K,5X,10H CURVATURE,E12.3,5H(RAD)
     113H AXIAL FORCE ,F12.3,5HCHECK,F10.3)
      GO TO 140
  130 WRITE(6,16)
   16 FORMAT(1X,10HSLOPE ZERO)
```

```
140 CONTINUE
    CPE=EPC
    EPC=EPC-0.0001
    IF(CPE.LT.5.0E-04.AND.CPE.GT.1.0E-04) EPC=CPE-0.00001
    IF(EPC.LE.0.0) GO TO 320
340 CONTINUE
    JJ=JJ+1
    GO TO 320
313 WRITE(6,21)
 21 FORMAT(15H NO CONVERGENCE)
500 WRITE(6,22)
 22 FORMAT(12H XBAR.GT.THK)
320 CONTINUE
    P=P-2.0
    IF(P.GE.(-15.0)) GO TO 330
    STOP
  1 FORMAT(6F6.3,E12.5,F6.3,E12.5)
  2 FORMAT(1X,5H FY,F7.3,4H FPC,F6.3,2H B,F6.3,2H D,F6.3,4H ASC,F6.3,
   14H AST,F6.3,5H ES,E12.5,4H THK,F6.3,7H SHRINK,E12.5)
  3 FORMAT(2I5)
  4 FORMAT(6F10.5,I5)
    END
    FUNCTION POLY(Z)
    COMMON/S1/A1,A2,A3
    POLY=A1*Z**4+A2*Z**3+A3*Z**2
    RETURN
    END
    FUNCTION PIKE(Z)
    COMMON/S2/B1,B2,B3
    PIKE=B1*Z**3+B2*Z**2+B3*Z
    RETURN
    END
    SUBROUTINE TENCO(SLOPE,THK,EPC,DOG,XBAR,B,TC,ARM,FPC)
C   THIS SUBROUTINE ASSUMES CONCRETE STRESS-STRAIN CURVE
C   FOR TENSION IS A MIRROR IMAGE OF THAT FOR COMPRESSION
C   UP TO A STRAIN OF 0.00015
    COMMON/S2/B1,B2,B3
    BTMS=EPC-SLOPE*THK
    STRAW=0.00015
    WARTS=DOG-STRAW
    EX=STRAW/SLOPE
    IF(BTMS.GT.WARTS) GO TO 200
    ARM=2.0*EX/3.
    TC=B*(PIKE(STRAW))*(EX/STRAW)*(FPC/4.4)
    GO TO 100
200 IF(BTMS.GT.0.) GO TO 300
    EX=THK-XBAR
    ROM=DOG-BTMS
    ARM=0.66667*(THK-XBAR)
    TC=B*(PIKE(ROM))*(EX/ROM)*(FPC/4.4)
    GO TO 100
300 ARM=0.
    TC=0.
100 CONTINUE
```

```
RETURN
END
SUBROUTINE STEEL(FS,FY,EPS,EPY)
FS=FY*(((EPS+EPY)-ABS(EPY-EPS))/(2.*EPY))
RETURN
END
FUNCTION PINE(Z)
COMMON/S2/B1,B2,B3
PINE=B1*Z**4+B2*Z**3+B3*Z**2
RETURN
END
SUBROUTINE STRAIN(Y,X,B1,B2,B3,B4)
Y=4.*B1*X**3+3.*B2*X*X+2.*B3*X+B4
RETURN
END
```

CD TOT 0200

B3. STRAIN DISTRIBUTION FROM DEMEC READINGS

```
C     PROGRAM TO PROCESS LONG-TERM DEMEC READINGS.
C     ZEROS ARE INITIAL DEMEC READINGS.
C     X1,X2,X3 ARE GAUGE LOCATIONS FROM INSIDE FACE.
C     COMPRESSION IS POSITIVE
      DIMENSION ZERO1(30),ZERO2(30),ZERO3(30),X1(30),X2(30),X3(30),
     1Y1(30),Y2(30),Y3(30),Y1ERR(30),Y3ERR(30),TITLE(13),STRO(30),
     2STR1(30),STR2(30),STR3(30),STR4(30)
      READ(5,1)NGAGE,NLOAD
      DO 10 I=1,NGAGE
      READ(5,2)ZERO1(I),ZERO2(I),ZERO3(I),X1(I),X2(I),X3(I)
   10 WRITE(6,2)ZERO1(I),ZERO2(I),ZERO3(I),X1(I),X2(I),X3(I)
      DO 100 II=1,NLOAD
      READ(5,6)(TITLE(J),J=1,13)
      WRITE(6,7)(TITLE(J),J=1,13)
      READ(5,3)((Y1(I),Y2(I),Y3(I)),I=1,NGAGE)
      DO 20 I=1,NGAGE
      STR1(I)=(ZERO1(I)-Y1(I))*10.
      STR2(I)=(ZERO2(I)-Y2(I))*10.
      STR3(I)=(ZERO3(I)-Y3(I))*10.
      IF((STR1(I)-STR3(I)).LT.0.0) GO TO 30
      SLOPE=(STR2(I)-STR1(I))/(X2(I)-X1(I))
      STRO(I)=STR1(I)-X1(I)*SLOPE
      STR4(I)=STRO(I)+8.*SLOPE
      Y3ERR(I)=STR3(I)-STRO(I)-X3(I)*SLOPE
      Y1ERR(I)=0.0
      GO TO 20
   30 SLOPE=(STR2(I)-STR3(I))/(X2(I)-X3(I))
      STRO(I)=STR3(I)-X3(I)*SLOPE
      STR4(I)=STRO(I)+8.*SLOPE
      Y1ERR(I)=STR1(I)-STRO(I)-X1(I)*SLOPE
      Y3ERR(I)=0.0
   20 CONTINUE
      WRITE(6,4)
      WRITE(6,5)((I,STRO(I),STR4(I),Y1ERR(I),Y3ERR(I)),I=1,NGAGE)
  100 CONTINUE
      STOP
    1 FORMAT(2I3)
    2 FORMAT(6F10.3)
    3 FORMAT(3F10.3)
    4 FORMAT(1X,11HSECTION NO.,5X,15HSTRAIN INSIDE,5X,14HSTRAIN OUTSIDE,
     13X,15HDIFFERENCES--Y1,10X,2HY2)
    5 FORMAT(4X,I5,11X,F10.3,7X,F10.3,6X,F10.4,6X,F10.4)
    6 FORMAT(13A6)
    7 FORMAT(1X,13A6)
      END
```

CD TOT 0049

B4. SHORT-TERM ANALYSIS

```
C     FIRST STAGE PROGRAM FOR SMALL ELEMENT SOLUTION FOR CONCRETE FRAME
C     THIS VERSION REQUIRES LOADS AND REACTIONS TO BE INPUT FOR
C     EACH LOAD INCREMENT.
C     NLOAD IS NUMBER OF LOAD INCREMENTS.
C     PROGRAM FOR MOMENT CURVATURE WITH AXIAL FORCE.
C     ES IS STEEL MOMENT OF INERTIA.
C     AST IS TOTAL AREA OF STEEL.
C     AC IS EFFECTIVE AREA OF CONCRETE.
C     HOR IS APPLIED HORIZONTAL LOAD.
C     VERT IA APPLIED VERTICAL LOAD.
C     P AND V READ IN ARE BASE REACTIONS POSITIVE IN A RIGHT HAND
C     ORTHOGONAL COORDINATE SYSTEM.
      DIMENSION X(100),Y(100),PHI(100),XM(100),R(100),THETA(100),ANG(10
     1),ONG(100),D(100),GOOF(200)
      DIMENSION AXFOR(100),SHFOR(100),ICN(100),XMULT(100)
      READ(5,509)NLOAD
  509 FORMAT(I3)
      READ(5,8)EC,ES,AST,AC
C     SLOP IS SLOPE AT POINT 0
C     SLIP IS SLOPE AT POINT N
      READ(5,1)N,XXL,COL,BEAM
    1 FORMAT(I3,3F10.3)
      DO 1000 IJ=1,NLOAD
      READ(5,2)P,V,XM(1),HOR,VERT
      READ(5,14)SHRINK,X(1),Y(1),SLOP,XN,YN,SLIP
   14 FORMAT(E8.1,2F10.5,E10.3,2F10.5,E10.3)
      XSTART=X(1)
      YSTART=Y(1)
      WRITE(6,15)SHRINK,SLOP
   15 FORMAT(1X,10HSHRINKAGE ,E12.5,5X,10HSLOPE AT 0,E12.5)
      PST=P
      VST=V
      CROX=100.
      CROY=100.
      CROM=100.
      GOOF(1)=10.
      TRIAL=10.
      ITCH=1
      WRITE(6,5)P,V,XXL,N,COL,HOR,VERT,BEAM
      WRITE(6,4)
      Z=-P
      XMULT(1)=(XM(1)/ABS(XM(1)))*(512.-2.5*Z)
      CALL CURVA(XM(1),SHRINK,Z,PHI(1),XMULT(1))
      WRITE(6,5)XM(1),X(1),Y(1),PHI(1),P,V,I
  500 CONTINUE
      X(1)=XSTART
      Y(1)=YSTART
      Z=-P
      XMULT(1)=(XM(1)/ABS(XM(1)))*(512.-2.5*Z)
      CALL CURVA(XM(1),SHRINK,Z,PHI(1),XMULT(1))
      I=0
      AXFOR(1)=P
      SHFOR(1)=V
```

```
      PRD=XXL
      XMSTA=XM(I)*(COL+4.)/COL
      CALL BASE(ANG(I),XMSTA,SLOP,Z,XBIT,YBIT)
      X(I)=X(I)+XBIT
      Y(I)=Y(I)+YBIT
      ITER=1
      ITEM=1
      ITEC=1
      DO 40 I=1,N
      IKOUNT=0
   30 R(I)=1./PHI(I)
      IKOUNT=IKOUNT+1
      THETA(I+1)=XXL/R(I)
      ANG(I+1)=ANG(I)+THETA(I+1)
      UNG(I)=ABS(ANG(I))
      UNG(I+1)=ABS(ANG(I+1))
      COFUN=ABS(COS(UNG(I))-COS(UNG(I+1)))
      SIFUN=ABS(SIN(UNG(I+1))-SIN(UNG(I)))
      IF((ANG(I+1)/ANG(I)).LT.0.0)SIFUN=ABS(SIN(UNG(I+1))+SIN(UNG(I)))
      D(I)=ABS(R(I))
      ABC=ANG(I)+THETA(I+1)/2.
      BBC=ABS(ABC)
      IF(PRD.GT.(2.*COL+BEAM)) GO TO 100
      IF(PRD.GT.(COL+BEAM)) GO TO 80
      IF(PRD.GT.(COL+BEAM/2.)) GO TO 70
      IF(PRD.GT.COL) GO TO 60
      DELX=D(I)*COFUN
      DELY=D(I)*SIFUN
      IF(ANG(I+1).GT.0.0.AND.R(I).GT.0.0) GO TO 92
      DELXX=DELX
      DELYY=-DELY
      GO TO 90
   92 DELX=-DELX
      DELXX=DELX
      DELYY=-DELY
   90 X(I+1)=X(I)+DELX
      Y(I+1)=Y(I)+DELY
      AXFOR(I+1)=P
      SHFOR(I+1)=V
      XM(I+1)=XM(I)+P*DELXX+V*DELYY
C     PUT TEMPORARY APPROXIMATION TO PLASTIC HINGE IN.
      XMULT(I+1)=(XM(I+1)/ABS(XM(I+1)))*(S12.-2.5*Z)
      IF(XM(I+1).GT.ABS(XMULT(I+1))) XM(I+1)=ABS(XMULT(I+1))
      IF(XM(I+1).LT.(-ABS(XMULT(I+1)))) XM(I+1)=-ABS(XMULT(I+1))
      CALL CURVA(XM(I+1),SHRINK,Z,RII,XMULT(I+1))
      PHI(I)=(PHI(I)+RII)/2.
      IF(IKOUNT.GE.200) GO TO 400
      PHI(I+1)=PHI(I)
      IF(ABS(PHI(I)-RII).LE.1.0E-06) GO TO 38
      IF(ABS((PHI(I)-RII)/RII).GE.0.01) GO TO 30
   38 PRD=PRD+XXL
   40 CONTINUE
      GO TO 100
   60 CONTINUE
```

```
      IF(ITER.NE.1) GO TO 61
      PORT=P
      P=V+HOR
      Z=-P
      V=PORT
      ITER=2
      IF((COL+BEAM/2.-PRD).LT.XXL) ITER=1
   61 DELX=D(I)*SIFUN
      DELY=-D(I)*COFUN
      IF(ANG(I+1).GT.0.0.AND.ANGER(I).GT.0.0) GO TO 63
      DELXX=-DELY
      DELYY=DELX
      GO TO 90
   63 DELYY=DELX
      DELY=-DELY
      DELXX=-DELY
      GO TO 90
   70 CONTINUE
      IF(ANG(I).GE.(-2.0E-05)) GO TO 74
C     THIS  CHECK IS TO MAKE SURE THAT THE SLOPE WILL GO POSITIVE NEAR
C     THE CENTRE OF THE BEAM.
      ANGER=-ANG(I)
      PORT=V
      V=P-HOR
      P=PORT
      IF(PRD.GT.(COL+BEAM/2.+XXL))P=PORT-VERT
      DELP=35.6*ANGER
      DELV=21.0*ANGER
      DELM=952.0*ANGER
      P=P+DELP
      V=V-DELV
      XM(I)=XM(I)+DELM
      IF(ABS(XM(I)).GE.ABS(XMULT(I))) GO TO 1100
      GO TO 300
   74 CONTINUE
      IF(ITER.NE.1) GO TO 71
      V=V+VERT
      ITER=2
      IF((COL+BEAM-PRD).LT.XXL) ITER=1
   71 DELX=D(I)*SIFUN
      DELY=D(I)*COFUN
      IF(ANG(I+1).LT.0.0) GO TO 73
      DELXX=-DELY
      DELYY=DELX
      GO TO 90
   73 DELY=-DELY
      DELXX=-DELY
      DELYY=DELX
      GO TO 90
   80 CONTINUE
      IF(ITER.NE.1) GO TO 81
      HART=P
      P=V
      Z=P
```

```
      V=PART
      ITEC=2
   81 DELX=-D(I)*COFUN
      DELY=-D(I)*SIFUN
      IF(ANG(I+1).GT.0.0.AND.R(I).GT.0.0) GO TO 83
      DELXX=DELX
      DELYY=-DELY
      GO TO 90
   83 DELXX=-DELX
      DELYY=-DELY
      DELX=-DELX
   19 FORMAT(1X,6HPASSED)
      GO TO 90
  100 CONTINUE
      INK=COL/XXL
      XP=-((XM(I+1)-XM(I+1-INK))*(COL+4.))/COL-XM(I+1-INK)
      CALL BASE(ANGST,XP,SLIP,Z,XBIT,YBIT)
      X(I+1)=X(I+1)-XBIT
      Y(I+1)=Y(I+1)-YBIT
      XERR=X(I+1)-XN
      YERR=Y(I+1)-YN
      SLOER=ANG(I+1)-ANGST
      ABEX=ABS(XERR)
      ABEY=ABS(YERR)
      ABEM=ABS(SLOER)
      P=P-VERT
      V=V-HOR
      SUMER=ABEX+ABEY+ABEM*100.
      GOOF(ITCH+1)=SUMER
      IF(GOOF(ITCH+1).LT.GOOF(ITCH)) GO TO 260
      GO TO 262
  260 IF(GOOF(ITCH+1).LT.TRIAL) GO TO 261
      GO TO 263
  261 TRIAL=GOOF(ITCH+1)
      XMTR=XM(I)
      PTR=P
      VTR=V
  263 IF(ITCH.LT.15) GO TO 262
      IF((GOOF(ITCH-1)-GOOF(ITCH+1)).GT.0.1) GO TO 262
      XM(I)=XMTR
      P=PTR
      V=VTR
      IF(ITCH.LT.50) GO TO 265
      IF(ITCH.LT.100) GO TO 266
      GO TO 262
  265 GOOF(50)=GOOF(ITCH)
      GOOF(51)=GOOF(ITCH+1)
      ITCH=50
      GO TO 262
  266 GOOF(100)=GOOF(ITCH)
      GOOF(101)=GOOF(ITCH+1)
      ITCH=100
  262 CONTINUE
      IF(SUMER.LT.0.05) GO TO 900
```

```
C       CHANGES IN REACTIONS AT 0 ARE BASED ON AN ELASTIC DETERMINATION
C       OF THE FORCES REQUIRED TO REMOVE THE COORDINATE ERRORS AT N.
        SOMER=CROX+CROY+CROM
        CROX=XERR
        CROY=YERR
        CROM=SLOER
        DELV=0.65*XERR+21.0*SLOER
        DELP=0.376*YERR+35.6*SLOER
        DELM=41.6*XERR-17.8*YERR+932.8*SLOER
        DULV=DELV
        DULP=DELP
        DULM=DELM
        IF(ABS(DELP).LT.0.01) DELP=0.01*DELP/ABS(DELP)
        IF(ABS(DELV).LT.0.01)DELV=0.01*DELV/ABS(DELV)
        IF(ABS(DELM).LT.0.1)DELM=0.1*DELM/ABS(DELM)
        IF(SOMER.LT.SUMER) GO TO 800
        GO TO 810
  800   DIF1=ABEX-ABEY
        IF(DIF1.GT.0.) GO TO 811
        DIF2=ABEY-ABEM*100.
        IF(DIF2.GT.0.) GO TO 812
        DELV=0.0
        DELP=0.0
        GO TO 810
  811   DIF3=ABEX-ABEM*100.
        IF(DIF3.GT.0.) GO TO 813
        DELV=0.
        DELP=0.
        GO TO 810
  812   DELV=0.
        DELM=0.
        GO TO 810
  813   DELP=0.
        DELM=0.
  810   CONTINUE
        WRITE(6,2222)XERR,YERR,SLOER,SUMER,DELP,DELV,DELM,XM(1),XM(15),
       1XM(20),XM(29),ITCH
 2222   FORMAT(1X,4F10.5,3F7.3,4F10.3,I3)
        WRITE(6,2223)ANGST,SLIP,ANG(I+1),ANG(I)
 2223   FORMAT(1X,4F10.6)
        ITCH = ITCH+1
        IF(ITCH.GT.125) GO TO 50
        IF(ITCH.GT.50) GO TO 51
        IF(ABS(XM(I)).GE.ABS(XMULT(I))) GO TO 1100
        IF(ABS(DELP).GT.0.1) DELP=(DELP/ABS(DELP))*0.1
        IF(ABS(DELV).GT.0.1) DELV=(DELV/ABS(DELV))*0.1
        IF(ABS(DELM).GT.5.) DELM=(DELM/ABS(DELM))*5.
        P=P+DELP
        V=V+DELV
        XM(I)=XM(I)-DELM
        GO TO 500
   51   IF(DELV.EQ.0.0.AND.DELP.EQ.0.0) GO TO 52
        IF(DELV.EQ.0.0.AND.DELM.EQ.0.0) GO TO 53
        DELP=0.01*DULP/ABS(DULP)
```

```
      DELM=0.1*DOLM/ABS(DOLM)
      GO TO 54
   52 DELV=0.01*DOLV/ABS(DOLV)
      DELP=0.01*DOLP/ABS(DOLP)
      GO TO 54
   53 DELV=0.01*DOLV/ABS(DOLV)
      DELM=0.1*DOLM/ABS(DOLM)
   54 CONTINUE
      IF(ITCH.GT.75) GO TO 200
      IF(ABS(DELP).GT.0.1) DELP=(DELP/ABS(DELP))*0.1
      IF(ABS(DELV).GT.0.1) DELV=(DELV/ABS(DELV))*0.1
      IF(ABS(DELM).GT.5.) DELM=(DELM/ABS(DELM))*5.
      P=P+DELP
      V=V+DELV
      XM(1)=XM(1)-DELM
      GO TO 300
  200 CONTINUE
      IF(ABS(DELP).GT.0.1)DELP=(DELP/ABS(DELP))*0.1
      IF(ABS(DELV).GT.0.1) DELV=(DELV/ABS(DELV))*0.1
      IF(ABS(DELM).GT.5.) DELM=(DELM/ABS(DELM))*5.
      P=P+DELP/2.
      V=V+DELV/2.
      XM(1)=XM(1)-DELM/2.
      GO TO 300
 1100 P=PSI/2.
      V=VSI/2.
      XM(1)=XM(1)/4.
      IF(XM(1).LT.(-32.*P))XM(1)=-32.*P
      GO TO 300
  669 III=I-1
      WRITE(6,56) ITCH,SUMER
      WRITE(6,670)III
  670 FORMAT(1X,25HPLASTIC HINGE AT SECTION ,I2/1X,33HTHIS PROGRAM NO LO
     1NGER APPLICABLE)
      GO TO 1111
  400 P=AXFOR(1)
      V=SHFOR(1)
   50 WRITE(6,7)
  900 WRITE(6,666)
  666 FORMAT(1X,7HSECTION,3X,6HMOMENT,3X,11HAXIAL FORCE,3X,11HSHEAR FOR
     1E,6X,1HX,6X,1HY,5X,9HCURVATURE,7X,5HANGLE)
      NN=N+1
      DO 668 I=1,NN
  668 ICN(I)=I-1
      WRITE(6,667)((ICN(I),XM(I),AXFOR(I),SHFOR(I),X(I),Y(I),PHI(I),
     1ANG(I)),I=1,NN)
  667 FORMAT(4X,I2,4X,F8.3,4X,F8.3,6X,F8.3,3X,F8.4,2X,F8.4,2X,E12.5,2X,
     1E12.5)
      DO 671 I=1,NN
      TRIM=XM(I)
      IF(ABS(TRIM).GE.ABS(XMULT(I))) GO TO 669
  671 CONTINUE
      WRITE(6,16)XN,YN,SLIP
   16 FORMAT(1X,25H MEASURED COORDS AT N (,F10.4,1H,,F10.4,1H),5X,10HSL
```

```
     1PE AT X,E12.5)
      WRITE(6,17)XERR,YERR,SLOER
   17 FORMAT(1X,4HXERR,F10.5,2X,4HYERR,F10.5,2X,5HSLOER,E12.5)
      GOOF(I)=10.
      TRIAL=10.
      WRITE(6,56)ITCH,SOMER
   56 FORMAT(1X,4HITCH,I4,5HSOMER,F10.7)
 1000 CONTINUE
 1111 STOP
    2 FORMAT(5F10.5)
    3 FORMAT(1X,1HP,F10.5,2X,1HV,F10.5,2X,14HELEMENT LENGTH,F7.5,2X,15H
     1NO. OF ELEMENTS,I3,2X,11HCOL LENGTH,F10.5/1X,16HHORIZONTAL FORCE,
     2F10.5,5X,14HVERTICAL FORCE,F10.5,5X,11HBEAM LENGTH,F10.5)
    4 FORMAT(5X,6HMOMENT,8X,1HX,10X,1HY,7X,9HCURVATURE,5X,11HAXIAL FORC
     1,3X,11HSHEAR FORCE,3X,11HELEMENT NO.)
    5 FORMAT(3X,F10.5,1X,F10.5,1X,F10.5,1X,E12.5,1X,F10.3,1X,F10.3,6X,I
     1)
    7 FORMAT(6H NO GO)
    8 FORMAT(2E10.5,2F7.5)
      END
      SUBROUTINE CORVA(XM,SHRINK,P,PHI,XMULT)
C     THIS SUBROUTINE CALCULATES CURVATURE FOR A GIVEN MOMENT
C     FROM THE MOMENT-CURVATURE GRAPHS AND THE CURVE FITTING PROGRAMS.
      XMCR=(XM/ABS(XM))*((75.-1.25*P)-(1.+0.025*P)*SHRINK*1.0E+05)
      PHICR=(XM/ABS(XM))*(1.07+0.02*P+SHRINK*1.4E+05)*1.0E-04
      IF(ABS(XM).LE.ABS(XMCR)) GO TO 20
      SLOPE=(6.0E+05+1.0E+07*SQRT(SHRINK))*(1.0+0.003*P)
      PHI=PHICR+(XM-XMCR)/SLOPE
      GO TO 100
   20 PHI=XM/(1.94E+06)
  100 CONTINUE
      RETURN
      END
      SUBROUTINE AXSTR(DX,DY,P,EC,ES,AST,AC,XXL,ABC)
      XN=ES/EC
      F=P*COS(ABC)
      STRAIN=F/(EC*(AC+XN*AST))
      DL=STRAIN*XXL
      DX=DL*SIN(ABC)
      DY=DL*COS(ABC)
      RETURN
      END
      SUBROUTINE BASE(ANG,XM,SLOPE,Z,XBIT,YBIT)
C     THIS SUBROUTINE CALCULATES THE ROTATION OF THE STEEL BASE.
      STRT=((-XM/7.567)+Z)/25114.
      STRC=((XM/7.567)+Z)/25114.
      ABSTR=ABS(STRT-STRC)
      EXI=-ATAN(ABSTR/7.567)
      ABEX=-EXI
      SLORP=-SLOPE
      ANG=-ATAN(SLORP)+EXI
      BIT=4.0*(1.0+(STRT+STRC)/2.)
      XBIT=BIT*SIN(SLORP)-4.*SIN(ANG)
      YBIT=BIT*COS(SLORP)+4.*COS(ANG)
      RETURN
      END
```

B5. SUSTAINED LOAD ANALYSIS

```
C     SECOND STAGE PROGRAM FOR SMALL ELEMENT SOLUTION OF RC FRAME
C     ES IS STEEL MOMENT OF INERTIA.
C     AST IS AREA OF TENSION OR COMPRESSION STEEL.
C     AC IS TOTAL CROSS-SECTION AREA.
C     HOR IS APPLIED HORIZONTAL LOAD.
C     VERT IA APPLIED VERTICAL LOAD.
C     P AND V READ IN ARE BASE REACTIONS POSITIVE IN A RIGHT HAND
C     ORTHOGONAL COORDINATE SYSTEM.
      REAL INST
      DIMENSION UU(30,25),UUF1(30,25),PEEP(30,25)
      DIMENSION X(100),Y(100),PHI(100),XM(100),R(100),THETA(100),ANG(100
     1),UNG(100),D(100),XMULT(100)
      DIMENSION AXFOR(100),SHFOR(100),ICK(100)
      DIMENSION OUTST(100),INST(100),GOOF(130)
  401 READ(5,8) ES,AST,AC,CYL,SFY,H,SSY,M,UC,UT,TCF
    8 FORMAT(E10.3,6F10.5/I3,2E12.5,F10.5)
C     UC IS STRAIN AT THE OUTSIDE FIBRE
C     UT IS STRAIN AT THE INSIDE FIBRE
C     COMPRESSION IS POSITIVE.
      WRITE(6,8)ES,AST,AC,CYL,SFY,H,SSY,M,UC,UT,TCF
      AS=AST
C     EC IS THE CONCRETE MODULUS OF ELASTICITY FOR LOW STRAINS.
      EC=1131.*CYL
      IF(H.LE.0.00025)EC=1184.*CYL
      CSHR=2.*AS*H*ES/((AC-2.*AS)*EC)
      WRITE(6,301)CSHR
  301 FORMAT(1X,28HSHRINKAGE STRAIN IN CONCRETE,E11.3)
      CROX=100.
      CROY=100.
      CROM=100.
      ITCH=1
      GOOF(1)=10.0
      TRIAL=10.0
C     SLOP IS SLOPE AT POINT 0
C     SLIP IS SLOPE AT POINT N
      READ(5,1)N,XXL,COL,BEAM
    1 FORMAT(I3,3F10.3)
      READ(5,14)X(1),Y(1),SLOP,XN,YN,SLIP
   14 FORMAT(2F10.4,E10.3,2F10.4,E10.3)
      WRITE(6,206)X(1),Y(1),SLOP
  206 FORMAT(1X,23H MEASURED COORDS AT 1 (,F10.4,1H,,F10.4,1H),3X,
     110HSLOPE AT 1,E12.5)
      XSTART=X(1)
      YSTART=Y(1)
      FCII=CYL
      DECIDE =0.0
      T0=0.0
      T1=0.0
      T2=0.0
      DL=0.
      NN=N+1
      DO 101 II=1,NN
      DO 101 JJ=1,M
  101 PEEP(II,JJ)=0.0
      READ(5,2)P,V,XM(1),HOR,VERT
```

```
      WRITE(6,5)P,V,XXL,N,COL,HOR,VERT,BEAM
      PST=P
      VST=V
  300 CONTINUE
      GO TO 525
  501 CONTINUE
      READ(5,2)P,V,XM(1),HOR,VERT
      READ(5,14)X(1),Y(1),SLOP,AN,YN,SLIP
      WRITE(6,510)HOR,VERT
  510 FORMAT(1X,3HHOR,F10.6,3X,4HVERT,F10.6)
      GO TO 525
  530 READ(5,511)T2,HOR,VERT,P,V,XM(1),DECIDE
  511 FORMAT(7F10.3)
      COEF(1)=1.0
      READ(5,14)X(1),Y(1),SLOP,AN,YN,SLIP
      WRITE(6,512)T1,T2,HOR,VERT
  512 FORMAT(1X,2HT1,F10.3,2HT2,F10.3,3HHOR,F10.3,4HVERT,F10.3)
      CALL CREEP(T0,T1,T2,U0,PEEP,N,M)
      IF(T2.LE.120.) GO TO 105
      CYL=FCTI*(1.0+TCF)
      GO TO 525
  105 CYL=FCTI*(1.0+TCF*T2/120.)
  525 X(1)=XSTART
      Y(1)=YSTART
      I=0
      III=I+1
      DELXX=0.0
      DELYY=0.0
      Z=-P
      XMULT(1)=(XM(1)/ABS(XM(1)))*(512.-2.5*Z)
      PP=P
      UCR=UC
      UTR=UT
      KIK=1
  313 CONTINUE
      DO 310 II=1,600
      CALL STEEL(UC,UT,PS1,PS2,AS,SF,SSY,H)
      CALL AFORCE(UC,UT,PS1,PS2,PCAL,PP,N,PEEP,U0,III,CYL,KIK,COMM)
      IF(ABS(UC+UT).GT.0.1) GO TO 311
      IF(II.GT.550)WRITE(6,801)P,PCAL,PS1,PS2,UC,UT,II
      CALL STEEL(UC,UT,PS1,PS2,AS,SF,SSY,H)
      CALL XBMX(UC,UT,PS1,PS2,BMXCAL,BAX,XM(III),PP,V,PEEP,U0,
     1III,CYL,DELXX,DELYY,M,KIK,COMM)
      IF(ABS(UC+UT).GT.0.1) GO TO 311
      IF(II.GT.550)WRITE(6,801)BAX,BMXCAL,PS1,PS2,UC,UT,II
  801 FORMAT(1X,6E12.5,I4)
      PERROR=ABS((PP-PCAL)/PP)
      IF(II.GT.100.AND.ABS(BAX).GT.100.0)PERROR=0.0
      XBMER=ABS((BAX-BMXCAL)/BAX)
      IF(ABS(BAX).LT.15.)XBMER=ABS((BAX-BMXCAL)/10.)
      IF(ABS(BAX).GE.500.) GO TO 201
      IF(PERROR.GT.0.01) GO TO 310
      IF(XBMER.LT.0.01) GO TO 312
      GO TO 310
  201 IF(ITCH.LT.50)ITCH=50
      GO TO 312
```

```
310 CONTINUE
311 UC=UCK
    UT=UTK
    KIK=KIK+1
    IF(KIK.LE.2) GO TO 313
    GO TO 50
312 KIK=1
    PHI(1)=(UC-UT)/8.
    OUTST(1)=UC
    INST(1)=UT
    AXFOR(1)=P
    SHFOR(1)=V
    PRD=XXL
    XMSTA=XM(1)*(COL+4.)/COL
    CALL BASE(ANG(1),XMSTA,SLOP,Z,XBIT,YBIT)
    X(1)=X(1)+XBIT
    Y(1)=Y(1)+YBIT
    ITER=1
    ITEM=1
    ITEC=1
    IKOUNT=0
    DO 40 I=1,N
    III=I+1
    IKOUNT=IKOUNT+1
 30 R(I)=1./PHI(I)
    THETA(I+1)=XXL/R(I)
    ANG(I+1)=ANG(I)+THETA(I+1)
    UNG(I)=ABS(ANG(I))
    UNG(I+1)=ABS(ANG(I+1))
    COFUN=ABS(COS(UNG(I))-COS(UNG(I+1)))
    SIFUN=ABS(SIN(UNG(I+1))-SIN(UNG(I)))
    IF((ANG(I+1)/ANG(I)).LT.0.0)SIFUN=ABS(SIN(UNG(I+1))+SIN(UNG(I)))
    D(I)=ABS(R(I))
    ABC=ANG(I)+THETA(I+1)/2.
    BBC=ABS(ABC)
    IF(PRD.GT.(2.*COL+BEAM)) GO TO 100
    IF(PRD.GT.(COL+BEAM)) GO TO 80
    IF(PRD.GT.(COL+BEAM/2.)) GO TO 70
    IF(PRD.GT.COL) GO TO 60
    DELX=D(I)*COFUN
    DELY=D(I)*SIFUN-DL
    IF(ANG(I+1).GT.0.0.AND.R(I).GT.0.0) GO TO 92
    DELXX=DELX
    DELYY=-DELY
    GO TO 90
 92 DELX=-DELX
    DELXX=DELX
    DELYY=-DELY
 90 X(I+1)=X(I)+DELX
    Y(I+1)=Y(I)+DELY
    AXFOR(I+1)=P
    SHFOR(I+1)=V
    KIK=1
    UCK=UC
```

```
      UTK=UT
 2000 CONTINUE
      DO 400 II=1,600
      CALL STEEL(UC,UT,PS1,PS2,AS,SFY,SSY,H)
      CALL AFORCE(UC,UT,PS1,PS2,PCAL,PP,M,PEEP,UU,III,CYL,KIK,CONR)
      IF(ABS(UC+UT).GT.0.1) GO TO 2001
      IF(II.GT.550)WRITE(6,801)P,PCAL,PS1,PS2,UC,UT,II
      CALL STEEL(UC,UT,PS1,PS2,AS,SFY,SSY,H)
      CALL XBMX(UC,UT,PS1,PS2,BMXCAL,BAX,XM(I),PP,V,PEEP,UU,
     1III,CYL,DELXX,DELYY,M,KIK,CONR)
      IF(ABS(UC+UT).GT.0.1) GO TO 2001
      IF(II.GT.550)WRITE(6,801)BAX,BMXCAL,PS1,PS2,UC,UT,II
C     PUT TEMPORARY APPROXIMATION TO PLASTIC HINGE IN.
      IF(ABS(BAX).GE.ABS(XMULT(I))) GO TO 202
      PERROR=ABS((PP-PCAL)/PP)
      IF(II.GT.100.AND.ABS(BAX).GT.100.0)PERROR=0.0
      XBMER=ABS((BAX-BMXCAL)/BAX)
      IF(ABS(BAX).LT.15.)XBMER=ABS((BAX-BMXCAL)/10.)
      IF(ABS(PERROR*P).LT.0.1) GO TO 411
      IF(PERROR.GT.0.01) GO TO 400
      GO TO 411
  202 IF(ITCH.LT.50)ITCH=50
      BAX=XMULT(I)
      GO TO 410
  411 CONTINUE
      IF(ABS(XBMER*BAX).LT.1.0) GO TO 410
      IF(XBMER.LT.0.01) GO TO 410
  400 CONTINUE
 2001 UC=UCK
      UT=UTK
      KIK=KIK+1
      IF(KIK.LE.2) GO TO 2000
      GO TO 50
  410 RIT=(UC-UT)/8.0
      DL=-(UC+UT)*XXL/2.
      XM(I+1)=BAX
      XMULT(I+1)=(XM(I+1)/ABS(XM(I+1)))*(512.-2.5*Z)
      OUTST(I+1)=UC
      INST(I+1)=UT
      PHI(I)=(PHI(I)+RIT)/2.
      PHI(I+1)=PHI(I)
      IF(ABS(PHI(I)-RIT).LE.1.0E-06) GO TO 38
      IF(ABS((PHI(I)-RIT)/RIT).GE.0.01) GO TO 30
   38 PRD=PRD+XXL
      IF(IROUNT.GT.1) GO TO 40
      UCO=UC
      UTO=UT
   40 CONTINUE
      GO TO 100
   60 CONTINUE
      IF(ITER.NE.1) GO TO 61
      PORT=P
      P=V+HOR
      Z=-P
      PP=P
```

```
      V=PORT
      ITER=2
      IF((COL+BEAM/2.-PRD).LT.XXL) ITER=1
   61 DELX=D(I)*SIFUN-DL
      DELY=-D(I)*COFUN
      IF(ANG(I+1).GT.0.0.AND.R(I).GT.0.0) GO TO 63
      DELXX=-DELY
      DELYY=DELX
      GO TO 90
   63 DELYY=DELX
      DELY=-DELY
      DELXX=-DELY
      GO TO 90
   70 CONTINUE
      IF(ANG(I).GE.(-2.0E-03)) GO TO 74
C     THIS  CHECK IS TO MAKE SURE THAT THE SLOPE WILL GO POSITIVE NEAR
C     THE CENTRE OF THE BEAM.
      ANGER=-ANG(I)
      PORT=V
      V=P-HOR
      P=PORT
      IF(PRD.GT.(COL+BEAM/2.+XXL))P=PORT-VERT
      DELP=35.6*ANGER
      DELV=21.0*ANGER
      DELM=952.8*ANGER
      P=P+DELP
      V=V-DELV
      XM(I)=XM(I)+DELM
      GOOF(ITCH+1)=10.
      IF(ABS(XM(I)).GE.ABS(XMULT(I))) GO TO 1100
      GO TO 300
   74 CONTINUE
      IF(ITEM.NE.1) GO TO 71
      V=V+VERT
      ITEM=2
      IF((COL+BEAM-PRD).LT.XXL) ITEM=1
   71 DELX=D(I)*SIFUN-DL
      DELY=D(I)*COFUN
      IF(ANG(I+1).LT.0.0) GO TO 73
      DELXX=-DELY
      DELYY=DELX
      GO TO 90
   73 DELY=-DELY
      DELXX=-DELY
      DELYY=DELX
      GO TO 90
   80 CONTINUE
      IF(ITEC.NE.1) GO TO 81
      PART=P
      P=V
      Z=P
      PP=-P
      V=PART
      ITEC=2
   81 DELX=-D(I)*COFUN
```

```
      DELY=-D(I)*SIFUN-DL
      IF(ANG(I+1).GT.0.0.AND.R(I).GT.0.0) GO TO 83
      DELXX=DELX
      DELYY=-DELY
      GO TO 90
   83 DELXX=-DELX
      DELYY=-DELY
      DELX=-DELX
      GO TO 90
  100 CONTINUE
      INK=COL/XXL
      XP=-((XM(I+1)-XM(I+1-INK))*(COL+4.))/COL-XM(I+1-INK)
      CALL BASE(ANGST,XP,SLIP,Z,XBIT,YBIT)
      X(I+1)=X(I+1)-XBIT
      Y(I+1)=Y(I+1)-YBIT
      XERR=X(I+1)-XN
      YERR=Y(I+1)-YN
      SLOER=ANG(I+1)-ANGST
      ABEX=ABS(XERR)
      ABEY=ABS(YERR)
      ABEM=ABS(SLOER)
      P=P-VERT
      V=V-HOR
      SUMER=ABS(XERR)+ABS(YERR)+100.*ABS(SLOER)
      GOOF(ITCH+1)=SUMER
      IF(GOOF(ITCH+1).LT.GOOF(ITCH))GO TO 260
      GO TO 262
  260 IF(GOOF(ITCH+1).LT.TRIAL) GO TO 261
      GO TO 263
  261 TRIAL=GOOF(ITCH+1)
      XMTR=XM(1)
      PTR=P
      VTR=V
  263 IF(ITCH.LT.15) GO TO 262
      IF((GOOF(ITCH-1)-GOOF(ITCH+1)).GT.0.1) GO TO 262
      XM(1)=XMTR
      P=PTR
      V=VTR
      IF(ITCH.LT.50) GO TO 265
      IF(ITCH.GT.50.AND.ITCH.LT.100) GO TO 266
      GO TO 262
  265 GOOF(50)=GOOF(ITCH)
      GOOF(51)=GOOF(ITCH+1)
      ITCH=50
      GO TO 262
  266 GOOF(100)=GOOF(ITCH)
      GOOF(101)=GOOF(ITCH+1)
      ITCH=100
  262 CONTINUE
      IF(SUMER.LT.0.03) GO TO 809
      IF(ITCH.GT.75.AND.SUMER.LT.0.05) GO TO 809
      IF(ITCH.GT.100.AND.SUMER.LT.0.1) GO TO 809
C     CHANGES IN REACTIONS AT O ARE BASED ON AN ELASTIC DETERMINATION
C     OF THE FORCES REQUIRED TO REMOVE THE COORDINATE ERRORS AT N.
      SOMER=CROX+CROY+CROM
```

```
      CROX=XERR
      CROY=YERR
      CROM=SLOER
      DELV=0.65*XERR+21.0*SLOER
      DELP=0.376*YERR+35.6*SLOER
      DELM=41.6*XERR-17.6*YERR+752.8*SLOER
      DOLV=DELV
      DOLP=DELP
      DOLM=DELM
      IF(ABS(DELP).GT.0.1)DELP=(DELP/ABS(DELP))*0.1
      IF(ABS(DELV).GT.0.1)DELV=(DELV/ABS(DELV))*0.1
      IF(ABS(DELM).GT.5.) DELM=(DELM/ABS(DELM))*5.
      IF(ABS(DELP).LT.0.01) DELP=0.01*DELP/ABS(DELP)
      IF(ABS(DELV).LT.0.01) DELV=0.01*DELV/ABS(DELV)
      IF(ABS(DELM).LT.0.1) DELM=0.1*DELM/ABS(DELM)
      IF(SOMER.LT.SUMER) GO TO 1800
      GO TO 1810
 1800 DIF1=ABEX-ABEY
      IF(DIF1.GT.0.) GO TO 1811
      DIF2=ABEY-ABEM*100.
      IF(DIF2.GT.0.) GO TO 1812
      DELV=0.
      DELP=0.
      GO TO 1810
 1811 DIF3=ABEX-ABEM*100.
      IF(DIF3.GT.0.) GO TO 1813
      DELV=0.
      DELP=0.
      GO TO 1810
 1812 DELV=0.
      DELM=0.
      GO TO 1810
 1813 DELP=0.
      DELM=0.
 1810 CONTINUE
      WRITE(6,224)ITCH,XERR,YERR,SLOER,SOMER,TRIAL
      ITCH=ITCH+1
      IF(ITCH.GT.120) GO TO 222
      GO TO 223
  222 WRITE(6,225)((XM(I),AXFOR(I),SMFOR(I),OUTST(I),INST(I),X(I),Y(I),
     1PHI(I)),I=1,MM)
  225 FORMAT(1X,3F10.5,2E12.5,2E10.4,E12.5)
  224 FORMAT(1X,I5,5E12.5)
  223 CONTINUE
      IF(ITCH.GT.125) GO TO 50
      IF(ITCH.GT.50) GO TO 151
      IF(ABS(XM(1)).GE.ABS(XMOLT(1))) GO TO 1100
      IF(ABS(DELP).GT.0.1)DELP=(DELP/ABS(DELP))*0.1
      IF(ABS(DELV).GT.0.1)DELV=(DELV/ABS(DELV))*0.1
      IF(ABS(DELM).GT.5.) DELM=(DELM/ABS(DELM))*5.
      P=P+DELP
      V=V+DELV
      XM(1)=XM(1)-DELM
      GO TO 300
```

```
 151 IF(DELV.EQ.0.0.AND.DELP.EQ.0.0) GO TO 52
     IF(DELV.EQ.0.0.AND.DELM.EQ.0.0) GO TO 53
     DELP=0.01*DDLP/ABS(DDLP)
     DELM=0.1*DDLM/ABS(DDLM)
     GO TO 54
  52 DELV=0.01*DDLV/ABS(DDLV)
     DELP=0.01*DDLP/ABS(DDLP)
     GO TO 54
  53 DELV=0.01*DDLV/ABS(DDLV)
     DELM=0.1*DDLM/ABS(DDLM)
  54 CONTINUE
     IF(ITCH.GT.75) GO TO 200
     IF(ABS(DELP).GT.0.1)DELP=(DELP/ABS(DELP))*0.1
     IF(ABS(DELV).GT.0.1)DELV=(DELV/ABS(DELV))*0.1
     IF(ABS(DELM).GT.5.) DELM=(DELM/ABS(DELM))*5.
     P=P+DELP
     V=V+DELV
     XM(1)=XM(1)-DELM
     GO TO 300
 200 P=P+DELP/2.
     V=V+DELV/2.
     XM(1)=XM(1)-DELM/2.
     IF(ITCH.GT.80) GO TO 300
     WRITE(6,225)((XM(I),AXFOR(I),SHFOR(I),OUTST(I),INST(I),X(I),Y(I),
    1PHI(I)),I=1,NN)
     GO TO 300
1100 P=PST/2.
     V=VST/2.
     XM(1)=XM(1)/4.
     IF(XM(1).LT.(-32.*P)) XM(1)=-32.*P
     GO TO 300
 669 III=I-1
     WRITE(6,56)ITCH,SUMER
     WRITE(6,670)III
 670 FORMAT(1X,25HPLASTIC HINGE AT SECTION ,I2/1X,33HTHIS PROGRAM NO LO
    1NGER APPLICABLE)
     GO TO 900
 869 UC=UCO
     UT=UTO
     WRITE(6,3333)XMOTM,XP
3333 FORMAT(1X,2E12.5)
     WRITE(6,250) ITCH
 250 FORMAT(1X,4HITCH,I4)
     ITCH=1
     WRITE(6,666)
 666 FORMAT(1X,7HSECTION,3X,6HMOMENT,3X,11HAXIAL FORCE,3X,11HSHEAR FORC
    1E,6X,1HX,8X,1HY,1X,40HSTRAINS--   OUTSIDE FIBRE      INSIDE FIBRE)
     DO 668 I=1,NN
 668 ICK(I)=I-1
     WRITE(6,667)((ICK(I),XM(I),AXFOR(I),SHFOR(I),X(I),Y(I),OUTST(I),
    1INST(I)),I=1,NN)
 667 FORMAT(4X,I2,4X,F8.3,4X,F8.5,6X,F8.5,5X,F8.4,2X,F8.4,12X,E12.5,
    14X,E12.5)
     DO 671 I=1,NN
```

```
      TRIM=XM(I)
      IF(ABS(TRIM).GE.ABS(XMULT(I))) GO TO 669
  671 CONTINUE
      WRITE(6,16)XN,YN,SLIP
   16 FORMAT(1X,23H MEASURED COORDS AT N (,F10.4,1H,,F10.4,1H),5X,10HSLO
     1PE AT N,E12.5)
      WRITE(6,17)XERR,YERR,SLOER
   17 FORMAT(1X,4HXERR,F10.5,2X,4HYERR,F10.5,2X,5HSLOER,E12.5)
      WRITE(6,56)ITCH,SUMER
   56 FORMAT(1X,4HITCH,I4,5HSUMER,F10.7)
      TRIAL=10.0
      GOOF(1)=10.0
      IF(DECIDE.LE.0.5) GO TO 550
      GO TO 501
   50 WRITE(6,7)
      IF(SUMER.LT.0.5) GO TO 669
   51 IF(DECIDE.GT.0.5) GO TO 900
      READ(5,511)T2,HOR,VERT,P,V,XM(1),DECIDE
      READ(5,14)X(1),Y(1),SLOP,XN,YN,SLIP
      WRITE(6,511)T2,HOR,VERT,P,V,XM(1),DECIDE
      GO TO 51
  900 WRITE(6,205)II
  205 FORMAT(1X,I4)
      STOP
    2 FORMAT(5F10.3)
    3 FORMAT(1X,1HP,F10.3,2X,1HV,F10.3,2X,14HELEMENT LENGTH,F7.3,2X,15HN
     10. OF ELEMENTS,I3,2X,11H COL LENGTH,F10.3/1X,16HHORIZONTAL FORCE,
     2F10.3,3X,14HVERTICAL FORCE,F10.3,3X,11HBEAM LENGTH,F10.3)
    7 FORMAT(6H NO GO)
      END
      SUBROUTINE BASE(ANG,XM,SLOPE,Z,XBIT,YBIT)
C     THIS SUBROUTINE CALCULATES THE ROTATION OF THE STEEL BASE.
      STRT=((-XM/7.567)+Z)/25114.
      STRC=((XM/7.567)+Z)/25114.
      ABSTR=ABS(STRT-STRC)
      EXI=-ATAN(ABSTR/7.567)
      ABEX=-EXI
      SLORP=-SLOPE
      ANG=-ATAN(SLORP)+EXI
      BIT=4.0*(1.0+(STRT+STRC)/2.)
      XBIT=BIT*SIN(SLORP)-4.*SIN(ANG)
      YBIT=BIT*COS(SLORP)+4.*COS(ANG)
      RETURN
      END
      SUBROUTINE CREEP(T0,T1,T2,CC,PEEP,N,M)
      DIMENSION CC(30,25),CCF1(30,25),PEEP(30,25)
      SSRR=SHRINK(T1,T2)
      IF(T1.GT.0.0) GO TO 67
      DO 69 I=1,N
      DO 69 J=1,M
      CLU=CC(I,J)
      IF(CLU.GT.0.0) GO TO 73
      PEEP(I,J)=PEEP(I,J)+SSRR
      GO TO 85
```

```
   73 PEEP(I,J)=A(CLO)+B(CLO)*ALOG10(T2)+SSRR
      UUF1(I,J)=CLO
      GO TO 69
   83 UUF1(I,J)=0.0
   69 CONTINUE
      GO TO 80
   67 DO 75 I=1,N
      DO 75 J=1,M
      CLO=UU(I,J)-PEEP(I,J)
      IF(CLO.GT.0.0) GO TO 79
      PEEP(I,J)=PEEP(I,J)+SSRR
      GO TO 82
   79 OLDO=CLO-UUF1(I,J)
      IF(OLDO.GT.0.0) GO TO 100
      ODLO=-OLDO
      IF(T1.EQ.T2) GO TO 200
      SOLD=(AA(ODLO)+BB(ODLO)*ALOG10(T2-T1))*0.6667
      GO TO 101
  200 SOLD=0.
      GO TO 101
  100 CONTINUE
      IF(T1.EQ.T2) GO TO 201
      SOLD=AA(OLDO)+BB(OLDO)*ALOG10(T2-T1)
      PEEP(I,J)=PEEP(I,J)+B(CLO)*(ALOG10(T2)-ALOG10(T1))+SSRR+SOLD
      GO TO 102
  201 SOLD=0.
      PEEP(I,J)=PEEP(I,J)+B(CLO)*(ALOG10(T2)-ALOG10(T1))+SSRR+SOLD
      GO TO 102
  101 PEEP(I,J)=PEEP(I,J)+B(CLO)*(ALOG10(T2)-ALOG10(T1))
     1-SOLD+SSRR
  102 UUF1(I,J)=CLO
      GO TO 75
   82 UUF1(I,J)=0.0
   75 CONTINUE
   80 T0=T1
      T1=T2
      WRITE(6,915)SSRR
  915 FORMAT(5X,F10.6//)
      WRITE(6,913)((PEEP(I,J),J=1,M),I=1,N)
  913 FORMAT(10X,10F10.6)
      RETURN
      END
      FUNCTION SHRINK(T1,T2)
      IF(T1-1.0)86,86,87
   86 SHRINK=-0.000111+0.000224*ALOG10(T2)
      GO TO 88
   87 IF(T2-700.)94,94,95
   94 SHRINK=0.000224*(ALOG10(T2)-ALOG10(T1))
      GO TO 88
   95 SHRINK=0.000518+0.000111-0.000224*ALOG10(T1)
   88 RETURN
      END
      FUNCTION A(CLO)
      FL=CLO-0.0005
      A=-1050500.*FL**3-970.363*FL**2-0.575562*FL-0.000177
      RETURN
```

```
      END
      FUNCTION B(CLU)
      FL=CLU-0.0005
      B=1858390.*FL**3+1775.29*FL**2+1.90502*FL+0.000732
      RETURN
      END
      FUNCTION AA(OLDU)
      FL=OLDU-0.0005
      AA=-1030500.*FL**3-970.863*FL**2-0.575662*FL-0.000177
      RETURN
      END
      FUNCTION BB(OLDU)
      FL=OLDU-0.0005
      BB=1858390.*FL**3+1775.29*FL**2+1.90502*FL+0.000732
      RETURN
      END
      SUBROUTINE AFORCE(UC,UT,PS1,PS2,PCAL,P,M,PEEP,UU,I,CYL,KIN,CSHR)
      DIMENSION UU(30,25),PEEP(30,25)
      DM=M
      PCAL=PS1+PS2
      DO 600 J=1,M
      DJ=J
      UU(I,J)=UC-(DJ-0.5)/DM*(UC-UT)-CSHR
      W=UU(I,J)-PEEP(I,J)
      IF(W+0.00015)600,603,603
  603 CCC=CONCF(W,CYL)
      PCAL=PCAL+(64.0/DM)*CCC
  600 CONTINUE
      UP=0.0001*(P-PCAL)/ABS(20.*ABS(P))
      IF(KIN.GT.1)UP=((P-PCAL)/ABS(P-PCAL))*1.0E-04/(100.*P)
      IF(ABS(UC-UT).LT.1.0E-07)UP=((P-PCAL)/ABS(P-PCAL))*1.0E-07
      UC=UC+UP
      UT=UT+UP
      RETURN
      END
      SUBROUTINE XBMX(UC,UT,PS1,PS2,BMXCAL,BAX,XM,P,V,PEEP,
     1UU,I,CYL,DELXX,DELYY,M,KIN,CSHR)
      DIMENSION UU(30,25),PEEP(30,25)
      DM=M
      BMXCAL=PS1*(-2.625)+PS2*2.625
      DO 610 J=1,M
      DJ=J
      UU(I,J)=UC-(DJ-0.5)/DM*(UC-UT)-CSHR
      W=UU(I,J)-PEEP(I,J)
      IF(W+0.00015)610,613,613
  613 CCC=CONCF(W,CYL)
      BMXCAL=BMXCAL+(64.0/DM)*(4.0-((DJ-0.5)/DM)*8.0)*CCC
  610 CONTINUE
      BAX=XM+P*DELXX+V*DELYY
      SAX=ABS((UC-UT)/UC)
      IF(SAX-0.05)675,671,671
  675 UMX=0.0001*(BAX-BMXCAL)/ABS(10.*BAX)
      IF(ABS(BAX).LT.10.)UMX=1.0E-05*(BAX-BMXCAL)
```

```
      GO TO 658
671   UMX=ABS(UC-UT)*(BAX-BMXCAL)/ABS(10.*BAX)
      IF(ABS(BAX).LT.10.)UMX=1.0E-06*(BAX-BMXCAL)
658   CONTINUE
      IF(KIK.GT.1)UMX=((BAX-BMXCAL)/ABS(BAX-BMXCAL))*ABS(UC-UT)/ABS(BAX)
      IF(ABS(UC-UT).LT.1.0E-07)UMX=((BAX-BMXCAL)/ABS(BAX-BMXCAL))*1.0E-0
     17
      UT=UT-UMX
      UC=UC+UMX
      RETURN
      END
      SUBROUTINE STEEL(UC,UT,PS1,PS2,AS,SFY,SSY,H)
      SS1=0.828125*UT+0.171875*UC+H
      SS2=0.828125*UC+0.171875*UT+H
      IF(SS1)501,501,502
502   PS1=AS*SFY*(SSY+SS1-SQRT((SSY+SS1)**2-4.*SSY*SS1))/(2.0*SSY)
      GO TO 503
501   VAN=ABS(SS1)
      PS1=-AS*SFY*(SSY+VAN-SQRT((SSY+VAN)**2-4.*SSY*VAN))/(2.0*SSY)
503   IF(SS2)504,504,505
505   PS2=AS*SFY*(SSY+SS2-SQRT((SSY+SS2)**2-4.*SSY*SS2))/(2.0*SSY)
      GO TO 506
504   VAN=ABS(SS2)
      PS2=-AS*SFY*(SSY+VAN-SQRT((SSY+VAN)**2-4.*SSY*VAN))/(2.0*SSY)
506   CONTINUE
      RETURN
      END
      FUNCTION CONCF(W,CYL)
      QU=W-1.27367/10.0**3
      CONCF=CYL/4000.*(-1.79697*10.**12*QU**4+2.12561*10.0**11*QU**3
     1-9.30356*10.**8*QU**2+1.19956*10.**6*QU+3529.01)
      RETURN
      END
```

CD TOT 0057

APPENDIX C - TENSILE TESTS ON REINFORCEMENT

TABLE C1 EFFECT OF HEAT TREATMENT ON STRENGTH OF REINFORCING STEEL

(ALL SAMPLES WERE #6 DEFORMED BARS)

TYPE OF SPECIMEN	METHOD OF HEATING	HEAT TREATMENT	NO. OF SAMPLES	YIELD STRENGTH (PSI) (AVG)	ULTIMATE TENSILE STRENGTH (AVG)	F*
STRAIGHT	NIL	COLD	3	59,300	109,000	0
STRAIGHT	ACETYLENE TORCH	HEATED LOCALLY TO PLASTIC STATE COOLED IN STILL AIR AT 70°F	3	59,500	109,200	0
STRAIGHT	ACETYLENE TORCH	HEATED LOCALLY TO PLASTIC STATE COOLED IN SAND	2	60,000	109,200	0
BENT 45° THEN STRAIGHT WHILE HOT	ACETYLENE TORCH	HEATED LOCALLY TO PLASTIC STATE. COOLED IN STILL AIR AT 70°F	3	NOT WELL DEFINED	107,000 - 110,000	1
STRAIGHT	FURNACE	WHOLE BAR HEATED TO 1500°F. COOLED IN STILL AIR AT 70°F	3	60,000	105,000	3

* F DENOTES NUMBER OF SAMPLES WHICH FAILED IN THE HEAT AFFECTED ZONE

AVG. YIELD STRENGTH WHERE WELL DEFINED = 59,800 PSI:STANDARD DEVIATION = 420 PSI

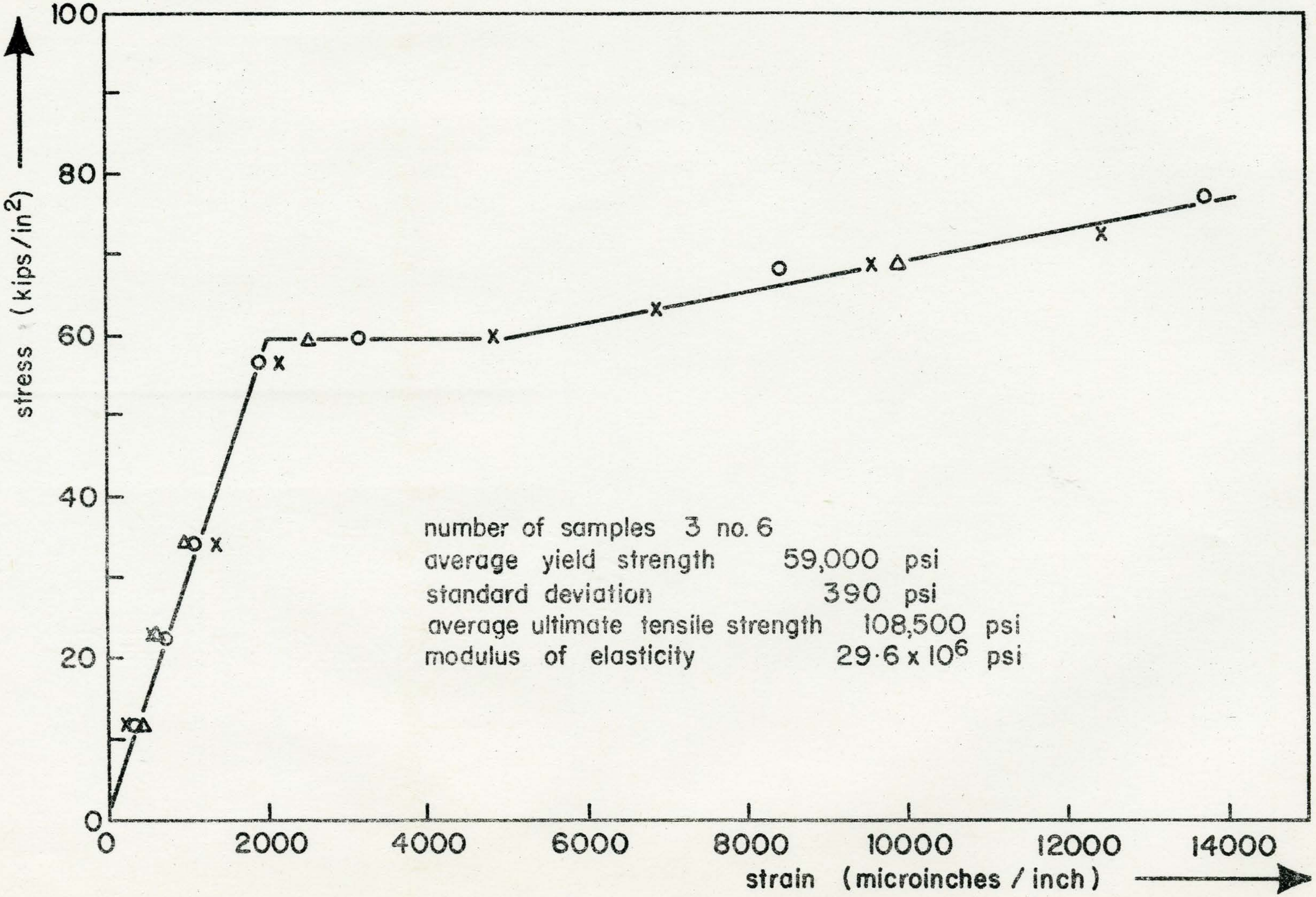

FIGURE C1 Stress-strain relationship for reinforcing steel.

BIBLIOGRAPHY

1. BARNARD, P.R., "Limit Design, Past, Present and Future," Engineering Journal, June, 1966.

2. BREENE, J.E., and Ferguson, P.M., "The Restrained Long Column as Part of a Rectangular Frame," Journal A.C.I. Proc., May, 1964.

3. "Building Code Requirements for Reinforced Concrete," (ACI 318-63), American Concrete Institute, 1963.

4. COHN, M.Z., "Optimum Limit Design for Reinforced Concrete Continuous Beams," Institute of Civil Engineering, April, 1965.

5. DRYSDALE, R.G., "The Behaviour of Slender Reinforced Concrete Columns Subjected to Sustained Biaxial Bending," Ph.D. Thesis, University of Toronto, 1967.

6. FLUCK, P.G., and Washa, G. W., "Creep of Plain and Reinforced Concrete," Journal A.C.I. Proc., April, 1958.

7. FREUDENTHAL, A.M. and Roll, F., "Creep and Creep Recovery of Concrete under High Compressive Stress," Journal A.C.I. Proc., June, 1958.

8. FURLONG, R.W. and Ferguson, P.M., "Tests on Frames with Columns in Single Curvature," accepted for publication in Symposium on Columns, American Concrete Institute.

9. GAEDE, K., "Knicken von Stahlbetonstaben unter Kurz - und Langzeitbelastung," Deutscher Ausschuss Fur Stahlbeton, Berlin, 1958.

10. GLUCKLICH, J., and Ishai, O., "Creep Mechanism in Cement Mortar," Journal A.C.I. Proc., July, 1962.

11. GRAY, D.C., "Prediction of the Effects of Creep on Concrete under Non-Uniform Stress," M. Eng. Thesis, McMaster University, 1968.

12. GREEN, R., "Behaviour of Unrestrained Reinforced Concrete under Sustained Load," Ph.D. Thesis, University of Texas, 1966.

13. KRIEG, K.H., "Einfluss des Betonkiechens auf die Knicksicherheit Krummer Stahlbetonstabe," Beton und Stahlbetonbau, February, 1954.

14. LEHMAN, D., "Short Term Beahviour of Long Columns in Reinforced Concrete Frames Subjected to Sidesway," M.A.Sc. Thesis, University of Toronto, 1968.

15. L'Hermite,"Idees Actuelles sur la Technologie du Beton," Document Technique du Batiment et des Travaux Publics, Paris, 1955.

16. LYSE, A., "Shrinkage and Creep of Concrete," Magazine of Concrete Research, November, 1959.

17. MANUEL, R.F. and MacGregor, J.G., "The Beahviour of Restrained Reinforced Concrete Columns under Sustained Load," Ph.D. Thesis, University of Alberta, 1966.

18. NEAL, B.G., "The Plastic Methods of Structural Analysis," Chapman & Hall, London, 1956.

19. NEVILLE, A.M., "Properties of Concrete," Sir Isaac Pitman and Sons Ltd., London, 1963.

20. ROSS, A.D., "Creep of Concrete under Variable Stress," Journal A.C.I. Proc., March, 1958.

21. SAWYER, H.A., "Design of Concrete Frames for Two Failure Stages," International Symposium on Flexural Mechanics of Reinforced Concrete, Miami, 1964.

22. SHANK, J.R., "The Mechanics of Plastic Flow of Concrete," Journal A.C.I. Proc., Nov. 1935.